Evolution and Molecular Mechanisms of Thermal Tolerance Plasticity in Reef-Building Corals

By

LESLIE GUERRERO
DISSERTATION

Submitted in partial satisfaction of the requirements for the degree of

DOCTOR OF PHILOSOPHY

in

Integrative Genetics and Genomics

in the

OFFICE OF GRADUATE STUDIES

of the

UNIVERSITY OF CALIFORNIA

DAVIS

Approved:

Rachael Bay, Chair

Janine LaSalle

Anne Todgham

Committee in Charge

2024

TABLE OF CONTENTS

ACKNOWLEDGEMENTS

This dissertation would not have been possible without the unwavering support of Rachael Bay. Rachael, you demonstrated the incredible ability to hold me to the standards of a collaborator while also giving me the space to make mistakes, learn, and grow. You believed in me when my own confidence faltered, and the compassion you modeled will continue to shape how I treat others–and myself. Together, we pursued some pretty bold scientific goals, and I will always be grateful that you stayed with me on the topsy-turvy rollercoaster of risks we took. Thank you for sharing your passion for corals, scientific creativity, and lifelong learning with me.

Thank you to all the members of the Bay Lab for creating an incredibly supportive community that enriched my scientific journey. I'm deeply grateful for all the insightful conversations we shared. Brenda Cameron, your invaluable advice and experience made exploring these scientific questions possible. Special thanks to Maddie, Brooke and Nicole. Maddie, I truly admire your positivity, your scientific curiosity and the supportive way you approach mentorship. Thanks for always offering a place to stay. Brooke, your enthusiasm is infectious, and your courage is both admirable and inspiring. I'm grateful you were always just a phone call away. Nicole, I am so glad our paths crossed in the Bay Lab, and I'm especially thankful for your continued friendship.

Thank you to the larger UC Davis biological sciences community for your support and for nurturing my scientific curiosity across a wide range of systems. I gained diverse experiences and skills, and I was given amazing opportunities to explore new ideas and take risks. I truly believe my scientific journey was only possible at UC Davis. Special thanks to Julin Maloof, Amanda Schrager-Lavelle, Dan Starr, Sean Burgess, JoAnne Engebrecht, Natalie Cain, Courtney Bone, and, last but not least, Venecia Valdez.

Thank you to the institutional support at UC Davis, including my dissertation committee, the UC Davis Genome Center, CMSI, the EVE office, and my graduate group, IGG. I am also grateful to the funding sources that made this work possible: the National Science Foundation, the American Philosophical Society, the H. A. Lewin Family Fellowship, and the UC Davis and Humanities Grad Research Award.

Thank you to my friends and family for your unwavering support and patience as I navigated the growth that comes with facing challenges.

Finally, thank you, Marcus Wolf. Sharing your passion for the natural world has been a true gift since the day we met. You've helped me through some incredibly difficult times with your grounded perspective, lightheartedness, and love. Thank you for always nerding out about science with me and for always identifying trees for me.

ABSTRACT

Organisms must respond to environmental cues to maintain homeostasis, with gene expression driving phenotypic variation. Variation in gene expression response to environmental stress varies across individuals, populations, and species and can determine tolerance to stressors. Understanding links between gene expression and tolerance is especially urgent in species vulnerable to climate change, such as reef-building corals. *Acropora,* the largest genus of corals, are ecologically significant, as reefs support marine biodiversity and human communities, yet are particularly vulnerable to climate-induced warming. Previous research linked gene expression variation to thermal tolerance, making *Acropora* an ideal system for exploring two fundamental questions, which I investigate in this dissertation: 1) What epigenetic mechanisms explain variation in gene expression at the individual level? and 2) How does the evolution of gene expression responses affect thermal tolerance across species?

In Chapter 1, I investigated the role of the epigenetic mechanism, DNA methylation, in driving gene expression changes coupled with enhanced thermal tolerance. In *A. nana*, individuals exhibiting thermal tolerance plasticity, or thermal acclimation, also have a reduced gene expression response to heat stress, a form of gene expression plasticity. DNA methylation is a chemical modification of DNA associated with overall mean gene expression and gene expression variability in invertebrates. I integrated RNA-seq and WGBS data to test the hypothesis that the heat stress genes with reduced expression responses to heat stress in acclimated individuals undergo a shift in DNA methylation throughout the thermal acclimation period. I found no relationship between the change in the heat-stress gene expression response in acclimated individuals and changes in DNA methylation following thermal acclimation. This result is likely due to the complexities of molecular interactions of DNA methylation with other gene expression regulators.

In Chapter 2, I explored the role of chromatin accessibility in the gene expression response to heat stress using the species *A. millepora*. Chromatin accessibility is unexplored in reef-building coral species but is an epigenetic mechanism that plays a role in higher-level gene expression regulation in other species. I performed 3'TagSeq on samples subject to a heat stress assay to evaluate the gene

expression response to heat stress. In parallel, I performed ATAC-seq on samples from ambient conditions (i.e., no stress treatment) to investigate baseline regions of open chromatin regions in *A. millepora.* By integrating these two data sets, I found a relationship between chromatin accessibility and gene expression and gene expression variation. Further, open chromatin promoters play a small but significant role in promoting a rapid gene expression response to heat stress.

In Chapter 3, I investigated the evolution of thermal tolerance and gene expression responses across eight *Acropora* species. Gene expression responses to heat stress are reduced in heat-tolerant individuals and populations, suggesting that this reduced response is a general thermal tolerance mechanism in corals. I estimated the relative thermal tolerances of multiple individuals across species and, using 3'TagSeq, found that thermally tolerant species exhibit a reduced gene expression response compared to thermally sensitive species. This suggests that similar mechanisms may be leading to thermal tolerance across levels of organization.

Overall, my findings lead to a better understanding of the mechanisms governing gene expression variation and thermal tolerance in corals, and phenotypic plasticity more broadly. These insights are critical for understanding organismal resilience to climate change and can inform conservation strategies at the molecular level.

Patterns of methylation and transcriptional plasticity during thermal acclimation in a reef-building coral

Authors: Leslie Guerrero and Rachael Bay

Abstract

Phenotypic plasticity can buffer organisms against short-term environmental fluctuations. For example, previous exposure to increased temperatures can increase thermal tolerance in many species. Prior studies have found that acclimation to higher temperature can influence the magnitude of transcriptional response to subsequent acute thermal stress (hereafter, “transcriptional response modulation”). However, mechanisms mediating this gene expression response and, ultimately, phenotypic plasticity remain largely unknown. Epigenetic modifications are good candidates for modulating transcriptional response, as they broadly correlate with gene expression. Here, we investigate changes in DNA methylation as a possible mechanism controlling shifts in gene expression plasticity and thermal acclimation in the reef-building coral *Acropora nana*. We find that gene expression response to acute stress is altered in corals acclimated to different temperatures, with many genes exhibiting a dampened response to heat stress in corals pre-conditioned to higher temperatures. At the same time, we observe shifts in methylation during both acclimation (11 days) and acute heat stress (24 hours). We observed that the acute heat stress results in shifts in gene-level methylation and elicits an acute transcriptional response in distinct gene sets. Further, acclimation-induced shifts in gene expression plasticity and differential methylation also largely occur in separate sets of genes. Counter to our initial hypothesis no overall correlation between the magnitude of differential methylation and the change in gene expression plasticity. We do find a small but statistically significant overlap in genes exhibiting both dampened expression response and shifts in methylation (14 genes), which could be candidates for further inquiry. Overall, our results suggest transcriptional response modulation occurs independently from methylation changes induced by thermal acclimation.

Introduction

Increased intensity and frequency of climate anomalies has led to physiological stress, population decline, and species redistribution across the globe. One potential mechanism for buffering against extreme climate fluctuations is adaptive phenotypic plasticity–phenotypic changes occurring within an individual's lifetime that promote greater fitness in response to environmental triggers (Gienapp et al. 2008; Merilä and Hendry 2014). The ability of organisms to undergo phenotypic plasticity is seemingly ubiquitous

across the tree of life (Gotthard and Nylin 1995; Sultan 2000; Agrawal 2001; Santillán and Mackey 2008; Sorek and Cossart 2010), and plastic phenotypes can vary widely among taxa, including shifts in physiology, morphology, or behavior (Sultan 2000; Ghalambor et al. 2010). The degree of plasticity can vary between individuals, populations, and species demonstrating the diversity and evolvability of trait plasticity (Dingemanse and Wolf 2013; Gunderson and Stillman 2015; Putnam et al. 2016; Kenkel and Matz 2016; Kelly 2019; Mallard et al. 2020). Climate change is predicted to interfere with the reliability of environmental stimuli for plastic responses in natural populations by increasing climate variability or forcing species redistributions, shifting selection pressure on phenotypic plasticity (Bonamour et al., 2019; Kelly, 2019). Accordingly, building a mechanistic understanding of adaptive plasticity can aid in predictions of when adaptive plasticity might be sufficient to buffer against the ongoing effects of climate change.

Phenotypic plasticity often results from gene expression shifts caused by environmental triggers (Schlichting & Pigliucci, 1993; Schlichting & Pigliucci, 1995; Schlichting & Smith, 2002). While differing baseline gene expression is associated with variation in several climate-relevant phenotypes (Hamdoun et al. 2003; Dayan et al. 2015; DeBiasse and Kelly 2016; Gibbons et al. 2017), recent evidence from transcriptomic studies reveals that the magnitude of gene expression response to climatic stressors, rather than the constitutive level of expression, may determine the outcome. For example, four genotypes of wheat seedlings acclimated to drought had a reduced physiological response to a 48-hour water stress assay and lower magnitudes of expression of drought response genes than the non-acclimated counterparts (Amoah et al., 2019). Similarly, plasticity in thermal tolerance(i.e., thermal acclimation) in corals followed by short-term thermal exposure was associated with a reduced gene expression response of heat-stress genes (Bay & Palumbi, 2015; Bellantuono et al., 2012). Lastly, a reciprocal transplant experiment revealed that a higher capacity for transcriptional plasticity in a coral population was associated with survival during thermal stress (Kenkel & Matz, 2016). Together these studies highlight the potential for gene expression plasticity to facilitate adaptive phenotypic plasticity. However,

mechanisms driving such transcriptional modifications remain elusive (Hamdoun et al. 2003; López-Maury et al. 2008; Barshis et al. 2013; Gleason and Burton 2015; Mallard et al. 2020; Logan and Cox 2020). How environmental signals are translated to changes in gene expression plasticity remains a fundamental question. Understanding these mechanisms will aid in predicting when we expect adaptive plasticity to occur and the potential limits.

DNA methylation offers a potential intermediate between environmental change and gene expression plasticity (Eirin-Lopez & Putnam, 2019). DNA methylation–a stable yet reversible covalently attached methyl group to nucleotides–is an epigenetic mechanism that putatively affects gene expression plasticity by interacting with transcriptional regulators (Jones, 2012; LaSalle et al., 2013). DNA methylation dynamics are influenced by the environment and these shifts are associated with a genotype's potential for phenotypic plasticity (Putnam et al., 2016; Dixon et al., 2018). Interestingly, methylation distribution and density vary among genomic features within a single genome and are associated with different gene expression patterns. For instance, the methylation of cytosines in cytosine-guanine dinucleotide motifs (CpG) within coding sequences, or gene body methylation, is associated with hypomethylated promoters and correlated with expression magnitude and variation in invertebrate species (Jones, 2012; Li et al., 2018; Dixon et al., 2018; Dixon & Matz, 2022). In particular, genes regularly expressed to maintain basal homeostatic processes or housekeeping genes tend to be more highly methylated than environmentally responsive genes (Gatzmann et al., 2018; Dixon et al., 2018). In cnidarians, heavily methylated intragenic transposable elements can explain hypermethylated gene bodies (Ying et al. 2022). However, high methylation of intragenic transposable elements in cnidarians does not affect gene expression levels (Ying et al. 2022). Altogether these studies highlight the complex relationship between DNA methylation and gene expression patterns.

Despite links between baseline methylation and gene expression (Gatzmann et al. 2018; Anastasiadi et al. 2018; Dixon and Matz 2022), whether environmentally-induced shifts in methylation lead to shifts in

gene expression is unclear. By coupling transcriptome and methylome analyses across six invertebrate species, Dixon and Matz show that changes in gene body methylation do not explain global changes in gene expression (Dixon & Matz, 2022). A common-garden experiment performed on full-sibling families of *Crassostrea virginica* show that, while gene expression patterns are driven by sampling location, DNA methylation is driven by genetic differences between families, suggesting methylation does not facilitate global changes in gene expression (Johnson et al., 2021). Comparative analysis between *Arabidopsis thaliana* and *Eutrema salsugineum*, a species that has lost gene body methylation, shows gene function and histone modifications are indistinguishable between the two species suggesting a minimal relationship between gene body methylation and transcription (Muyle et al., 2022; Bewick et al., 2016). Nevertheless, gene body methylation is conserved across plants, fungi, and animals, suggesting functional significance despite conflicting conclusions about the relationship with gene expression (Muyle et al., 2021; Entrambasaguas et al., 2021; Dixon & Matz, 2022; He et al., 2020; Zeng et al., 2018).

Here, we examine the association between gene body methylation and transcriptional plasticity observed during rapid thermal acclimation in the reef-building coral species *Acropora nana*. Particularly vulnerable to ocean warming, reef-building coral species within the Acropora genus are of significant conservation concern due to bleaching-induced mortality following acute warming events. As long-lived benthic marine invertebrates, thermal acclimation, the ability to increase thermal tolerance following exposure to sublethal elevated temperatures, is one of the few mechanisms corals have to respond to short-term environmental fluctuations (Middlebrook et al., 2008). Thermal acclimation is associated with altered magnitudes of transcriptional response to subsequent acute heat stress, a phenomenon we refer to as "transcriptional response modulation". This modulation in coral heat response genes during imminent acute thermal challenge suggests the presence of molecular pathway(s) that presumably i) preserve the memory of previous thermal exposure and ii) mediate an altered transcriptional response leading to stress resilience (Bellantuono et al., 2012; Bay & Palumbi, 2015; Hackerott et al., 2021). We leveraged a previously published experiment in which *Acropora nana* fragments were acclimated to elevated but

sublethal temperatures and then treated with an acute heat stress assay (Bay & Palumbi, 2015). Bleaching under acute heat stress was reduced in acclimated individuals (Bay & Palumbi, 2015). Bay and Palumbi then measured gene expression following the heat stress assay to characterize the transcriptional response to heat stress between acclimated and non-acclimated individuals. Within that experiment, individuals acclimated to higher temperatures were shown to have a reduced transcriptional response to heat stress. For the subset of the genes exhibiting a modulated expression response to heat stress, we aimed to explore whether these genes undergo changes in methylation during the acclimation treatment leading up the heat stress assay. Simultaneously investigating gene body methylation and gene expression patterns associated with increased thermal tolerance following acclimation, we addressed the following questions: i) Are there shifts in gene body methylation during acclimation to elevated temperatures? and ii) Do shifts in methylation correspond to reduced transcriptional plasticity in the same genes?

Methods

Experimental Design

The samples used in this study were taken from a previously published acclimation experiment, and details on the experimental setup can be found in that paper (Figure 1.1 A; Bay & Palumbi, 2015). Briefly, we took whole small colonies of *Acropora nana* (Studer, 1878) from the reef on Ofu Island, American Samoa, and placed them in outdoor aquaria for acclimation. Three colonies were placed in each tank, with two tanks per acclimation treatment, totaling six colonies per acclimation treatment and 18 colonies in total. Due to logistical constraints, genotype was not replicated across acclimation treatments. The original study had an ambient (29°C), elevated (31°C), and variable (29-33°C daily) acclimation treatment to mimic *in situ* thermal fluctuation. We only used samples from the two stable treatments (29°C and 31°C) for our purposes. This 2°C temperature difference was sufficient to induce thermal acclimation and is within the typical thermal range. At different time points throughout the experiment, we sampled branches from each colony and subjected them to an acute heat stress assay to test thermal tolerance. For the heat stress assay, two branches were sampled from each colony; one was held at an

ambient control temperature (29°C) for 24 hours while the other was subjected to heat stress consisting of a three-hour ramp to 34°C followed by five hours at 34°C, then a decline to 29°C for approximately one hour. This temperature profile was designed to mimic tidal fluctuations in temperature at this location and expose variation in bleaching among samples. The heated samples were incubated at 29°C overnight for the remainder of the 24-hour assay. At 6:00 AM the following morning, branches were cut in half and preserved in 95% ethanol and RNA stabilizing solution (70g Ammonium Sulfate /100ml solution, 10 mM EDTA, 25 mM Sodium Citrate, 5.4 pH) for downstream analysis. To assess thermal tolerance after heat stress, we measured chlorophyll concentration as a proxy for bleaching (Ritchie, 2008). Figure 1.1 B, redrawn from Bay & Palumbi (2015), shows the increase in thermal tolerance (reflected in higher chlorophyll content of heat-stressed samples) for 31°C acclimated corals than 29°C acclimated corals after 11 days. In this study, we examine samples in the acclimation treatments for either 0 days (i.e., collected the previous day and held at 29°C overnight) or 11 days. Note that this means the Day 0 samples in the 31°C tank never actually experienced 31°C acclimation.

RNASeq

Six samples per treatment group, totaling 48 samples, were extracted and sequenced for RNASeq. Sample preservation, library prep, cDNA sequencing, and read trimming are described in Bay & Palumbi 2015. We aligned trimmed reads to the *Acropora millepora* genome using STAR aligner software (v. 2.7.0e) (Dobin et al. 2013; Fuller et al. 2020). Filtering parameters that optimized alignment were: --outFilterScoreMinOverLread 0, --outFilterMatchNminOverLread 0, --outFilterMatchNmin 0, --outFilterMismatchNmax 4. We used HTSeq v. 0.9.1 to count all reads that mapped to genes, including reads that map to multiple genes(--nonunique all), using the annotated gene models provided with the *Acropora millepora* reference genome (Anders et al., 2015; Fuller et al. 2020). We expect that a congener alignment may have resulted in some reads failing to map due to the divergence between *Acropora millepora* and *Acropora nana,* thus, these reads were excluded from the remainder of the analyses.

To quantify the symbiont composition within each sample, we aligned RNASeq reads to Symbiodinium goreaui (GenBank accession number: AF333515) and Durusdinium trenchii (GenBank accession number: LC718590) ITS2 sequences using the STAR aligner software (v. 2.7.0e) (LaJeunesse 2001, Dobin et al. 2013, Mihirogi et al. 2023). We used the STAR option --outFilterMultimapNmax 1 to ensure that STAR reports only the best alignment for each read. We counted the number of reads that uniquely aligned to each ITS2 sequence in each sample.

Whole-genome bisulfite sequencing

We extracted DNA from the same branches used for RNA-Seq (6 samples per treatment group, totaling 48 samples) using the Qiagen DNeasy Blood & Tissue Kit (Cat. No. 69504). Genomic DNA was sent to Novogene (Sacramento), and Methyl-MaxiSeq libraries were prepared from 300 ng of genomic DNA digested with 2 units of Zymo Research's dsDNA Shearase™ Plus (Cat. No. E2018-50). The fragments produced were end-blunted, 3'-terminal-A extended, then purified using the Zymo Research DNA Clean & Concentrator™ kit (Cat. No. D4003). The A-tailed fragments were ligated to pre-annealed adapters containing 5'-methylcytosine instead of cytosine. Bisulfite treatment of the fragments was done using the EZ DNA Methylation–Lightning kit (Zymo Research, Cat. No. D5030). PCR was performed with Illumina TruSeq indices, and the size and concentration of the fragments were confirmed on the Agilent 2200 TapeStation. Before sequencing, samples were spiked with Illumina's PhiX Control library. Sequencing was performed using the Novaseq 6000 platform with Paired-End 150 (PE150) reads, aiming for a target coverage of 30x based on the 500 Mb *Acropora* millepora estimated genome size. The average raw read coverage achieved was 23x.

To analyze WGBS reads, we used Trim Galore! Version 0.6.3 to filter out reads that were less than 20 nt long along with their read-mate (Krueger 2019). We clipped the 5' ends of the reads to remove possible methylation bias (--clip_R1 10 --clip_R2 10). We aligned trimmed reads to the *Acropora millepora* genome using bwa-meth with default settings (Fuller et al. 2020; Pedersen et al. 2014). We used

SAMtools view (Version 1.9) to filter by excluding unmapped reads, mapped reads with unmapped mates, and/or reads that failed platform quality thresholds (-F 524) (Li et al. 2009). We kept reads with a minimum mapping quality of 2 (-q 2) (Li et al. 2009). To filter out PCR duplicates, we used Picard MarkDuplicates (Version 2.20.2) with default settings (Picard). Finally, to extract methylation calls, we used MethylDackel (https://github.com/dpryan79/MethylDackel). This output summarizes the strand-specific frequency of cytosines and thymines (a proxy for unmethylated cytosine). In downstream statistical analyses, these frequencies are converted to a percentage of DNA methylation at each CpG dinucleotide. As we did not have full genomic data for *A. nana,* we were unable to mask possible C to T substitutions between the *A. millepora* reference genome and *A. nana* samples. The minimum depth of methylation calls was set to 10, and the maximum variant fraction was set to 0.75 to exclude possible non-cytosine alleles at reference CpG sites.

Differential gene expression and heat response gene identification

We analyzed differential gene expression using R Package DESeq2 v. 1.36.0 (Love et al. 2014, R Core Team 2022). First, we filtered for genes with a depth of at least 10 reads in all samples and normalized data with the variance stabilizing transformation. We performed a PCA to investigate the relationship between acclimation and heat stress treatment groups. We identified heat response genes by comparing the heat-stressed samples to their corresponding control counterparts that had not undergone thermal acclimation (29°C at Day 0 and Day 11, and 31°C at Day 0). Since thermal acclimation can lead to the downregulation of a subset of stress response genes, transcriptional data from thermally acclimated samples were excluded from identifying the heat response genes. We calculated the $\log_2$ fold-change between heat-stressed and control samples and performed $\log_2$ fold-change shrinkage with the 'ashr' method to account for the strong variation in $\log_2$ fold-change associated regions of low read counts (Love et al. 2014; Stephens 2017). Heat response genes are defined by a $|\log_2 \text{fold-change}| > 2$ and Benjamini-Hochberg false discovery rate (BH p_{adj}) < 0.01. We classified a total set of heat response genes from the union of the significant differential expression within any of the three sample sets: 29°C (Day 0

and Day 11) and 31°C (Day 0). A more conservative set of "core" heat stress genes were identified by the intersection of the significant heat stress genes across all three contrasts. We analyzed Gene Ontology (GO) terms with the R package, topGO v. 2.50.0 (Alexa and Rahnenfuhrer 2022). We compared the list of "core" heat response genes against a background of all genes that passed our quality filters. Enriched GO terms were identified with the classic Fisher's test with a p-value < 0.01 and at least 10 transcripts within each category.

Quantifying transcriptional response modulation

Previously, we found no change in gene expression during acclimation but rather a change in the magnitude of gene expression response to heat stress in corals pre-conditioned at higher temperatures (Bay and Palumbi 2015). Here, we quantified this "transcriptional response modulation" using R Package DESeq2 v. 1.36.0 (Love et al. 2014, R Core Team 2022). DESeq2 estimates the interaction term coefficient for each gene and uses the Wald test to test if the interaction term is statistically different from zero (Love et al. 2014). The predictors of the coefficient terms are the levels of the experimental design (Love et al. 2014). In our case, the experimental conditions are acclimation temperature and heat stress treatment, with the Wald test quantifying the interaction between the two. To avoid the confounding factor of Day, we used heat stress treatment and control samples from the acclimation temperature control, 29°C (Day 11), and the acclimation treatment, 31°C (Day 11), for comparison to capture the effect of thermal acclimation. We identified two categories of transcriptional response modulation: amplified and dampened expression. Transcripts with amplified expression had a higher magnitude of expression response induced by heat stress in samples acclimated to 31°C than those acclimated to 29°C (Wald statistic > 0 and BH $p_{adj} < 0.1$). Transcripts with dampened expression had a smaller magnitude of expression response (Wald statistic < 0 and BH $p_{adj} < 0.1$) (Love et al. 2014). To test if amplified and dampened genes have different mean expressions, we $\log_{10}$-transformed each transcript's average normalized count values and performed a two-sample t-test. We analyzed Gene Ontology (GO) terms with the R package, topGO v. 2.50.0 (Alexa and Rahnenfuhrer 2022). We compared lists of amplified and

dampened genes against a background of all genes that passed our quality filters. Enriched GO terms were identified with the classic Fisher's test with a p-value < 0.01 and at least 10 transcripts within each category.

Effects of treatment on DNA methylation

We used methylKit to analyze CpG methylation calls in R (Akalin et al. 2012, R Core Team 2022). We maintained CpG sites in the 'methylRawDB' if there was a coverage count minimum of at least 10, had a maximum cut-off in the 99.9 percentile of read counts covering the site, and was covered in all the samples. We performed principal coordinate analysis (PCoA) using the Bray-Curtis dissimilarity of DNA methylation sites to visualize the relationship between acclimation and heat stress treatment groups. We recalculated the PCoA after removing the following four outliers: 29°C acclimation treatment (Day 11) heat stress sample replicate 1, 29°C acclimation treatment (Day 11) heat stress control replicate 1, 31°C acclimation treatment (Day 11), heat stress treatment replicate 1 and 31°C acclimation treatment (Day 11), heat stress treatment replicate 3.

We assessed the distribution of methylation across CpG sites and genes in our data set. We used methylKit to summarize percent methylation across CpG sites and genes (Akalin et al. 2012). CpG sites were included in the 'methylRawDB' if there was a coverage count minimum of at least 10 and had a maximum cut-off in the 99.9 percentile of read counts covering the site. For the CpG site methylation distribution, we used the methylKit 'unite' function to collate the methylation data and calculate the methylation percentage where the site was covered in at least 3 replicates per treatment from distinct colonies. For the gene-level methylation distribution, we created a GRanges object by importing annotated *A. millepora* gene models furnished with the reference genome (Lawrence et al. 2009; Fuller et al. 2020). Then we used the methylKit 'unite' function to collate the methylation data, integrate the methylation data with the GRanges object, and calculate the methylation percentage where the gene was covered in at least 3 replicates per treatment.

Previous studies have found that environmental shifts can alter global methylation levels (Putnam et al. 2016; Metzger and Schulte 2017). We conducted distinct tests to examine heat stress and acclimation induced effects within our dataset. We combined methylation data across all samples with the methylKit 'unite' function (Lawrence et al. 2009; Akalin et al. 2012; Fuller et al. 2020). We calculated the average percent of methylation at each CpG site covered in at least 3 replicates per treatment across all treatment groups. We excluded missing data from the average methylation percent calculation. We tested the effect of heat stress and acclimation treatments on global CpG methylation percent with an ANOVA. An important caveat is that since we were unable to account for C-to-T substitutions in our data, these substitutions may artificially increase unmethylated calls at CpG sites, potentially resulting in decreased variance in methylation (Supp. Methods). While this artifact could affect baseline methylation levels, it should not impact inferences about differential methylation, though artificial reduction in methylation variance due to C-T polymorphisms could also result in false positives.

We tested whether DNA methylation percent varies between genomic features and if there were feature-specific changes in methylation following acclimation. First, we were interested in the methylation percentage within and between genomic features. We created a GRanges object by importing annotated *A. millepora* exons and introns (Lawrence et al. 2009; Fuller et al. 2020). We created a GRanges object by importing BED files that define predicted coordinates of promoters, transcription start sites (TSS), long interspersed nuclear element (LINE) repeats, short interspersed nuclear element (SINE) repeats, and rolling circle (RC) repeats in the *A. millepora* genome (https://github.com/Groves-Dixon-Matz-laboratory/benchmarking_coral_methylation/tree/master/windowStats) (Dixon and Matz 2021). We integrated the feature-specific GRanges objects with methylation data across all samples and calculated the methylation percentage where the region was covered in at least 3 replicates per treatment with the methylKit 'unite' function (Akalin et al. 2012). We calculated the average percent of methylation at each promoter, TSS, exon, intron, LINE repeat, SINE repeat, and RC repeat across all samples. We excluded

missing data from the average methylation percent calculation. We used an ANOVA followed by a Tukey's HSD test to test whether DNA methylation varies across genomic features.

Next, we investigated gene-level differential methylation due to heat stress. We created a GRanges object by importing annotated *A. millepora* genes and then integrated this object with methylation data across all samples with the methylKit 'unite' function (Lawrence et al. 2009; Akalin et al. 2012; Fuller et al. 2020). We set 'min.per.group' to 3 and performed gene-level differential methylation analysis using methylKit's 'calculateDiffMeth' function to determine genes with different methylation between heat-stressed and control groups (Akalin et al. 2012). The heat assay and control groups were formed by pooling all heat-stress and control samples, respectively, across all acclimation treatment groups: 29°C (Day 0), 31°C (Day 0), 29°C (Day 11), and 31°C (Day 11). We set the minimum percentage change threshold to 25% difference between heat-stressed and control groups. The results were corrected for false discovery rate using a q-value threshold of 0.05. After calculating the change in DNA methylation between heat stress treatments, we analyzed Gene Ontology (GO) terms with the R package, topGO v. 2.50.0 (Alexa and Rahnenfuhrer 2022). We compared differentially methylated genes against a background of all genes that passed our quality filters. Enriched GO terms were identified with the classic Fisher's test with a p-value < 0.01 and at least 10 genes within each category.

We hypothesize that thermal acclimation may lead to changes in DNA methylation, which forms the primary focus of our study. We investigated differences in methylation due to acclimation at the CpG site and gene levels. To capture the effect of thermal acclimation, we formed the acclimation control group by pooling 29°C (Day 11) heat stress treatment and control samples, and we formed the acclimation treatment group by pooling 31°C (Day 11) heat stress treatment and control samples. We used the same filtering criteria as when assaying differences in methylation due to heat stress. After calculating the change in DNA methylation between acclimation and controls, we analyzed GO terms as explained above.

Relationship between gene expression and DNA methylation

First, we tested the relationship between gene expression and average methylation percent within each coding region by performing a linear regression between the $\log_{10}$ transformed means of expression counts and the average percent methylation of genes in all samples. To test this relationship, we used the linear regression function in base R where the base mean of expression for each gene was the response variable and the average percent of gene-level methylation was the predictor variable (R Core Team 2022). We used ANOVA to determine effect strength and significance.

Then, we tested the relationship between heat stress gene expression plasticity and average methylation percent within each coding region. We used R Package DESeq2 v. 1.36.0 to calculate the $\log_2$ fold-change between all heat-stressed and control samples. All heat-stressed and control samples were collated with gene-level methylation percent data. We then performed a linear regression between the gene-level $\log_2$ fold-change standard errors and percent methylation. We used the linear regression function in base R (R Core Team 2022). The standard error was the dependent variable, and the percent methylation was the independent variable. We used ANOVA to determine effect strength and significance.

Relationship between transcriptional response modulation and change in gene level methylation

Our central hypothesis was that shifts in DNA methylation during acclimation result in transcriptional response modulation. In other words, genes with differential methylation between acclimation treatments would be those whose expression response to acute heat stress was either dampened or amplified in 31°C acclimated samples compared to those acclimated at 29°C. We merged acclimation-induced differential methylation data with the analysis of transcriptional response modulation (see above). We collated the measure of transcriptional response modulation–the interaction term coefficient–and difference in methylation percent for each gene. We tested the relationship between transcriptional response modulation and change in the gene-level percent DNA methylation using the linear regression function in

base R, where for each gene, the measure of transcriptional response modulation was the dependent variable and methylation difference was the independent variable (R Core Team 2022). We used ANOVA to determine effect strength and significance. Finally, we tested the difference in average percent methylation of amplified and dampened genes using a two-sample unpaired wilcoxon test.

Results

RNASeq

We aligned RNASeq reads to the *Acropora millepora* reference genome (Fuller et al. 2020). An average of 7.9 million reads (about 56%) of reads uniquely mapped to one locus in each sample. Across all samples, 97,272 reads mapped to symbiodinium ITS2 sequences, with the majority of reads mapping to the *Durusdinium trenchii* ITS2 sequence across all samples (Figure 1.S1).

Gene expression

We performed differential gene expression analysis to identify heat response genes and to quantify transcriptional response modulation associated with acclimation at higher temperatures. After filtering, 27,501 transcripts were included in the analysis. PCA of gene expression data shows clustering based on heat stress treatment along the first PC axis (Figure 1.2 A). While control samples were tightly clustered, there was more variation within heat-stressed samples along PC2. While we did not see clustering in the PCA based on acclimation treatment, all 31°C acclimated heat-stressed samples were among the highest PC2 values, though they overlapped with 29°C acclimated samples. We classified heat response genes by contrasting the control and heat stress sample gene expression. There were 4,714 heat response genes from the 29°C (Day 0) samples, 2,285 heat response genes from the 31°C (Day 0) samples, and 1,368 heat response genes in the 29°C (Day 11) samples. We identified a “core” set of 733 of heat response genes shared across all three contrasts. GO term analysis shows that 98 biological processes GO terms (BP) were enriched in the core set of heat response genes (Table 1.S1). The most significant biological processes were structure and tissue homeostasis and regulation of molecular functions (Table 1.S1). There

were also 9 molecular function (MF), and 6 cellular component (CC) GO terms enriched in this set (Table 1.S1).

To identify transcripts with transcriptional response modulation associated with acclimation, we tested for significant interaction between acclimation and acute treatments affecting expression values between heat stress and acclimation treatment. There were 206 amplified genes and 446 dampened genes, supporting our previous finding that response to heat stress was largely dampened in corals acclimated to higher temperatures (Bay and Palumbi 2015). We found no significant overlap between the core heat response genes and genes with transcriptional response modulation (18 shared genes, chi-square test, p = 0.806). However, we did find a significant overlap between the total set of heat response genes and genes with transcriptional response modulation (299 shared genes, chi-square test, p-value < 7.4e-51). Biological processes GO term associated with metabolic and transcript processing were enriched in the amplified gene set (Table 1.S2). Cellular component GO terms associated with mitochondrial components and cellular membranes were also enriched in the amplified gene set (Table 1.S2). In the dampened gene set, biological processes GO terms associated with DNA replication and metabolism were enriched, indicating these processes are attenuated following thermal acclimation (Table 1.S3). Molecular functions such as ATP-dependent activity, DNA binding, and ion transmembrane transporter activity were also reduced following heat stress due to thermal acclimation (Table 1.S3).

Whole-genome bisulfite sequencing

We performed whole-genome bisulfite sequencing to assay cytosine-guanine dinucleotide (CpG) motif methylation across our samples. After filtering for reads that match our threshold for base call and mapping quality, we had an average of 23,342,870 reads per sample. After depth filtering, there were 544,948 methylation calls from a minimum of 1 sample per treatment group, about 8% of all possible CpG sites. This low percentage is similar to previous reports of genome-wide DNA methylation in coral and other marine invertebrates (Li et al. 2018; Dixon et al. 2018; Ying et al. 2022). Filtering for sites

called in all samples yielded a total of 18,716 CpG sites. We performed PCoA from site calls to assess grouping by treatment. After removing 4 outliers from a preliminary PCoA (Figure 1.S2), we found no discrete clustering between acclimation or heat assay treatment groups (Figure 1.2 B). Removal of outliers was limited to visualization in Figure 1.2 B, and all samples were included in the remainder of the analyses. Next, we summarized DNA methylation across CpG sites and genes in this dataset. There is a bimodal distribution of the CpG sites, but we do not see a bimodal distribution at the gene level (Figures 1.S3 A and 1.S3 B). Previous studies report DNA methylation differences between genomic and intragenic features in corals, so we compared the average DNA methylation across these features in our data (Liew et al. 2018; Dixon and Matz 2021; Rodriguez-Casariego et al. 2022; Ying et al. 2022). We find that promoters and exons are hypomethylated relative to introns, LINE repeats, and RC repeats, aligning with previous studies (Figure 1.S3 C, Tukey HSD p-val < 0.0001) (Liew et al. 2018; Dixon and Matz 2021; Rodriguez-Casariego et al. 2022; Ying et al. 2022, but see Li et al. 2018 for DNA methylation of introns and exons in *Exaiptasia pallida*).

We tested global site and gene level changes in percent methylation following heat stress. At the global level, heat stress did not lead to changes in DNA methylation between samples (ANOVA, $F = 0.7925$, $p = 0.378$). However, we did find that heat stress did lead to differential methylation in 451 genes out of a total of 16,531 genes. A total of 205 genes were hypermethylated (≥ 25% increase), and 246 genes were hypomethylated (≥ 25% decrease), with significance determined by an FDR-adjusted q-value of ≤0.05. Five GO terms were enriched in this gene set, and most of these genes code for cellular components associated with intracellular structure and membrane-bound organelles (Table 1.S4).

We tested global site and gene level changes in percent methylation following acclimation. Acclimation did not lead to global changes in CpG methylation (ANOVA, $F = 0.6355$, $p = 0.4339$). We identified genes with differential methylation between 31°C Day 11 acclimated samples and 29°C Day 11

acclimation control samples. There were 416 differentially methylated genes out of the 15,837 genes where methylation could be summarized in at least 3 samples per treatment group. A total of 205 genes were hypermethylated, while 211 genes were hypomethylated. Two GO terms were enriched in this set of genes: GTPase activity (MF) and GTP binding (MF). GTPases are a protein superfamily associated with many essential cellular pathways in eukaryotes. Finally, there was significant overlap with genes that are differentially methylated following acclimation and heat stress (40 shared genes, chi-square test, p-value = 4.02e-12), indicating that thermal treatments largely lead to unique methylation signatures.

Relationship between gene expression and DNA methylation

We combined gene expression and DNA methylation datasets to examine the potential effects of DNA methylation on gene expression and transcriptional response modulation. There is a small effect but a significant relationship between baseline gene expression and gene-level baseline DNA methylation (r^2 = 0.033, $p < 2e-16$) (Figure 1.S4 A). This finding aligns with previous studies on gene expression and methylation in metazoans (Dixon and Matz 2022). We also saw a small negative correlation between DNA methylation percent and the standard error of the log2 fold change of heat stress gene expression, a measure that captures variation due to gene expression plasticity and transcriptional noise ($r^2 = 0.025$, $p < 2e-16$) (Figure 1.S4 B). Together, these results suggest that gene body methylation contributes to preserving baseline gene expression levels and defining the magnitude of gene expression variation. These patterns also explain differences in methylation and expression in genes with transcriptional response modulation. Overall, amplified genes exhibited higher DNA methylation levels compared to dampened genes (Figure 1.3 A) ($p < 0.001$) and displayed higher overall expression levels than dampened genes ($p < 0.0001$) (Figure 1.3 B).

We were able to investigate the effect of heat stress on DNA methylation independently of the effect of thermal acclimation. Genes that exhibited a shift in methylation in response to heat stress were not the same as the genes within the total set of heat response genes as there was no significant overlap between

the expression of the total set of heat stress response genes and differentially methylated genes following heat stress (101 shared genes, chi-square test, p-value = 0.170). This demonstrates the complexity of the molecular response induced by heat stress processes.

Our primary hypothesis for this study was that transcriptional response modulation was facilitated by shifts in DNA methylation following acclimation within the same genes (Figure 1.1 C). We found no relationship between transcriptional response modulation and differential methylation based on acclimation treatment (Figure 1.3 C). This is supported by the fact that neither amplified nor dampened genes exhibit broad significant changes in DNA methylation as a result of thermal acclimation treatment (Figure 1.S5). However, we did find a larger-than-expected overlap between dampened genes and acclimation-induced differentially methylated genes (14 shared genes, chi-square test, $p = 0.009$), perhaps suggesting that a subset of differentially methylated genes is also associated with transcriptional response modulation. On the other hand, there was no significant overlap between dampened genes and heat-stressed induced differentially methylated genes (9 shared genes, chi-square test, $p = 0.4470$). Moreover, the lack of overlap between amplified genes and differentially methylated genes after thermal acclimation (3 shared genes, chi-square test, $p = 1$) or heat stress (5 shared genes, chi-square test, $p = 0.3930$) provides evidence for a distinct association between specific dampened genes and acclimation-induced differential methylation. These findings further support the notion that gene body methylation plays a role in maintaining gene expression. However, despite overall correlations between expression, expression plasticity, and methylation, we did not find that short-term transcriptional modulation is associated with shifts in methylation. Instead, amplified and dampened genes resist methylation changes despite the dynamic methylation patterns observed during acute heat stress and thermal acclimation. While we cannot rule out the possibility that methylation changes may be occurring in large-effect upstream genes (see Supplementary materials for details on network analysis, Figure 1.S6), collectively, these results indicate that alterations in gene body methylation are not universally synchronizing the modulation of transcriptional response that we observe.

Discussion

Acclimation, a form of adaptive phenotypic plasticity, enables organisms to adjust their physiology to survive environmental fluctuations that may be otherwise lethal. Previous studies have shown that acclimation can be associated with shifts in the magnitude of gene expression response to a stressor, in other words, a shift in gene expression plasticity (here referred to as "transcriptional response modulation") (Bay and Palumbi 2015). However, the mechanisms preserving the memory of past environmental exposure and mediating gene expression plasticity remain to be resolved in many ecologically relevant species. Here, in the coral *Acropora nana,* we document differential methylation and differences in heat stress-induced gene expression plasticity between corals acclimated to different temperatures. We find no overall relationship between differential DNA methylation and shifts in gene expression plasticity at the gene level. Interestingly, a small number of genes exhibit both a shift in gene expression plasticity and a shift in methylation level. This observation leads us to propose that DNA methylation shifts are not a general mechanism for controlling short-term changes in plasticity but may be significant for specific genes. Future studies should focus on alternative mechanisms controlling gene expression plasticity during acclimation.

Gene expression plasticity is critical for homeostasis (Rivera et al. 2021). In a previous study using our same samples, Bay and Palumbi (2015) found transcriptional dampening–the reduction of gene expression plasticity in response to heat stress–in corals more resistant to bleaching due to acclimation at higher temperatures. Our reanalysis replicates these results, finding 446 genes have dampened expression due to the interaction of thermal pre-conditioning and heat stress. We also identify 206 genes with amplified expression, where the magnitude of gene expression response to heat stress is greater in corals acclimated to higher temperatures. GO term enrichment of amplified genes includes metabolic and transcript processing, mitochondrial components, and cellular membranes. Meanwhile, GO term enrichment of dampened genes is enriched for DNA replication and metabolism. The enrichment of GO

terms in amplified and dampened genes suggests that corals acclimated to higher temperatures may optimize gene expression to enhance stress-response pathways and diminish growth pathway gene expression following thermal acclimation (López-Maury et al. 2008, Table 1.S2 and Table 1.S3).

Timescales of molecular responses to environmental change

In ecological systems, an emerging hypothesis is that DNA methylation mediates adaptive phenotypic plasticity by fluctuating in response to environmental cues and interacting with chromatin-modifying proteins and transcription complexes resulting in altered gene expression (Eirin-Lopez and Putnam 2019; Vogt 2022). Following thermal acclimation, we identified differential methylation within 416 gene bodies relative to the non-acclimated samples. This aligns with previous studies finding DNA methylation shifts are associated with various environmental variables, a key aspect of a plasticity mediating mechanism (Putnam et al. 2016; Crisp et al. 2016; Metzger and Schulte 2017; Dixon et al. 2018; Liew et al. 2018; Eirin-Lopez and Putnam 2019; Dimond and Roberts 2020). In the vertebrate ecological model, threespine stickleback, DNA methylation variation was reported between cohorts of individuals raised in different temperatures, and DNA methylation changed in adults acclimated to different temperatures (Metzger and Schulte 2017). Recent studies in diverse coral genera reported DNA methylation changes in response to pH, symbiont associations, nutrient stress, and transplantation to novel environments (Putnam et al. 2016; Rodriguez-Casariego et al. 2018; Dixon et al. 2018; Liew et al. 2018; Dimond and Roberts 2020; Rodriguez-Casariego et al. 2021). After a 6-week exposure to acidic conditions, the global methylation percentage doubled in the environmentally sensitive coral species *Pocillopora damicornis* compared to control samples (Putnam et al. 2016). The shift in global DNA methylation brought the methylation percent to a similar level as the more environmentally robust species, *Montipora captitata* (Putnam et al. 2016). In another pH acclimation investigation where *Stylophora pistillata* coral replicates were kept in four pH environments for two years, changes in DNA methylation due to pH occurred in genes associated with growth and stress response processes (Liew et al. 2018). Together these studies suggest that shifts in methylation can be environmentally induced within the lifetime of an organism. Notably, our experiment

was much shorter than previous studies. In this timeframe, we do not observe global shifts in CpG methylation following thermal acclimation (Figure 1.2 B). Instead, we see localized methylation dynamics following the 11-day thermal acclimation, suggesting that on this timescale, shifts in methylation may be more finely controlled.

Timescales of DNA methylation and gene expression shifts may impact buffering against short-term fluctuations. In many systems, we know little about how quickly methyl groups can be added or removed from DNA. Our experiment explores two timescales: an 11-day acclimation and a 24-hour acute stress. Both are quite a bit shorter than many previous investigations. Within other non-model systems, environmental effects of the methylome have been reported within 48-72 hours of environmental stressors during development (Strader et al., 2020; Jones and Griffitt, 2022). Building on findings regarding DNA dynamics after brief stressor exposure, our study revealed that a 24-hour acute thermal stress induced differential expression of 5,531 genes and methylation changes in 451 genes. The 11-day thermal acclimation treatment led to changes in DNA methylation in 416 genes and transcriptional response modulation in 652 genes. DNA methylation can spontaneously occur thus variation can be driven by noise, interfering with the detection of a biological signal between DNA methylation and gene expression (Sanchez and Mackenzie, 2023). However, thermal acclimation and the acute heat stress treatment resulted in both hypermethylation and hypomethylation, indicating the addition and removal of methyl groups presumably by methylation machinery. Previous reports of gene body methylation in marine invertebrates indicate that detectable differences can accrue in a few months. For example, Strader et al. (2020) show that female purple sea urchins conditioned to different abiotic treatments for four months produced larvae with differential methylation in 684 genes. In another study, Dixon and colleagues report that highly methylated genes became less methylated, and lowly methylated genes became more methylated in *Acropora millepora* three months after transplant (Dixon et al. 2018). Other studies investigating temporal DNA methylation dynamics occur over seasonal timescales where seasonal methylation changes have been reported in gene promoters associated with phenological traits. For

example, changes in promoter methylation of transcriptional regulator genes have been identified in the great tit (*Parus major*), which covaries with female reproductive timing (Lindner et al. 2021). However, seasonal stability of gene body methylation across a year was observed in *Arabidopsis halleri* and was associated with stable gene expression (Ito et al. 2019). In the context of previous studies, our study suggests that changes in methylation can occur quite rapidly (within one day), suggesting it may contribute to short-term buffering against rapid environmental fluctuations.

Relationship between gene-level methylation and gene expression plasticity

We find that methylation is associated with the baseline gene expression level and variation across samples but shifts in methylation do not necessarily affect gene expression plasticity. Previous studies have documented the correlation between gene body methylation and expression across other invertebrate species (Gatzmann et al. 2018; Dixon and Matz 2022). Additionally, the baseline methylation level is known to be associated with the degree of gene expression plasticity; housekeeping genes have higher methylation levels than environmentally-inducible genes (Sarda et al. 2012; Dixon et al. 2014; Dimond and Roberts 2016; Gatzmann et al. 2018). We also see this association between baseline methylation and gene expression plasticity–expression is more variable in genes with lower methylation levels. A potential limitation in our results is in our inability to account for C-to-T substitutions between the reference species, *Acropora millepora*, and *Acropora nana*. Still, our results support the same relationships between methylation, baseline gene expression, and expression variation.

Despite the seemingly stable association between methylation and gene expression, we do not find strong evidence that shifts in methylation drive the transcriptional response modulation (Figure 1.3 C); genes with the biggest change in expression magnitude do not show significant changes in DNA methylation. Congruently, the genes with the largest change in DNA methylation following thermal acclimation do not demonstrate a shift in expression magnitude during the thermal challenge. Our findings align with those of Abbott and colleagues, who conducted an independent study on *Acropora millepora*. In their three-

week thermal acclimation experiment, which involved switching coral fragments from elevated thermal exposure to the control thermal environment at two sampling timepoints, they observed no association between shifts in gene body methylation and either reversible or irreversible shifts in gene expression (Abbott et al. 2024). Furthermore, there were no associations with shifts in the magnitude of gene expression changes (Abbott et al. 2024). Perhaps the general absence of shifts in methylation in genes showing altered plasticity indicates that significant changes in gene body methylation are suppressed in transcriptionally modified coral heat response genes (Muyle et al. 2021; Takuno et al. 2017).

The results also beg the question of whether the acclimation-induced shifts in methylation have a functional outcome and what that may be. One possibility is that there are trans-acting effects on gene expression, for example, if acclimation induces methylation in transcription factors (Moore et al. 2013; Anastasiadi et al. 2018; Lindner et al. 2020). Indeed, while we did not find an overall correlation between shifts in methylation and transcriptional response modulation, we did find a small but significant number of genes that exhibited shifts in both methylation and gene expression plasticity, providing candidates for future inquiry. While we find no overall relationship between differential DNA methylation and shifts in gene expression plasticity at the gene level, our gene-level approach limits our ability to identify the putative role of DNA methylation changes in genes with cascading effects in corals (Gomez-Campo et al. 2023). Another hypothesis is that DNA methylation shifts could follow changes in expression (Li et al 2018). This hypothesis is supported by the bimodal DNA methylation in housekeeping and environmentally responsive genes (Sarda et al. 2012; Dixon et al. 2014; Dimond and Roberts 2016; Gatzmann et al. 2018). Although we do not observe a change in gene expression during the acclimation treatment, it is possible that our sample timing does not capture a change in gene expression during the acclimation period. Another reason why we might not observe a change in the expression of genes with altered DNA methylation following acclimation is that DNA methylation changes are necessary to stabilize gene expression in altered environments (i.e., transcriptional homeostasis) (Li et al 2018). Since thermal acclimation results from multiple processes that functionally coalesce to shift the baseline

temperature at which homeostasis is maintained, it makes sense that acclimation-induced methylation changes would act to maintain transcriptional homeostasis during subsequent heat stress.

Opposing directions of gene expression plasticity suggest multiple mechanisms

Independent mechanisms operate separately on gene expression and gene expression plasticity across multiple metazoan species, as indicated by the poor correlation between gene expression and plasticity (Xiao et al. 2019). Gene expression is determined by many mechanisms, for example, transcription factor binding, eQTLs, and 3D chromatin organization (López-Maury et al. 2008). Meta-analyses of various metazoan species performed by Xiao and colleagues find that cis-elements and trans-acting factors promote gene expression plasticity, while epigenetic histone modifications–H3K36me3, H3K79me2 and H4K20me1–inhibit plasticity (Xiao et al. 2019). Here, we identify two modes of transcriptional response modulation: amplified and dampened expression plasticity. There is a relationship between the directionality of gene expression plasticity, gene body methylation, and overall expression (Figures 1.3 B and 1.3 C); amplified genes have higher overall expression and DNA methylation than dampened genes. The directional changes in expression plasticity, considered with gene body methylation level, may convey that distinct mechanisms are either increasing or decreasing expression plasticity, and the exact mechanism of plasticity mode may be particular to the genetic network (Herman and Sultan 2011). However, these two modes may not necessarily be acting independently as a small number of genes can largely influence gene expression plasticity (Schlichting and Smith 2002; López-Maury et al. 2008).

The relationship between amplified and dampened gene expression plasticity and DNA methylation might be explained by methylation interactions with other mechanisms that cause variation in gene expression. For example, Li and colleagues demonstrate the interaction between DNA methylation and epigenetic histone mark, histone 3 lysine 36 trimethylation (H3K36me3) in Aiptasia (Li et al. 2018). Typically found in gene bodies, this histone mark recruits DNA methyltransferase, which methylates cytosine nucleotides (Li et al. 2018; Weinberg et al. 2019). Li et al. found that DNA methylation was associated with a

reduction in transcriptional noise–an expression variation distinct from transcriptional plasticity–where methyl groups potentially inhibit access to cryptic promoters and affect the binding affinity of transcription factors (Li et al. 2018; Héberlé and Bardet 2019). Methylation-sensitive transcription factors have been identified across many phyla, indicating that interactions between DNA methylation and trans-acting factors may be conserved, yet, these remain to be identified in coral species (de Mendoza et al. 2019). Elucidating the relationship between amplified and dampened plasticity and DNA methylation will be an exciting direction for future research.

Conclusion

Prior to our study, gene body methylation was a compelling candidate for establishing a cellular memory of past environmental exposure to influence gene expression plasticity. DNA methylation is a labile chemical mark that can change based on the environment experienced by the organism (Eirin-Lopez and Putnam 2019). It is stable yet reversible, and environmentally responsive genes tend to have lower methylation than housekeeping genes (Gatzmann et al. 2018; Dixon and Matz 2022). Depending on the genomic context, this simple chemical mark is associated with different expression effects. Recent reports indicate that various phyla show no relationship between genome-wide changes in DNA methylation and change in gene expression plasticity (Bogan and Yi 2024, Dixon and Matz 2022, Duncan et al. 2022). Our study, along with the recent paper by Abbott and colleagues (Abbott et al. 2024), suggests that, more generally, cis-acting differential methylation of gene bodies is not directly responsible for shifts in gene expression plasticity. Our results and other reports of gene body methylation function suggest that the relationship between gene body methylation and gene expression is complex and may depend on gene-specific cis- and trans-factors and other epigenetics layers. Developing a more thorough understanding of the links between gene expression and epigenetic layers will further our understanding of ecologically important forms of phenotypic plasticity, including potential rates and limits to acclimation in the face of rising temperatures.

References

Abbott, E., Loockerman, C., & Matz, M. V. (2024). Modifications to gene body methylation do not alter gene expression plasticity in a reef-building coral. *Evolutionary Applications*, *17*(2), e13662.

Agrawal, A. A. (2001). Phenotypic plasticity in the interactions and evolution of species. *Science*, *294*(5541), 321–326.

Akalin, A., Kormaksson, M., Li, S., Garrett-Bakelman, F. E., Figueroa, M. E., Melnick, A., & Mason, C. E. (2012). methylKit: a comprehensive R package for the analysis of genome-wide DNA methylation profiles. *Genome Biology*, *13*(10), R87.

Alexa A, Rahnenfuhrer J (2023). topGO: Enrichment Analysis for Gene Ontology. R package version 2.52.0.

Amoah, J. N., Ko, C. S., Yoon, J. S., & Weon, S. Y. (2019). Effect of drought acclimation on oxidative stress and transcript expression in wheat (Triticum aestivum L.). *Journal of Plant Interactions*, *14*(1), 492–505.

Anastasiadi, D., Esteve-Codina, A., & Piferrer, F. (2018). Consistent inverse correlation between DNA methylation of the first intron and gene expression across tissues and species. *Epigenetics & Chromatin*, *11*(1). https://doi.org/10.1186/s13072-018-0205-1

Anders, S., Pyl, P. T., & Huber, W. (2015). HTSeq--a Python framework to work with high-throughput sequencing data. *Bioinformatics*, *31*(2), 166–169.

Barshis, D. J., Ladner, J. T., Oliver, T. A., Seneca, F. O., Traylor-Knowles, N., & Palumbi, S. R. (2013). Genomic basis for coral resilience to climate change. *Proceedings of the National Academy of Sciences of the United States of America*, *110*(4), 1387–1392.

Bay, R. A., & Palumbi, S. R. (2015). Rapid Acclimation Ability Mediated by Transcriptome Changes in Reef-Building Corals. *Genome Biology and Evolution*, *7*(6), 1602–1612.

Bellantuono, A. J., Granados-Cifuentes, C., Miller, D. J., Hoegh-Guldberg, O., & Rodriguez-Lanetty, M. (2012). Coral thermal tolerance: tuning gene expression to resist thermal stress. *PloS One*, *7*(11), e50685.

Bewick, A. J., Ji, L., Niederhuth, C. E., Willing, E.-M., Hofmeister, B. T., Shi, X., Wang, L., Lu, Z., Rohr, N. A., Hartwig, B., Kiefer, C., Deal, R. B., Schmutz, J., Grimwood, J., Stroud, H., Jacobsen, S. E., Schneeberger, K., Zhang, X., & Schmitz, R. J. (2016). On the origin and evolutionary consequences of gene body DNA methylation. *Proceedings of the National Academy of Sciences of the United States of America*, *113*(32), 9111–9116.

Bewick, A. J., Zhang, Y., Wendte, J. M., Zhang, X., & Schmitz, R. J. (2019). Evolutionary and experimental loss of gene body methylation and its consequence to gene expression. *G3* , *9*(8), 2441–2445.

BioProject. (n.d.). [dataset]. Retrieved June 20, 2024, from https://www.ncbi.nlm.nih.gov/bioproject/PRJNA1074434

Bogan, S. N., & Yi, S. V. (2024). Potential Role of DNA Methylation as a Driver of Plastic Responses to the Environment Across Cells, Organisms, and Populations. *Genome Biology and Evolution*, *16*(2). https://doi.org/10.1093/gbe/evae022

Bonamour, S., Chevin, L.-M., Charmantier, A., & Teplitsky, C. (2019). Phenotypic plasticity in response to climate change: the importance of cue variation. *Philosophical Transactions of the Royal Society of London. Series B, Biological Sciences*, *374*(1768), 20180178.

Crisp, P. A., Ganguly, D., Eichten, S. R., Borevitz, J. O., & Pogson, B. J. (2016). Reconsidering plant memory: Intersections between stress recovery, RNA turnover, and epigenetics. *Science Advances*, *2*(2), e1501340.

Dayan, D. I., Crawford, D. L., & Oleksiak, M. F. (2015). Phenotypic plasticity in gene expression contributes to divergence of locally adapted populations of Fundulus heteroclitus. *Molecular Ecology*, *24*(13), 3345–3359.

de Mendoza, A., Hatleberg, W. L., Pang, K., Leininger, S., Bogdanovic, O., Pflueger, J., Buckberry, S., Technau, U., Hejnol, A., Adamska, M., Degnan, B. M., Degnan, S. M., & Lister, R. (2019). Convergent evolution of a vertebrate-like methylome in a marine sponge. *Nature Ecology & Evolution*, *3*(10), 1464–1473.

DeBiasse, M. B., & Kelly, M. W. (2016). Plastic and Evolved Responses to Global Change: What Can We Learn from Comparative Transcriptomics? *The Journal of Heredity*, *107*(1), 71–81.

Dimond, J. L., & Roberts, S. B. (2016). Germline DNA methylation in reef corals: patterns and potential roles in response to environmental change. *Molecular Ecology*, *25*(8), 1895–1904.

Dimond, J. L., & Roberts, S. B. (2020). Convergence of DNA Methylation Profiles of the Reef Coral Porites astreoides in a Novel Environment. *Frontiers in Marine Science*, *6*, 792.

Dingemanse, N. J., & Wolf, M. (2013). Between-individual differences in behavioural plasticity within populations: causes and consequences. *Animal Behaviour*, *85*(5), 1031–1039.

Dixon, G. B., Bay, L. K., & Matz, M. V. (2014). Bimodal signatures of germline methylation are linked with gene expression plasticity in the coral Acropora millepora. *BMC Genomics*, *15*, 1109.

Dixon, G., Liao, Y., Bay, L. K., & Matz, M. V. (2018). Role of gene body methylation in acclimatization and adaptation in a basal metazoan. *Proceedings of the National Academy of Sciences of the United States of America*, *115*(52), 13342–13346.

Dixon, G., & Matz, M. (2021). Benchmarking DNA methylation assays in a reef-building coral. *Molecular Ecology Resources*, *21*(2), 464–477.

Dixon, G., & Matz, M. (2022). Changes in gene body methylation do not correlate with changes in gene expression in Anthozoa or Hexapoda. *BMC Genomics*, *23*(1), 234.

Dobin, A., Davis, C. A., Schlesinger, F., Drenkow, J., Zaleski, C., Jha, S., Batut, P., Chaisson, M., & Gingeras, T. R. (2013). STAR: ultrafast universal RNA-seq aligner. *Bioinformatics* , *29*(1), 15–21.

Duncan, E. J., Cunningham, C. B., & Dearden, P. K. (2022). Phenotypic Plasticity: What Has DNA Methylation Got to Do with It? *Insects*, *13*(2). https://doi.org/10.3390/insects13020110

Eirin-Lopez, J. M., & Putnam, H. M. (2019). Marine Environmental Epigenetics. *Annual Review of Marine Science*, *11*, 335–368.

Entrambasaguas, L., Ruocco, M., Verhoeven, K. J. F., Procaccini, G., & Marín-Guirao, L. (2021). Gene body DNA methylation in seagrasses: inter- and intraspecific differences and interaction with transcriptome plasticity under heat stress. *Scientific Reports*, *11*(1), 14343.

Fuller, Z. L., Mocellin, V. J. L., Morris, L. A., Cantin, N., Shepherd, J., Sarre, L., Peng, J., Liao, Y., Pickrell, J., Andolfatto, P., Matz, M., Bay, L. K., & Przeworski, M. (2020). Population genetics of the coral *Acropora millepora*: Toward genomic prediction of bleaching. *Science*, *369*(6501). https://doi.org/10.1126/science.aba4674

Gatzmann, F., Falckenhayn, C., Gutekunst, J., Hanna, K., Raddatz, G., Carneiro, V. C., & Lyko, F. (2018). The methylome of the marbled crayfish links gene body methylation to stable expression of poorly accessible genes. *Epigenetics & Chromatin*, *11*(1), 57.

Ghalambor, C. K., Angeloni, L. M., Carroll, S. P., Fox, C. W., & Westneat, D. F. (2010). *Evolutionary behavioral ecology*. Oxford University Press.

Ghalambor, C. K., McKAY, J. K., Carroll, S. P., & Reznick, D. N. (2007). Adaptive versus non-adaptive phenotypic plasticity and the potential for contemporary adaptation in new environments. *Functional Ecology*, *21*(3), 394–407.

Gibbons, T. C., Metzger, D. C. H., Healy, T. M., & Schulte, P. M. (2017). Gene expression plasticity in response to salinity acclimation in threespine stickleback ecotypes from different salinity habitats. *Molecular Ecology*, *26*(10), 2711–2725.

Gienapp, P., Teplitsky, C., Alho, J. S., Mills, J. A., & Merilä, J. (2008). Climate change and evolution: disentangling environmental and genetic responses. *Molecular Ecology*, *17*(1), 167–178.

Gleason, L. U., & Burton, R. S. (2015). RNA-seq reveals regional differences in transcriptome response to heat stress in the marine snail Chlorostoma funebralis. *Molecular Ecology*, *24*(3), 610–627.

Gomez-Campo, K., Sanchez, R., Martinez-Rugerio, I., Yang, X., Maher, T., Osborne, C. C., Enriquez, S., Baums, I. B., Mackenzie, S. A., & Iglesias-Prieto, R. (2023). Phenotypic plasticity for improved light harvesting, in tandem with methylome repatterning in reef-building corals. *Molecular Ecology*, e17246.

Gotthard, K., & Nylin, S. (1995). Adaptive Plasticity and Plasticity as an Adaptation: A Selective Review of Plasticity in Animal Morphology and Life History. *Oikos*, *74*(1), 3–17.

Guerrero, L., & Bay, R. (2024). Patterns of methylation and transcriptional plasticity during thermal acclimation in a reef-building coral [Dataset]. Dryad. https://doi.org/10.5061/dryad.76hdr7t3q

Gunderson, A. R., & Stillman, J. H. (2015). Plasticity in thermal tolerance has limited potential to buffer ectotherms from global warming. *Proceedings. Biological Sciences / The Royal Society*, *282*(1808), 20150401.

Hackerott, S., Martell, H. A., & Eirin-Lopez, J. M. (2021). Coral environmental memory: causes, mechanisms, and consequences for future reefs. *Trends in Ecology & Evolution*, *36*(11), 1011–1023.

Hamdoun, A. M., Cheney, D. P., & Cherr, G. N. (2003). Phenotypic plasticity of HSP70 and HSP70 gene expression in the Pacific oyster (Crassostrea gigas): implications for thermal limits and induction of thermal tolerance. *The Biological Bulletin*, *205*(2), 160–169.

He, C., Zhang, Z., Li, B., & Tian, S. (2020). The Pattern and Function of DNA Methylation in Fungal Plant Pathogens. *Microorganisms*, *8*(2). https://doi.org/10.3390/microorganisms8020227

Héberlé, É., & Bardet, A. F. (2019). Sensitivity of transcription factors to DNA methylation. *Essays in Biochemistry*, *63*(6), 727–741.

Herman, J. J., & Sultan, S. E. (2011). Adaptive transgenerational plasticity in plants: case studies, mechanisms, and implications for natural populations. *Frontiers in Plant Science*, *2*, 102.

Holliday, R., & Pugh, J. E. (1975). DNA modification mechanisms and gene activity during development. *Science*, *187*(4173), 226–232.

Ito, T., Nishio, H., Tarutani, Y., Emura, N., Honjo, M. N., Toyoda, A., Fujiyama, A., Kakutani, T., & Kudoh, H. (2019). Seasonal Stability and Dynamics of DNA Methylation in Plants in a Natural Environment. *Genes*, *10*(7). https://doi.org/10.3390/genes10070544

Johnson, K. M., Sirovy, K. A., & Kelly, M. W. (2021). Differential DNA methylation across environments has no effect on gene expression in the eastern oyster. *The Journal of Animal Ecology*. https://doi.org/10.1111/1365-2656.13645

Jones, P. A. (2012). Functions of DNA methylation: islands, start sites, gene bodies and beyond. *Nature Reviews. Genetics*, *13*(7), 484–492.

Kelly, M. (2019). Adaptation to climate change through genetic accommodation and assimilation of plastic phenotypes. *Philosophical Transactions of the Royal Society of London. Series B, Biological Sciences*, *374*(1768), 20180176.

Kenkel, C. D., & Matz, M. V. (2016). Gene expression plasticity as a mechanism of coral adaptation to a variable environment. *Nature Ecology & Evolution*, *1*(1), 14.

Krueger, F. (n.d.). *TrimGalore: A wrapper around Cutadapt and FastQC to consistently apply adapter and quality trimming to FastQ files, with extra functionality for RRBS data*. Github. Retrieved April 20, 2023, from https://github.com/FelixKrueger/TrimGalore

LaJeunesse, T. C. (2001). Investigating the biodiversity, ecology, and phylogeny of endosymbiotic dinoflagellates in the genus *symbiodinium* using the ITS region: in search of a "species" level marker. *Journal of Phycology*, *37*(5), 866–880.

LaSalle, J. M., Powell, W. T., & Yasui, D. H. (2013). Epigenetic layers and players underlying neurodevelopment. *Trends in Neurosciences*, *36*(8), 460–470.

Lawrence, M., Gentleman, R., & Carey, V. (2009). rtracklayer: an R package for interfacing with genome browsers. *Bioinformatics* , *25*(14), 1841–1842.

Li, H., Handsaker, B., Wysoker, A., Fennell, T., Ruan, J., Homer, N., Marth, G., Abecasis, G., Durbin, R., & 1000 Genome Project Data Processing Subgroup. (2009). The Sequence Alignment/Map format and SAMtools. *Bioinformatics* , *25*(16), 2078–2079.

Li, Y., Liew, Y. J., Cui, G., Cziesielski, M. J., Zahran, N., Michell, C. T., Voolstra, C. R., & Aranda, M. (2018). DNA methylation regulates transcriptional homeostasis of algal endosymbiosis in the coral model Aiptasia. *Science Advances*, *4*(8), eaat2142.

Liew, Y. J., Zoccola, D., Li, Y., Tambutté, E., Venn, A. A., Michell, C. T., Cui, G., Deutekom, E. S., Kaandorp, J. A., Voolstra, C. R., Forêt, S., Allemand, D., Tambutté, S., & Aranda, M. (2018). Epigenome-associated phenotypic acclimatization to ocean acidification in a reef-building coral. *Science Advances*, *4*(6), eaar8028.

Lindner, M., Laine, V. N., Verhagen, I., Viitaniemi, H. M., Visser, M. E., van Oers, K., & Husby, A. (2021). Rapid changes in DNA methylation associated with the initiation of reproduction in a small songbird. *Molecular Ecology*, *30*(15), 3645–3659.

Logan, M. L., & Cox, C. L. (2020). Genetic Constraints, Transcriptome Plasticity, and the Evolutionary Response to Climate Change. *Frontiers in Genetics*, *11*, 538226.

López-Maury, L., Marguerat, S., & Bähler, J. (2008). Tuning gene expression to changing environments: from rapid responses to evolutionary adaptation. *Nature Reviews. Genetics*, *9*(8), 583–593.

Love, M. I., Huber, W., & Anders, S. (2014). Moderated estimation of fold change and dispersion for RNA-seq data with DESeq2. *Genome Biology*, *15*(12), 550.

Mallard, F., Nolte, V., & Schlötterer, C. (2020). The Evolution of Phenotypic Plasticity in Response to Temperature Stress. *Genome Biology and Evolution*, *12*(12), 2429–2440.

Merilä, Juha, and Andrew P. Hendry. 2014. “Climate Change, Adaptation, and Phenotypic Plasticity: The Problem and the Evidence.” *Evolutionary Applications* 7 (1): 1–14.

Metzger, D. C. H., & Schulte, P. M. (2017). Persistent and plastic effects of temperature on DNA methylation across the genome of threespine stickleback (Gasterosteus aculeatus). *Proceedings. Biological Sciences / The Royal Society*, *284*(1864). https://doi.org/10.1098/rspb.2017.1667

Middlebrook, R., Hoegh-Guldberg, O., & Leggat, W. (2008). The effect of thermal history on the susceptibility of reef-building corals to thermal stress. *The Journal of Experimental Biology*, *211*(Pt 7), 1050–1056.

Mihirogi, Y., Kaneda, M., Yamagishi, D., Ishii, Y., Maruyama, S., Nakamura, S., Shimoyama, N., Oohori, C., & Hatta, M. (2023). Establishment of a New Model Sea Anemone for Comparative Studies on Cnidarian-Algal Symbiosis. *Zoological Science*, *40*(3), 235–245.

Moore, L. D., Le, T., & Fan, G. (2013). DNA methylation and its basic function. *Neuropsychopharmacology: Official Publication of the American College of Neuropsychopharmacology*, *38*(1), 23–38.

Muyle, A., & Gaut, B. S. (2019). Loss of Gene Body Methylation in Eutrema salsugineum Is Associated with Reduced Gene Expression. *Molecular Biology and Evolution*, *36*(1), 155–158.

Muyle, A. M., Seymour, D. K., Lv, Y., Huettel, B., & Gaut, B. S. (2022). Gene Body Methylation in Plants: Mechanisms, Functions, and Important Implications for Understanding Evolutionary Processes. *Genome Biology and Evolution*, *14*(4). https://doi.org/10.1093/gbe/evac038

Muyle, A., Ross-Ibarra, J., Seymour, D. K., & Gaut, B. S. (2021). Gene body methylation is under selection in Arabidopsis thaliana. *Genetics*, *218*(2). https://doi.org/10.1093/genetics/iyab061

Okano, M., Bell, D. W., Haber, D. A., & Li, E. (1999). DNA methyltransferases Dnmt3a and Dnmt3b are essential for de novo methylation and mammalian development. *Cell*, *99*(3), 247–257.

Pedersen, B. S., Eyring, K., De, S., Yang, I. V., & Schwartz, D. A. (2014). Fast and accurate alignment of long bisulfite-seq reads. In *arXiv [q-bio.GN]*. arXiv. http://arxiv.org/abs/1401.1129

Picard. (n.d.). Retrieved April 20, 2023, from http://broadinstitute.github.io/picard/

Putnam, H. M., Davidson, J. M., & Gates, R. D. (2016). Ocean acidification influences host DNA methylation and phenotypic plasticity in environmentally susceptible corals. *Evolutionary Applications*, *9*(9), 1165–1178.

R Core Team (2022). R: A language and environment for statistical computing. R Foundation for Statistical Computing, Vienna, Austria. https://www.R-project.org/.

Ritchie, R. J. (2008). Universal chlorophyll equations for estimating chlorophylls a, b, c, and d and total chlorophylls in natural assemblages of photosynthetic organisms using acetone, methanol, or ethanol solvents. *Photosynthetica*, *46*(1), 115–126.

Rivera, H. E., Aichelman, H. E., Fifer, J. E., Kriefall, N. G., Wuitchik, D. M., Wuitchik, S. J. S., & Davies, S. W. (2021). A framework for understanding gene expression plasticity and its influence on stress tolerance. *Molecular Ecology*, *30*(6), 1381–1397.

Rodriguez-Casariego, J. A., Cunning, R., Baker, A. C., & Eirin-Lopez, J. M. (2022). Symbiont shuffling induces differential DNA methylation responses to thermal stress in the coral Montastraea cavernosa. *Molecular Ecology*, *31*(2), 588–602.

Sanchez, R., & Mackenzie, S. A. (2023). On the thermodynamics of DNA methylation process. *Scientific Reports*, *13*(1), 8914.

Santillán, M., & Mackey, M. C. (2008). Quantitative approaches to the study of bistability in the lac operon of Escherichia coli. *Journal of the Royal Society, Interface / the Royal Society*, *5 Suppl 1*(Suppl 1), S29–S39.

Sarda, S., Zeng, J., Hunt, B. G., & Yi, S. V. (2012). The evolution of invertebrate gene body methylation. *Molecular Biology and Evolution*, *29*(8), 1907–1916.

Schlichting, C. D., & Pigliucci, M. (1993). Control of phenotypic plasticity via regulatory genes. *The American Naturalist*, *142*(2), 366–370.

Schlichting, C. D., & Pigliucci, M. (1995). Gene regulation, quantitative genetics and the evolution of reaction norms. *Evolutionary Ecology*, *9*(2), 154–168.

Schlichting, C. D., & Smith, H. (2002). Phenotypic plasticity: linking molecular mechanisms with evolutionary outcomes. *Evolutionary Ecology*, *16*(3), 189–211.

Sorek, R., & Cossart, P. (2010). Prokaryotic transcriptomics: a new view on regulation, physiology and pathogenicity. *Nature Reviews. Genetics*, *11*(1), 9–16.

Stephens, M. (2017). False discovery rates: a new deal. *Biostatistics* , *18*(2), 275–294.

Strader, M. E., Kozal, L. C., Leach, T. S., Wong, J. M., Chamorro, J. D., Housh, M. J., & Hofmann, G. E. (2020). Examining the Role of DNA Methylation in Transcriptomic Plasticity of Early Stage Sea Urchins:

Developmental and Maternal Effects in a Kelp Forest Herbivore. *Frontiers in Marine Science*, *7*. https://doi.org/10.3389/fmars.2020.00205

Sultan, S. E. (2000). Phenotypic plasticity for plant development, function and life history. *Trends in Plant Science*, *5*(12), 537–542.

Takuno, S., Seymour, D. K., & Gaut, B. S. (2017). The Evolutionary Dynamics of Orthologs That Shift in Gene Body Methylation between Arabidopsis Species. *Molecular Biology and Evolution*, *34*(6), 1479–1491.

Vogt, G. (2022). Epigenetics and Phenotypic Plasticity in Animals. In L. M. Vaschetto (Ed.), *Epigenetics, Development, Ecology and Evolution* (pp. 35–108). Springer International Publishing.

Weinberg, D. N., Papillon-Cavanagh, S., Chen, H., Yue, Y., Chen, X., Rajagopalan, K. N., Horth, C., McGuire, J. T., Xu, X., Nikbakht, H., Lemiesz, A. E., Marchione, D. M., Marunde, M. R., Meiners, M. J., Cheek, M. A., Keogh, M.-C., Bareke, E., Djedid, A., Harutyunyan, A. S., … Lu, C. (2019). The histone mark H3K36me2 recruits DNMT3A and shapes the intergenic DNA methylation landscape. *Nature*, *573*(7773), 281–286.

West, P. T., Li, Q., Ji, L., Eichten, S. R., Song, J., Vaughn, M. W., Schmitz, R. J., & Springer, N. M. (2014). Genomic distribution of H3K9me2 and DNA methylation in a maize genome. *PloS One*, *9*(8), e105267.

Xiao, L., Zhao, Z., He, F., & Du, Z. (2019). Multivariable regulation of gene expression plasticity in metazoans. *Open Biology*, *9*(12), 190150.

Ying, H., Hayward, D. C., Klimovich, A., Bosch, T. C. G., Baldassarre, L., Neeman, T., Forêt, S., Huttley, G., Reitzel, A. M., Fraune, S., Ball, E. E., & Miller, D. J. (2022). The Role of DNA Methylation in Genome Defense in Cnidaria and Other Invertebrates. *Molecular Biology and Evolution*, *39*(2). https://doi.org/10.1093/molbev/msac018

Zeng, Z., Sun, H., Vainio, E. J., Raffaello, T., Kovalchuk, A., Morin, E., Duplessis, S., & Asiegbu, F. O. (2018). Intraspecific comparative genomics of isolates of the Norway spruce pathogen (Heterobasidion parviporum) and identification of its potential virulence factors. *BMC Genomics*, *19*(1), 220.

Data Availability

Whole-genome bisulfite sequencing and RNASeq data are available in the NCBI BioProject database under the accession number PRJNA1074434. The metadata tables for gene expression and methylation data, a matrix of gene expression and a matrix of gene level methylation percentage are available of Dryad (doi:10.5061/dryad.76hdr7t3q). All R scripts for this study are available on GitHub (https://github.com/leaguerrero/project-anana-thermal-acclimation).

Figures and Tables

Figure 1.1: (A) Experimental design showing the acclimation treatments and how samples from each acclimation treatment were distributed for the heat stress assay. *Day 0 samples in the 31°C tank never actually experienced 31°C acclimation. (B) Plot of *chlorophyll a* concentration redrawn from previously performed study. Samples in the 31°C (Day 11) acclimation tank have a higher *chlorophyll a* concentration following the 5-h 34°C heat stress assay. (C) Prediction of the relationship between change in gene expression response to heat stress following acclimation and the change in average percent DNA methylation. The green ellipse symbolizes the hypothesized positive association between these variables. The purple ellipse symbolizes the alternative hypothesis if there is no relationship between the variables.

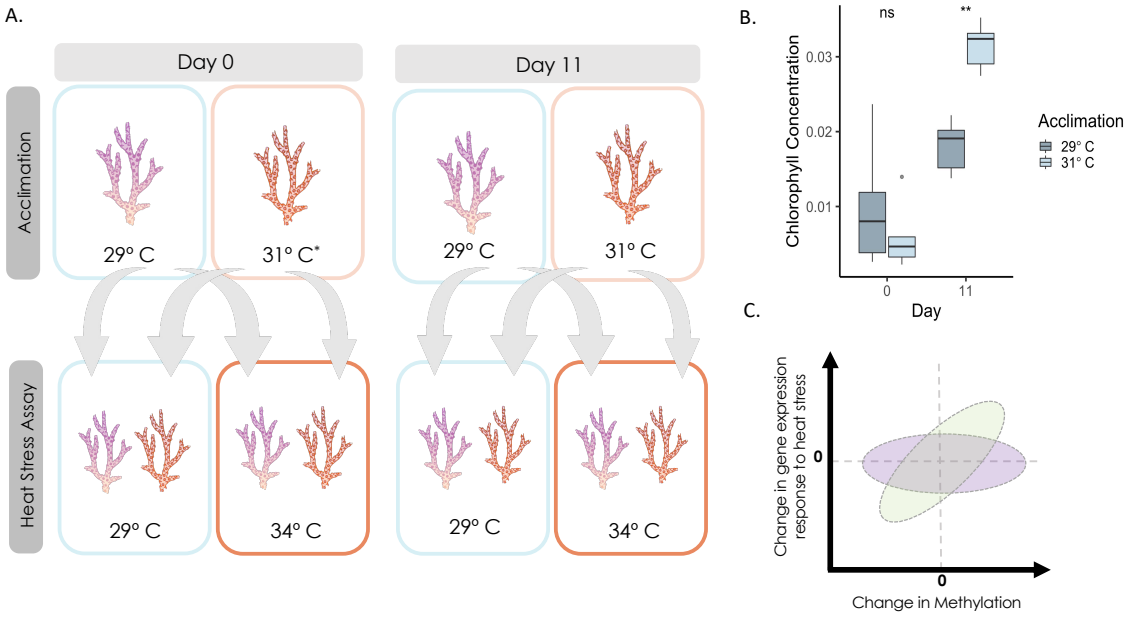

Figure 2.2: (A) PCA of gene expression showing tight cluster of control samples and variation within heat-stressed samples along PC2. (B) PCoA of DNA methylation showing no clustering between heat stress and control groups

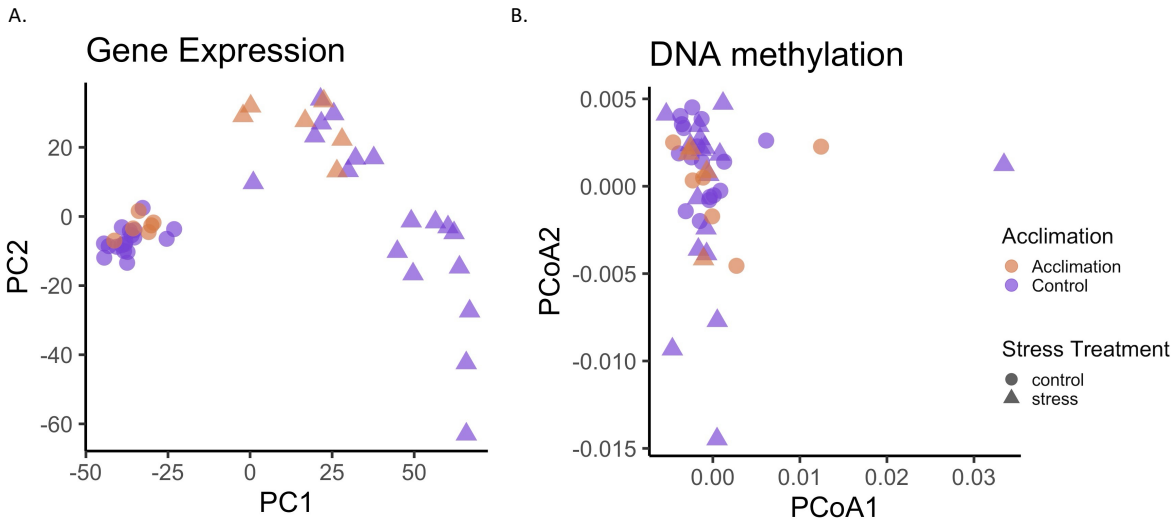

Figure 1.3: (A) Plot of mean percent methylation of amplified and dampened transcripts. ***$p < 0.001$. (B) Plot of the $\log_{10}$ of mean expression of amplified and dampened transcripts. ****$p < 0.0001$. (C) Scatterplot of acclimation-associated gene expression (i.e. Wald statistic) and DNA methylation changes. The oval represents the 99% CI. Legend colors depict genes with significant upregulation and downregulation following acclimation.

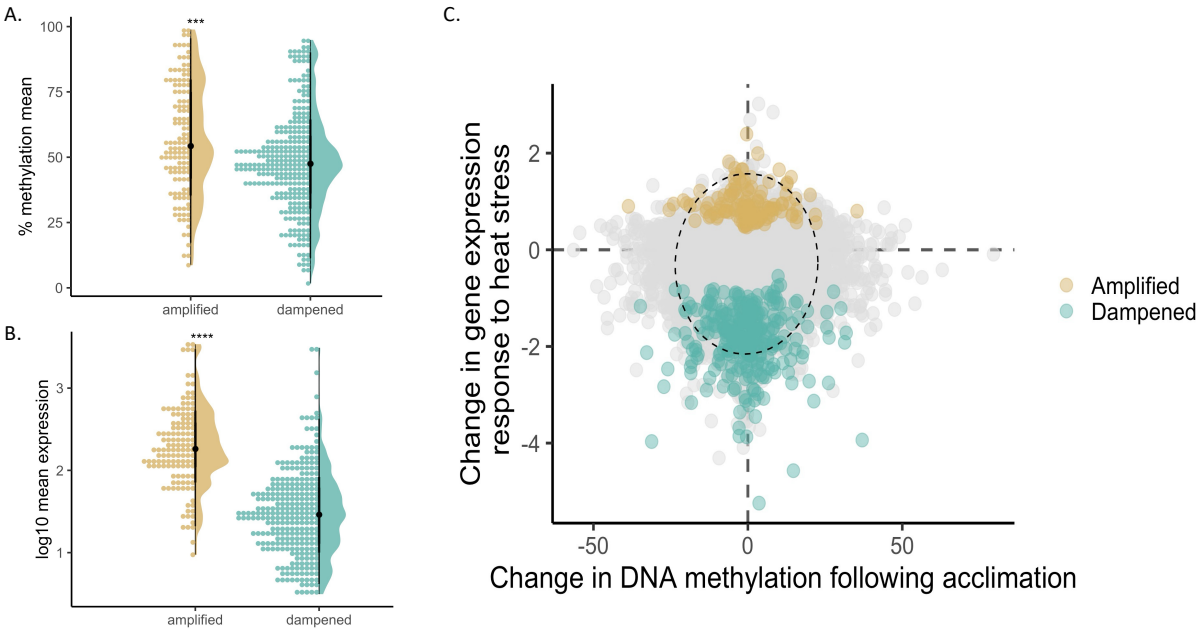

Supplemental Methods, Figures and Tables

Supplemental Methods

Accounting for *A.nana* C-to-T substitutions

Congener alignment can complicate methylation calling since C-to-T substitutions may be due to fixed genetic differences between *A. millepora* (reference genome species) and *A. nana* (query species) rather than the unmethylated cytosine conversion to thymine following bisulfite conversion. We used the RNASeq data to estimate how many C-to-T SNPs in the CpG dinucleotide motif exist in *A.nana* coding regions.

We used bcftools mpileup v 1.10.2 followed by bcftools call on sorted RNASeq BAM files data to call multiallelic SNPs between *A.nana* and *A. millepora.* We then used bcftools +fill-tags followed by bcftools convert to create annotated VCF files for downstream filtering. To filter for SNPs with an alternate allele frequency of 1 (i.e. fixed non-reference variants), a read depth of at least 10, variants present in at least 80% of the samples and a minimum genotype quality of 30. To identify C-to-T substitutions, we used bcftools view to identify SNPs where the reference was 'C' and the alternate was 'T'. This filtering we identified 186,786 fixed substitutions within our RNA-Seq data of 23,601 were C-to-T mutations.

In our analysis, we focus on CpG methylation, which means only C-to-T mutations in the CG context would be interpreted as unmethylated. We used samtools faidx to create a FASTA file of the reference dinucleotide motifs for each of the reported positions of the *A. nana* C-to-T SNPs. We found that 5,308 of C-to-T *A. nana* SNPs in the reference CpG motifs. Within *A. millepora* coding regions, there are 1,201,250 CGs. Based on these numbers, a rough estimate of the fraction of CGs that represent fixed differences between species is 0.47%. While we acknowledge the many caveats to this exact estimate (e.g. SNP estimates from RNA-Seq, variable coverage across genes, etc.), this does lead us to believe that a very small fraction of the CpG sites at which we are estimating methylation represent fixed substitutions between the two species.

Differential methylation enrichment in WGCNA expression modules

We conducted a network analysis to test whether genes that were differentially methylated between acclimation treatments were acting as 'hub genes', controlling larger-scale downstream expression changes. We used iterativeWGCNA based on the matrix of normalized gene expression counts to build a gene expression network. We defined 88 well supported modules representing 15,931 genes.
For each module, we conducted two tests. First, we ran an ANOVA testing the effects of heat stress treatment, acclimation treatment, and the interaction with the module eigenvector as the response variable. This tells us which gene expression modules are regulated according to our treatments and identified modules that exhibit the 'amplified' or 'dampened' gene expression response (i.e. those with significant interaction term). Second, we ran a Fisher's exact test to determine whether genes that were differentially methylated during acclimation were overrepresented in a module. Our expectation based on these tests was that if many differentially methylated genes were driving an overall gene expression pattern associated with acclimation response (the "Type I sub-network" from Gomez-Campo et al. 2023), we should see enrichment of methylation genes in modules that represent the gene expression to response to acclimation. We found six modules with enrichment of differentially methylated genes. However, none of these modules had significant acclimation or interaction terms.

We also did a second analysis to determine whether differentially methylated genes represented 'hub genes' – possible regulators of large-scale changes in gene expression ("Type II sub-networks" from Gomez-Campo et al.). We imported the network created with iterativeWGCNA into the R package *igraph*. This package allows us to calculate Kleinburg's hub centrality score for each gene in our network. We then tested whether differentially methylated genes were more likely to be hub genes than other genes in the network. We tested this hypothesis for two sets of genes (nodes): i) all genes in the network and ii) genes in modules with an acclimation effect. Supplementary Figure 6 shows the results for (i) but in both cases differentially methylated genes did not have higher hub scores than the null distribution based on all genes.

Based on these two analyses there is no evidence that differential methylation of hub genes is the mechanism for gene expression plasticity in our experiment (Figure S6). There are multiple reasons that our results likely differ from those in Gomez-Campo et al, the most obvious being that the timescale differs drastically, with the phenotypic plasticity we document occurring on much shorter timescales and resulting in far fewer methylation changes.

In invertebrates, network analysis may not capture biologically meaningful connectedness between gene expression hubs and changes in DNA methylation. Treatment driven differences in DNA methylation may not be detectable because the WGCNA framework assumes co-regulation of genes, and it remains to be determined that DNA methylation is co-regulated in invertebrates.

Supplemental Figures and Tables

Supplementary Table 1.S1: Gene Ontology (GO) terms of core heat response genes

Table shows the results from a GO enrichment analysis of the core set of heat response genes using the R package, topGO v. 2.50.0. We compared the list of "core" heat response genes against a background of all transcripts that passed our quality filters. Enriched GO terms were identified with the classic Fisher's test with a p-value < 0.01 and at least 10 transcripts within each category. GO terms are contained within ontology types: Biological Processes (BP), Cellular Components (CC), and Molecular Functions (MF).

Type	GO ID	Term	p-value
BP	GO:0060249	anatomical structure homeostasis	0.00012
BP	GO:0001894	tissue homeostasis	0.00013
BP	GO:0065009	regulation of molecular function	0.00013
BP	GO:0050896	response to stimulus	0.00016
BP	GO:0001503	ossification	0.00018
BP	GO:1901652	response to peptide	0.00018
BP	GO:0009888	tissue development	0.00019
BP	GO:1903037	regulation of leukocyte cell-cell adhesion	0.0003
BP	GO:0045859	regulation of protein kinase activity	0.00033
BP	GO:0001819	positive regulation of cytokine production	0.00035
BP	GO:0007159	leukocyte cell-cell adhesion	0.00038
BP	GO:0065008	regulation of biological quality	0.00049
BP	GO:0051607	defense response to virus	0.00049
BP	GO:0140546	defense response to symbiont	0.00049
BP	GO:0002833	positive regulation of response to biotic stimulus	0.00053
BP	GO:0008219	cell death	0.00062
BP	GO:0006950	response to stress	0.00071
BP	GO:0050863	regulation of T cell activation	0.00084
BP	GO:0050793	regulation of developmental process	0.00084
BP	GO:0043549	regulation of kinase activity	0.00089
BP	GO:0009887	animal organ morphogenesis	0.00101
BP	GO:0048771	tissue remodeling	0.00104
BP	GO:0033993	response to lipid	0.00112
BP	GO:0010941	regulation of cell death	0.0012
BP	GO:0032103	positive regulation of response to external stimulus	0.00128
BP	GO:0032496	response to lipopolysaccharide	0.0013
BP	GO:0032147	activation of protein kinase activity	0.00136
BP	GO:0002764	immune response-regulating signaling pathway	0.00148
BP	GO:0060562	epithelial tube morphogenesis	0.00158
BP	GO:0010557	positive regulation of macromolecule biosynthetic process	0.00172
BP	GO:0009725	response to hormone	0.00172
BP	GO:0001932	regulation of protein phosphorylation	0.00184
BP	GO:0044057	regulation of system process	0.00187
BP	GO:1901617	organic hydroxy compound biosynthetic process	0.00187
BP	GO:0045944	positive regulation of transcription by RNA polymerase II	0.00191
BP	GO:0009607	response to biotic stimulus	0.00191
BP	GO:0048871	multicellular organismal homeostasis	0.00191
BP	GO:1902105	regulation of leukocyte differentiation	0.00199

BP	GO:0045595	regulation of cell differentiation	0.00211
BP	GO:0048513	animal organ development	0.00212
BP	GO:0042221	response to chemical	0.00214
BP	GO:0006915	apoptotic process	0.00219
BP	GO:0002237	response to molecule of bacterial origin	0.0023
BP	GO:0010033	response to organic substance	0.00237
BP	GO:0050790	regulation of catalytic activity	0.00241
BP	GO:0051249	regulation of lymphocyte activation	0.00253
BP	GO:1903706	regulation of hemopoiesis	0.00256
BP	GO:0006066	alcohol metabolic process	0.0026
BP	GO:1901615	organic hydroxy compound metabolic process	0.00263
BP	GO:0048646	anatomical structure formation involved in morphogenesis	0.00266
BP	GO:1903131	mononuclear cell differentiation	0.00267
BP	GO:0048518	positive regulation of biological process	0.00277
BP	GO:0035239	tube morphogenesis	0.00289
BP	GO:0051091	positive regulation of DNA-binding transcription factor activity	0.00296
BP	GO:0043207	response to external biotic stimulus	0.00325
BP	GO:0051707	response to other organism	0.00325
BP	GO:0051247	positive regulation of protein metabolic process	0.00328
BP	GO:1901698	response to nitrogen compound	0.00338
BP	GO:0045893	positive regulation of DNA-templated transcription	0.00339
BP	GO:1903508	positive regulation of nucleic acid-templated transcription	0.00339
BP	GO:1902680	positive regulation of RNA biosynthetic process	0.00346
BP	GO:0006955	immune response	0.00368
BP	GO:0045597	positive regulation of cell differentiation	0.0037
BP	GO:0012501	programmed cell death	0.00372
BP	GO:0010035	response to inorganic substance	0.00375
BP	GO:0002253	activation of immune response	0.00382
BP	GO:0051338	regulation of transferase activity	0.0039
BP	GO:0002694	regulation of leukocyte activation	0.00392
BP	GO:0009891	positive regulation of biosynthetic process	0.00394
BP	GO:0006952	defense response	0.00449
BP	GO:0031328	positive regulation of cellular biosynthetic process	0.00452
BP	GO:0044093	positive regulation of molecular function	0.00452
BP	GO:0043410	positive regulation of MAPK cascade	0.00452
BP	GO:0048522	positive regulation of cellular process	0.00456
BP	GO:0070372	regulation of ERK1 and ERK2 cascade	0.00463
BP	GO:0042981	regulation of apoptotic process	0.00487
BP	GO:0051094	positive regulation of developmental process	0.00494
BP	GO:0044419	biological process involved in interspecies interaction between organisms	0.00497
BP	GO:0042592	homeostatic process	0.0053
BP	GO:0042391	regulation of membrane potential	0.00534
BP	GO:0009617	response to bacterium	0.00555
BP	GO:0070371	ERK1 and ERK2 cascade	0.00558
BP	GO:0051098	regulation of binding	0.00613
BP	GO:0032101	regulation of response to external stimulus	0.00629
BP	GO:0050865	regulation of cell activation	0.00632
BP	GO:0001816	cytokine production	0.00653
BP	GO:0043067	regulation of programmed cell death	0.00713
BP	GO:0001666	response to hypoxia	0.00725
BP	GO:0048856	anatomical structure development	0.00759
BP	GO:0019221	cytokine-mediated signaling pathway	0.0076
BP	GO:0051254	positive regulation of RNA metabolic process	0.00764
BP	GO:0010604	positive regulation of macromolecule metabolic process	0.00765
BP	GO:0002009	morphogenesis of an epithelium	0.00801
BP	GO:0043269	regulation of ion transport	0.00895

BP	GO:0001817	regulation of cytokine production	0.00914
BP	GO:0032502	developmental process	0.00951
BP	GO:0009628	response to abiotic stimulus	0.00979
BP	GO:0036293	response to decreased oxygen levels	0.00996
CC	GO:0031226	intrinsic component of plasma membrane	0.00011
CC	GO:0005615	extracellular space	0.00107
CC	GO:0098802	plasma membrane signaling receptor complex	0.00366
CC	GO:0005581	collagen trimer	0.00386
CC	GO:0005938	cell cortex	0.00396
CC	GO:0098552	side of membrane	0.00865
MF	GO:0005507	copper ion binding	0.0001
MF	GO:0001653	peptide receptor activity	0.00016
MF	GO:0005126	cytokine receptor binding	0.00024
MF	GO:0044389	ubiquitin-like protein ligase binding	0.0004
MF	GO:0031625	ubiquitin protein ligase binding	0.00078
MF	GO:0004497	monooxygenase activity	0.00133
MF	GO:0005102	signaling receptor binding	0.00158
MF	GO:0016705	oxidoreductase activity, acting on paired donors, with incorporation or reduction of molecular oxygen	0.00246
MF	GO:0016616	oxidoreductase activity, acting on the CH-OH group of donors, NAD or NADP as acceptor	0.00814

Supplementary Table 1.S2: Gene Ontology (GO) terms of Amplified Genes

Table shows the results from a GO enrichment analysis of amplified genes using topGO v. 2.50.0. We compared the list of amplified genes against a background of all transcripts that passed our quality filters. Enriched GO terms were identified with the classic Fisher's test with a p-value < 0.01 and at least 10 transcripts within each category. GO terms are contained within ontology types: Biological Processes (BP), Cellular Components (CC), and Molecular Functions (MF).

Type	GO ID	Term	p-value
BP	GO:1901566	organonitrogen compound biosynthetic process	0.0002
BP	GO:0009150	purine ribonucleotide metabolic process	0.00023
BP	GO:0009259	ribonucleotide metabolic process	0.00031
BP	GO:0019693	ribose phosphate metabolic process	0.00033
BP	GO:0006163	purine nucleotide metabolic process	0.00036
BP	GO:0042254	ribosome biogenesis	0.00036
BP	GO:0055086	nucleobase-containing small molecule metabolic process	0.00043
BP	GO:1901137	carbohydrate derivative biosynthetic process	0.00068
BP	GO:1901135	carbohydrate derivative metabolic process	0.0007
BP	GO:0072521	purine-containing compound metabolic process	0.00081
BP	GO:0022613	ribonucleoprotein complex biogenesis	0.00086
BP	GO:0090407	organophosphate biosynthetic process	0.00095
BP	GO:0009117	nucleotide metabolic process	0.001
BP	GO:0006753	nucleoside phosphate metabolic process	0.00108
BP	GO:0006397	mRNA processing	0.00151
BP	GO:0006396	RNA processing	0.00234
BP	GO:0032787	monocarboxylic acid metabolic process	0.00277
BP	GO:0044283	small molecule biosynthetic process	0.00614
BP	GO:0016071	mRNA metabolic process	0.00666
BP	GO:0043604	amide biosynthetic process	0.00721
BP	GO:0043603	cellular amide metabolic process	0.00761
BP	GO:0071704	organic substance metabolic process	0.0081
CC	GO:0005743	mitochondrial inner membrane	0.00019
CC	GO:1902494	catalytic complex	0.0002
CC	GO:0005739	mitochondrion	0.00025
CC	GO:1990904	ribonucleoprotein complex	0.00049
CC	GO:0019866	organelle inner membrane	0.00055
CC	GO:0005737	cytoplasm	0.00058
CC	GO:0005740	mitochondrial envelope	0.00069
CC	GO:0031966	mitochondrial membrane	0.0012
CC	GO:0031974	membrane-enclosed lumen	0.00344
CC	GO:0043233	organelle lumen	0.00344
CC	GO:0070013	intracellular organelle lumen	0.00344
CC	GO:0140513	nuclear protein-containing complex	0.00543
CC	GO:0140535	intracellular protein-containing complex	0.00558
MF	GO:0003824	catalytic activity	0.00432

Supplementary Table 1.S3: Gene Ontology (GO) terms of Dampened Genes

Table shows the results from a GO enrichment analysis of dampened genes using topGO v. 2.50.0. We compared the list of dampened genes against a background of all transcripts that passed our quality filters. Enriched GO terms were identified with the classic Fisher's test with a p-value < 0.01 and at least 10 transcripts within each category. GO terms are contained within ontology types: Biological Processes (BP), Cellular Components (CC), and Molecular Functions (MF).

Type	GO ID	Term	p-value
BP	GO:0006260	DNA replication	0.00081
BP	GO:0051276	chromosome organization	0.00214
BP	GO:0006259	DNA metabolic process	0.00702
CC	GO:0005694	chromosome	0.0031
MF	GO:0140657	ATP-dependent activity	0.0033
MF	GO:0003677	DNA binding	0.005
MF	GO:0015075	ion transmembrane transporter activity	0.0059
MF	GO:0005488	binding	0.0061
MF	GO:0005215	transporter activity	0.0069
MF	GO:0022836	gated channel activity	0.0084
MF	GO:0015318	inorganic molecular entity transmembrane transporter activity	0.0086
MF	GO:0005216	ion channel activity	0.0088

Supplementary Table 1.S4: Gene Ontology (GO) terms of Differentially Methylated Genes after Heat Stress Assay

Table shows the results from a GO enrichment analysis using topGO v. 2.50.0 of genes that have differential methylation following 24-hour heat stress assay. We compared the list of genes with a methylation percent change of at least 25% and a q-value ≤ 0.05 against a background of all genes included in the methylation dataset that passed our quality filters. Enriched GO terms were identified with the classic Fisher's test with a p-value < 0.01 and at least 10 transcripts within each category. GO terms are contained within ontology types: Biological Processes (BP), Cellular Components (CC), and Molecular Functions (MF). Note that no MF GO terms were enriched in this gene set.

Type	GO ID	Term	p-value
BP	GO:1901564	organonitrogen compound metabolic process	0.0043
CC	GO:0005622	intracellular anatomical structure	0.0018
CC	GO:0043231	intracellular membrane-bounded organelle	0.0032
CC	GO:0043227	membrane-bounded organelle	0.0033
CC	GO:0005737	cytoplasm	0.0057

Supplementary Figure 1.S1: The Bar plot shows the relative number of reads that align to *Symbiodinium goreaui* or *Durusdinium trenchii* in all samples.

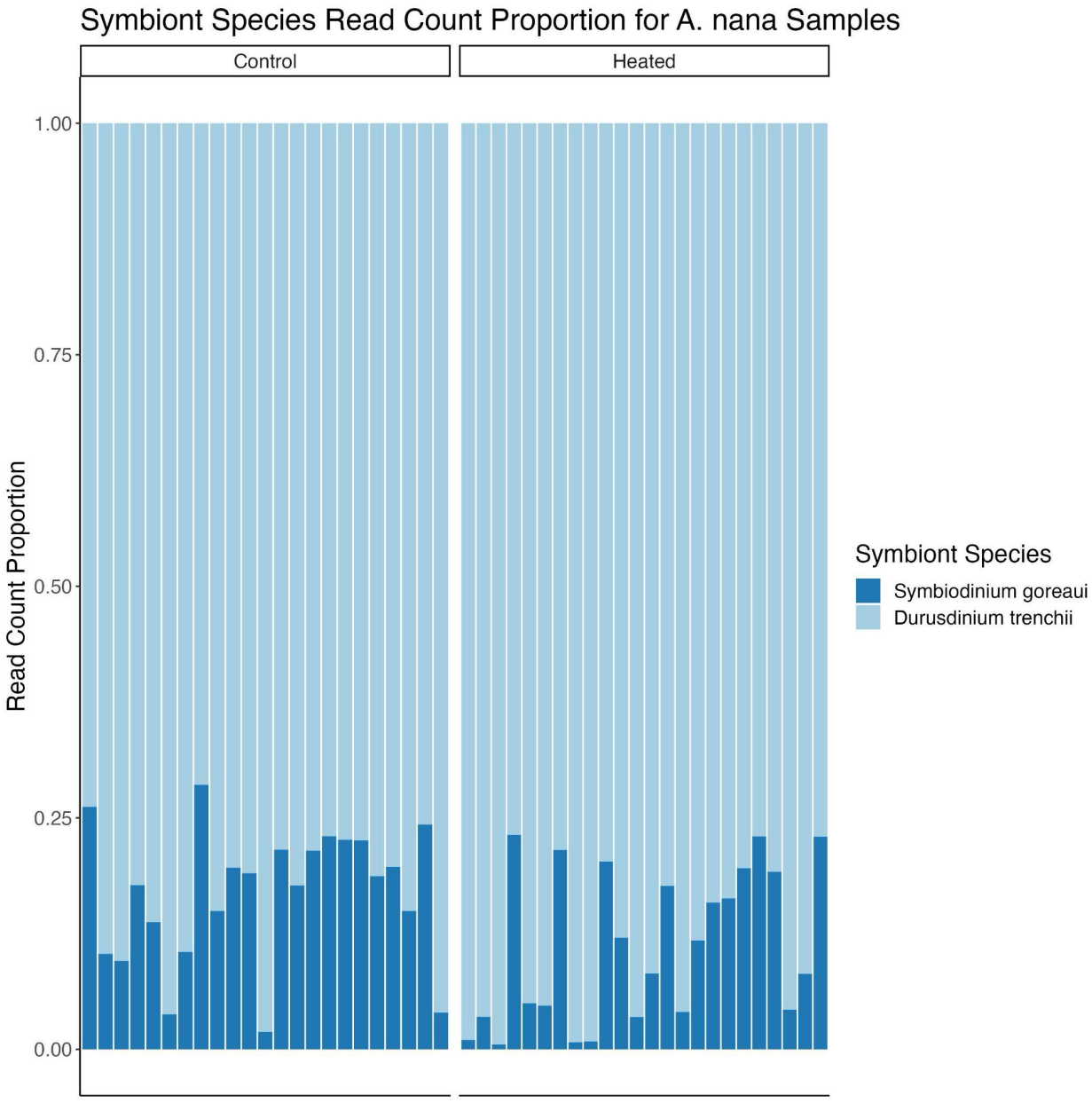

Supplementary Figure 1.S2. PCoA of DNA methylation before outliers (encircled) were removed.

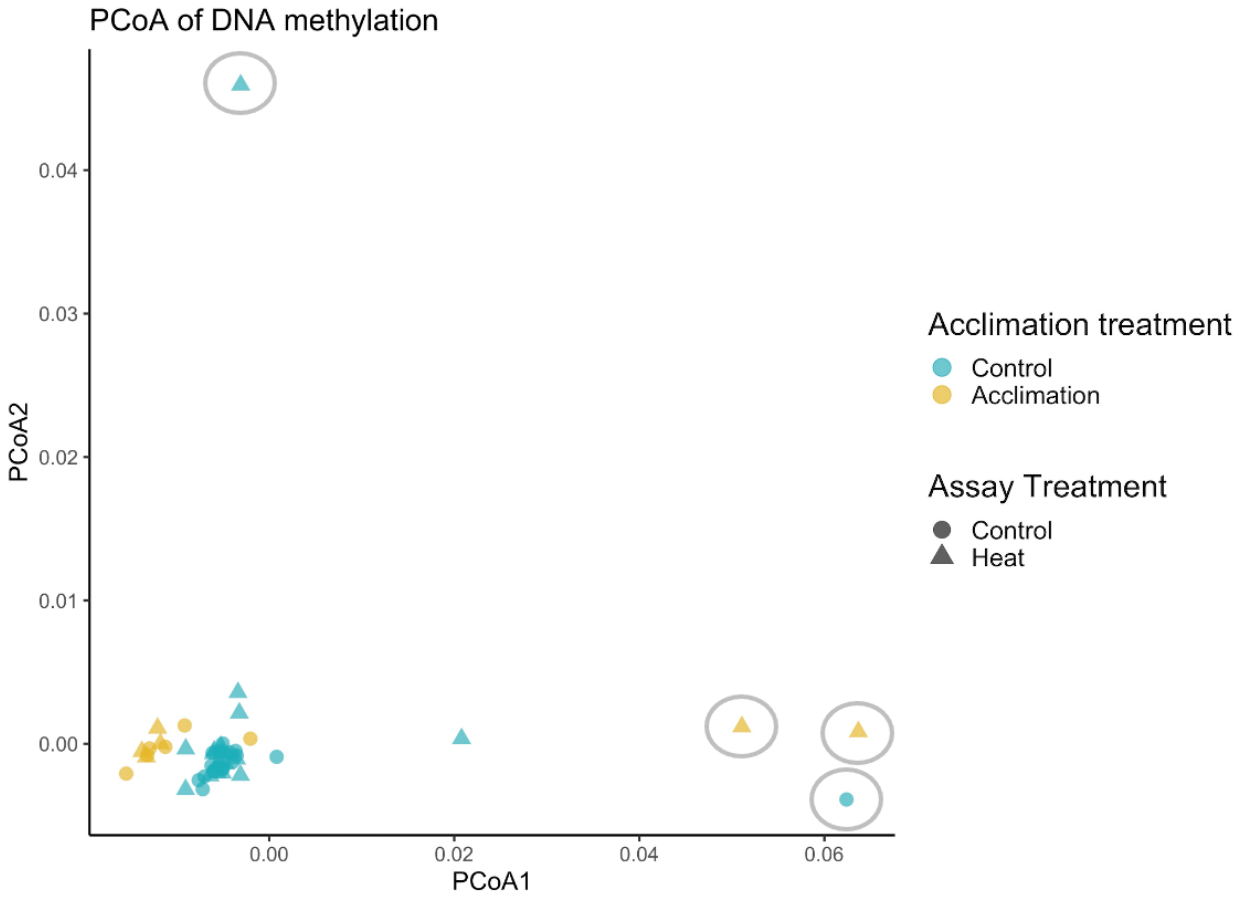

Supplementary Figure 1.S3: (A) Plot showing the bimodal distribution of CpG percent methylation across the genome. (B) Plot showing the distribution of gene-level percent methylation. (C)Distribution of percent methylation within genomic features. The dashed horizontal line represents the median of the feature-specific percent methylation means.

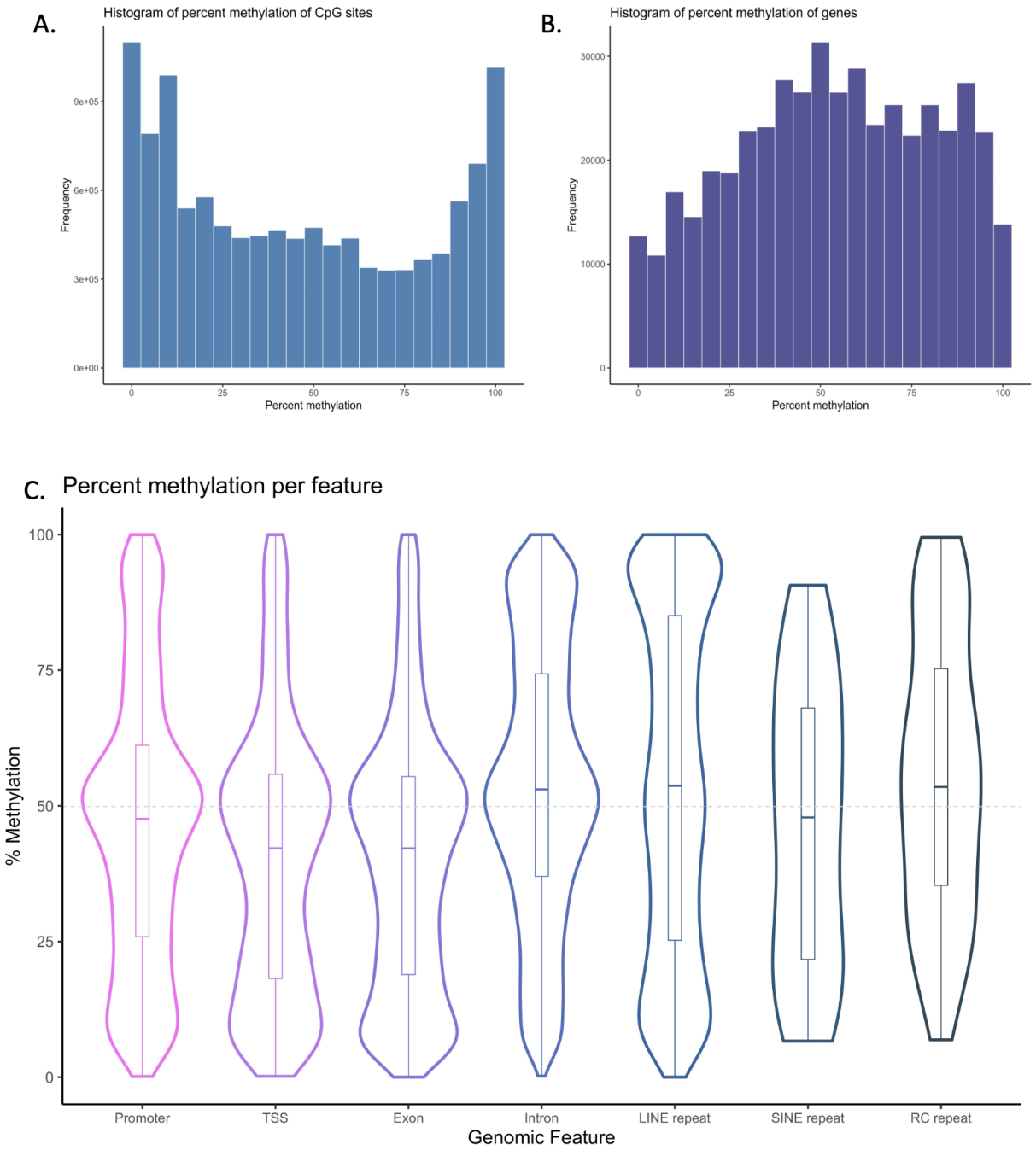

Supplementary Figure 1.S4: (A) Relationship between gene body methylation and baseline expression. On the x-axis is the average percent methylation of genes from all samples. On the y-axis is the $\log_{10}$ transformed expression means of transcripts from all samples. (B) Relationship between gene body methylation and variation in gene expression response to heat stress. On the x-axis is the average percent methylation of genes from all samples. On the y-axis is the standard error of the $\log_2$ fold change between heat stress and control samples.

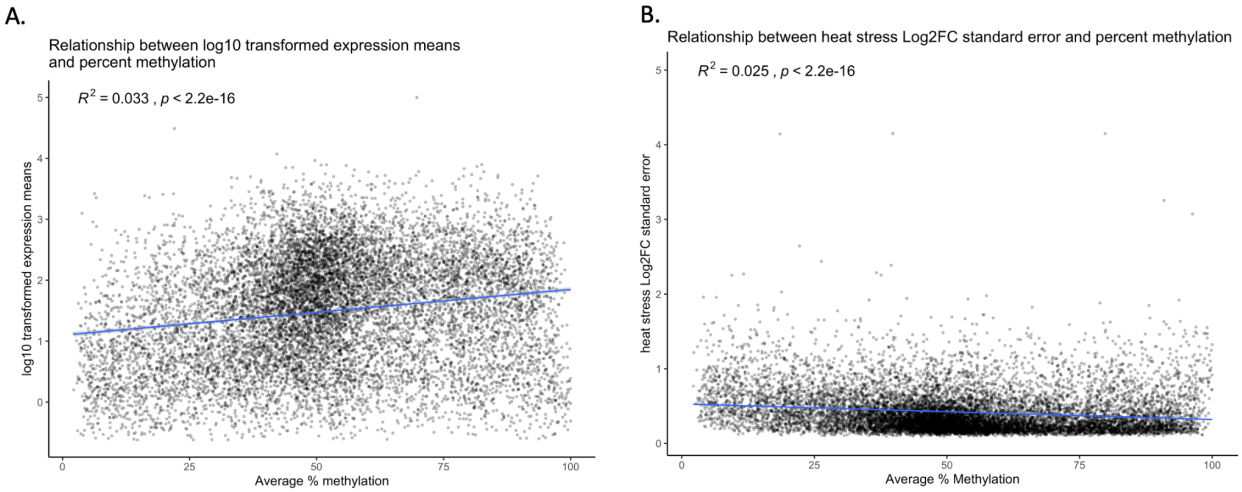

Supplementary Figure 1.S5: Boxplot of gene body percent methylation of amplified and dampened genes in thermally acclimated samples and the acclimation controls. A t-test was used to compare the means of percent methylation between genes with amplified expression and genes with dampened expression in acclimated samples and control samples.

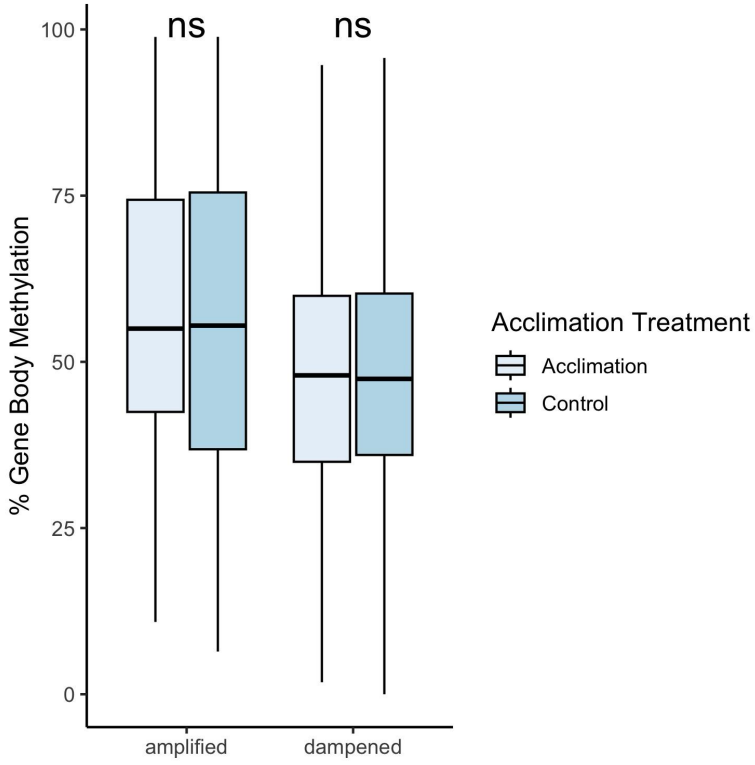

Supplementary Figure 1.S6: Hub scores for genes in iterativeWGCNA network. Gene categories are amplified (amp), dampened (damp), differentially methylated (meth), and none. Hub scores for ‘meth’ genes are not significantly different than ‘none’.

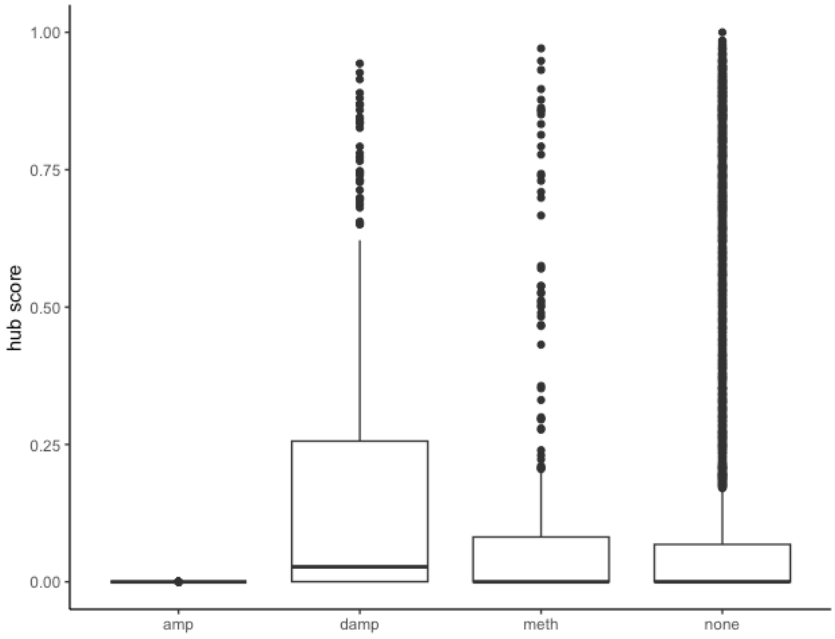

Chromatin accessibility and heat stress gene expression in the reef-building coral, *Acropora millepora*

Authors: Leslie Guerrero, Kenzie Pollard, and Rachael Bay

Abstract

Understanding how organisms regulate gene expression to maintain homeostasis in the face of environmental changes is critical, particularly in light of increasing climate stressors. DNA methylation in invertebrates is increasingly recognized as a mechanism associated with gene expression and other organismal processes, but recent studies suggest that methylation control of gene expression may not be acting on physiological timescales. Alternative epigenetic layers may provide more insight into short-term mechanisms of gene expression regulation. This study investigates the role of chromatin accessibility in influencing gene expression in the reef-building coral *A. millepora*, especially under heat stress conditions. Our findings reveal that highly accessible regions, or open chromatin, are predominantly located in distal intergenic regions, promoters, and introns. Genes with open promoters exhibit increased expression and reduced variability, suggesting that chromatin accessibility plays a significant role in influencing gene expression plasticity in response to heat stress. Functional enrichment of heat response genes with open chromatin promoters revealed functions in regulating immune responses, response to viruses, and gene expression, demonstrating the importance of chromatin accessibility in rapidly responding to environmental changes. By highlighting the complex interaction between chromatin and gene expression in *A. millepora*, this study contributes to new insights into short-term regulatory mechanisms important for responding to acute environmental stressors. This work establishes a foundation to investigate the interactions between chromatin accessibility and additional epigenetic layers, such as DNA methylation, and how the dynamics of these interacting epigenetic layers contribute to adaptive molecular and cellular responses, which will be critical for understanding coral resilience and informing conservation strategies.

Introduction

To maintain homeostasis in natural environments, organisms must effectively respond to external cues at both the cellular and molecular levels. A critical aspect of this response is the variation in gene expression, which ultimately contributes to shifts in phenotypes. However, the mechanisms by which gene expression is precisely mediated to respond to complex environmental signals remain a major

biological question. Epigenetics provides a valuable lens for understanding how environmental factors influence gene expression, leading to functional trait variation in natural populations (Kilvitis et al. 2014; Lamka et al. 2022). Defined as the study of molecular mechanisms that interact with DNA to modulate gene expression without altering the underlying sequence, epigenetics explores processes that are thought to play a crucial role in how organisms respond to biotic and abiotic factors such as temperature fluctuations, nutritional changes, and predator cues (Feil and Fraga 2012; Kilvitis et al. 2014; Noguera and Velando 2019). For example, in plants, abiotic stressors, such as drought and heat, influence changes in non-coding RNA expression, which is an epigenetic mechanism that regulates coding gene expression in a stress-specific manner (Di et al. 2014). Epigenetic mechanisms also are important for seasonal responses, reproductive trait fluctuations, and generating phenotypic variation in clonal species (Fishman and Tauber 2024; Jueterbock et al. 2020; Lindner et al. 2020).

A core objective of ecological epigenomics is to unravel the intricate interactions between epigenetic layers, gene expression regulation, and their ecological and evolutionary significance (Lamka et al. 2022). This endeavor has become increasingly important for predicting species' adaptive potential as climate change intensifies environmental stressors, particularly for long-lived species that cannot easily migrate to more favorable habitats (Eirin-Lopez and Putnam 2019; Hofmann 2017; Lancaster et al. 2022). Reef-building corals, which are highly vulnerable to ocean warming and other stressors, present a compelling system for studying the role of epigenetic mechanisms in regulating gene expression in response to abiotic stressors. Corals possess a marked ability to modulate their gene expression in response to acute environmental stress and, following environmental conditioning, have the capacity to finely-tune their gene expression for impending stressors (Bay and Palumbi 2015; Bellantuono et al. 2012). This suggests that molecular mechanisms can preserve the 'memory' of exposure to environmental cues and facilitate the necessary gene expression response to maintain homeostasis.

DNA methylation is the most extensively studied epigenetic mechanism in corals. Across various coral taxa, DNA methylation fluctuates in response to environmental changes (Dimond and Roberts 2016; Dimond and Roberts 2020; Dixon et al. 2018; Putnam et al. 2016; Rodriguez-Casariego et al. 2022). However, accumulating evidence indicates that shifts in DNA methylation following environmental fluctuations may play a negligible role in mediating gene expression changes (Abbott et al. 2024; Dixon and Matz 2022; Guerrero and Bay 2024; Rodriguez-Casariego et al. 2022; but see Gomez-Campo et al. 2023; Rodríguez-Casariego et al. 2020). Despite this, DNA methylation has established roles in suppressing transposable elements, maintaining transcriptional homeostasis, and correlating with higher overall gene expression (Dixon and Matz 2022; Guerrero and Bay 2024; Li et al. 2018; Rodriguez-Casariego et al. 2022; Ying et al. 2022). Altogether, DNA methylation in corals is hypothesized to act as a regulatory mechanism over adaptive timescales rather than a change in response to short-term environmental changes (Abbott et al. 2024). This raises important questions about the regulatory mechanisms acting at shorter timescales in corals.

Emerging interest in chromatin organization and accessibility has provided new insights into this epigenetic layer as a mediator of the stress response in cnidarian species, including corals (Rodriguez-Casariego et al. 2018; Roquis et al. 2022; Weizman and Levy 2019). Eukaryotic DNA is organized and tightly packed in the nucleus through physical interactions with octomer cores of histone proteins (Tsompana and Buck 2014). Regions of open chromatin result from post-translational histone modifications or histone variant substitutions that alter nucleosome structure, thereby facilitating DNA-binding processes such as transcription activation, DNA repair, and recombination (Tsompana and Buck 2014). Recent studies have shown that coral histones undergo post-translational modifications following stress events. For example, in *Acropora cervicornis*, phosphorylation of the histone variant H2.AX following nutrient and heat stress activates DNA repair processes (Rodriguez-Casariego et al. 2018). Similarly, in *Pocillopora acuta*, acute heat stress leads to clipping of canonical histone H3 amino acid tails, although the functional consequences of this modification remains to be explored (Roquis et al.

2022). Notably, studies in ATAC-seq and RNA-seq in the cnidarian model species *Exaiptasia pallida* have revealed that chromatin accessibility dynamics are influenced by thermal exposure, with exposed transcription factor binding motifs being linked to gene expression changes (Weizman and Levy 2019). However, the relationship between chromatin accessibility and gene expression in reef-building corals remains unexplored, a crucial step to enhance our understanding of epigenetic regulation in these ecologically vital species.

In this study, we use ATAC-seq to investigate regions of open chromatin and their relationship to gene expression variation broadly and to the heat stress gene expression response in particular in the reef-building coral, *Acropora millepora*. Specifically, we treated *A. millepora* fragments with an acute heat stress assay and performed 3'TagSeq to evaluate the heat stress gene expression response. We then performed ATAC-seq and assessed the relationship between promoter accessibility and overall expression and expression variation. Finally, we investigated whether the accessibility of chromatin promoters influences gene expression during heat stress. The relationship between open chromatin promoters and gene expression established here, through the integration of ATAC-seq and 3'TagSeq, sets the stage to broaden our understanding of short-term mechanisms driving gene expression changes in corals.

Methods

Experimental Design

Establishing thermal response

We acquired 74 fragments of *Acropora millepora*, comprised of 8 different genotypes, from Neptune Aquatics, Inc. in San Jose, California. We used these fragments to build a library of samples with varying thermal histories in an attempt to assay a more general heat stress response.The fragments underwent a 10-day conditioning period in the laboratory aquarium, which was maintained at 24.5°C. We maintained the salinity at 32 ppm as measured with a refractometer. To simulate variation in thermal exposure history, we incubated 24 fragments at 27°C for 7 days while keeping another 24 fragments at the control

temperature of 24.5°C, then returned all fragments to 24.5°C. Due to space limitations, we could not include fragments from all genotypes in every acclimation treatment. However, we ensured each genotype was represented in its respective thermal acclimation and control treatments. To characterize the thermal response, we performed five heat stress assays over the course of three weeks using a modified Coral Bleaching Automated Stress System (CBASS) protocol (Voolstra et al. 2020). The heat stress treatment involved a 3-hour thermal ramp from 24.5°C to 36°C, followed by a 3-hour hold at 36°C to simulate thermal stress conditions, and finally, thermal decline over the course of an hour back to 24.5°C. Temperature profiles were picked based on pilot experiments that tested for a temperature that induced an intermediate bleaching response that could capture variation among coral fragments. Heat stress assays were performed initially (Day 0) on 5 genotypes to capture baseline thermal tolerance (Figure 2.1). We followed with assays on days 7, 11, 14, and 21 on 4 fragments from 4 different genotypes with a thermal acclimation treatment and their respective controls (Figure 2.1). At the end of the heat stress assay, we dark-acclimated the fragments for an hour and analyzed each fragment using Pulse Amplitude Modulated (PAM) fluorometry, measuring efficiency of photosystem II (Fv/Fm). We used the Shapiro-Wilk test to determine the normality of Fv/Fm yield data. We used a Wilcoxon test to compare the average Fv/Fm values between control and heated samples.

After the PAM fluorometry, we captured images of the fragments with Kodak color standards using an iPhone (Kodak color separation guide and grayscale Q-13, Kodak, USA). We measured the red channel intensity using the methods described by Winters et al. (Winters et al. 2009). We used the Shapiro-Wilk test to determine the normality of red channel intensity data. We used a T-test to compare the average red channel intensity values between control and heated samples. Within an hour of completing the PAM fluorometry and color-standard photography, we flash-froze the fragments for RNA and protein extractions. We stored these tissue samples at -80°C until we were ready for molecular extractions.

We assayed the activity of glutathione reductase (GR), an emerging indicator of coral stress, for control and heat stress samples (Majerová and Drury 2022). In brief, we homogenized coral tissue by vortexing 1g of thawed coral clipping with 0.1mL of glass beads (Sigma-Aldrich, Mfr. Catalog ID g8772-10g) and 1 mL of filtered seawater (sl35) in a microcentrifuge tube. We used compound microscopy to check that symbiont cell integrity was maintained, thus minimizing the risk of symbiont GR contamination. We isolated coral tissue from symbionts by centrifuging samples at 800 g for 5 minutes. We centrifuged supernatants containing coral cells at 14,000g for 10 minutes to remove cellular debris. We collected the supernatant and quantified total protein using the Broad Range Qubit assay (Thermo Fisher Scientific, Mfr Catalog ID A50668). We used the EnzyChrom Glutathione Reductase kit (BioAssays, Mfr Catalog ID ECGR-100) to measure GR absorbance and calculate GR activity following manufacturer instructions. The plate reader we used to measure absorbance at 412 nm was a Spectramax M2 (Molecular Devices, San Jose, CA). We normalized the GR activity with the total protein concentration for each sample. We used the Shapiro-Wilk test to determine the normality of the normalized GR activity data. We used a Wilcoxon test to compare the average GR activity values between control and heated samples.

Molecular Preparation and Sequencing

3’TagSeq

We used 3’TagSeq to profile gene expression responses to heat stress. Our samples, while all exposed to similar heat stress, comprised a range of thermal histories. We extracted RNA from fifty-eight samples using the E.Z.N.A. HP Total RNA Isolation Kit (Omega Bio-Tek, Mfr. Catalog ID R6812) using instructions and the optional DNase I Digestion Protocol supplied by the manufacturer. We stored extracted RNA at -80°C. We sent RNA to the DNA Technologies and Expression Analysis Core at the UC Davis Genome Center for library preparation and sequencing. Barcoded 3'Tag-Seq libraries prepared using the QuantSeq FWD kit (Lexogen, Vienna, Austria) for multiplexed sequencing according to the manufacturer's recommendations. The fragment size distribution of the libraries was verified via micro-capillary gel electrophoresis on a Bioanalyzer 2100 (Agilent, Santa Clara, CA). The libraries were quantified by fluorometry on a Qubit instrument (LifeTechnologies, Carlsbad, CA), and pooled in

equimolar ratios. Fifty-eight libraries were sequenced on one lane of an Aviti sequencer (Element Biosciences, San Diego, CA) with single-end 100 bp reads. The sequencing generated more than 4 million reads per library.

We trimmed the reads of the universal Illumina adapters and bases on the 3' end of the read with a sequencing quality score of less than 10 using Cutadapt (v. 4.1) (Martin 2011). To separate intracellular symbiont reads from coral reads, we used BBsplit (v. 38.22) to bin reads that align to either the *Symbiodinium goreaui* or the *A. millepora* genome (reefgenomics.org, Bushnell 2014, Fuller et al. 2020). To optimize TagSeq read binning, we adjusted the BBsplit maxindel argument to '100K'. We mapped the *A. millepora* reads to the *A. millepora* reference genome using the STAR aligner (v. 2.7.10b) (Dobin et al. 2013). We used HTSeq (v. 2.0.3) to count all the reads that mapped to genes, including reads that mapped to multiple locations (--nonunique all) using the annotated gene models provided with the *A. millepora* reference genome (Anders et al. 2015).

ATAC-seq

We assayed 'open,' or hyper-accessible, chromatin in *A. millepora* using ATAC-seq (Buenrostro et al. 2015). Due to failed reactions, we were unable to do ATAC-seq in the same fragments used for gene expression. However, our study explores a more general connection between chromatin accessibility and gene expression in *A. millepora.* We acquired four fragments of *A. millepora*, each of a different genotype, from Neptune Aquatics, Inc. in San Jose, California. The fragments were stored in the laboratory aquarium overnight. The following morning, we performed nuclear preparations for sequencing regions of open chromatin by modifying previously published protocols (Ackermann et al. 2016; Buenrostro et al. 2015; Weizman and Levy 2019). The fragments used for ATAC-seq were not subject to any heat stress as we focused on open chromatin regions at baseline conditions. We first isolated tissue from the skeleton by scraping the tissue with a sterile scalpel into ice-cold 1x PBS buffer. We slowly pipetted the PBS buffer and tissue mixture up and down 10 times in a petri dish over ice to

break up and evenly distribute the tissue in the buffer. We pipetted 750 µL of the mixture into a mini 40 µm cell strainer fit into a 1.5 mL microcentrifuge tube to isolate coral cells. To facilitate the passage of the sample through the strainer and collection of filtrate into the microcentrifuge tube, we gently tapped the microcentrifuge tube bottom on the lab bench until most of the PBS-cell mixture had strained through the filter. After collecting the filtrate, we centrifuged the sample tubes at 1500g for 5 minutes at 4°C. We pipetted off the supernatant and resuspended the isolated cells in 500 µL of fresh ice-cold 1x PBS buffer. To pellet cells with symbionts, we centrifuged the samples at 600g for 10 minutes at 4°C. We collected and resuspended the supernatant in fresh ice-cold 1x PBS. We centrifuged the sample tubes at 1500g for 5 minutes at 4°C and pipetted off the supernatant.

To isolate the nuclei from the total cellular debris, we resuspended the cell pellet in 50 µL of lysis buffer consisting of 0.25 µL of 10% NP40 added to 49.75 µL of resuspension buffer (10 mM Tris-HCl, 10 mM NaCl, 3 mM $MgCl_2$). We incubated the cells in the lysis buffer on ice for 3 minutes. Following the 3-minute incubation, we centrifuged the mixture at 300g for 10 minutes at 4°C. We removed the supernatant with cellular debris and repeated the 3-minute incubation in the lysis buffer followed by the 10-minute centrifuge. We removed the supernatant and suspended nuclei in 100 µL of fresh ice-cold resuspension buffer. We centrifuged this mixture at 300g for 10 minutes at 4°C. We removed the supernatant and resuspended the nuclei in 100 µL fresh ice-cold resuspension buffer. To estimate the number of nuclei we collected per genotype, we stained 10 µL of suspended nuclei with DAPI to visualize and count nuclei using a hemocytometer and fluorescent microscopy (Life Technologies EVOS FL Color, Mfr Catalog ID AMEFC4300).

To perform the tagmentation, we added 2.5 µL of Tn5 Transposase suspended in 1X TD Buffer (Nextera DNA sample preparation kit; Illumina, cat. no. FC-121-1030), for every 50,000 nuclei. We incubated this reaction for 30 minutes at 37°C. We purified the DNA using the MinElute Reaction Cleanup Kit (Qiagen, Mfr. Catalog ID 28204).

We performed 20 cycles of PCR using the NEBNext High-Fidelity 2X PCR Master Mix (NEB, Mfr. Catalog ID M0541S) to generate sequencing libraries. We purified the libraries using AMPure XP beads (Beckman Coulter, Mfr. Catalog ID A63880). We used the Agilent High Sensitivity DNA Bioanalysis Kit (Agilent, Mfr. Catalog ID 5067-4626) to assess the quality of the purified libraries and that the expected fragment sizes of amplified ATAC-seq libraries were present (Buenrostro et al. 2015). We pooled the purified libraries and had samples sequenced at the DNA Technologies and Expression Analysis Core at the UC Davis Genome Center. DNA was sequenced using Illumina NextSeq to generate 75 bp PE reads intending to achieve 120 million read pairs total.

We used Cutadapt (v. 4.1) to trim Nextera adapter sequences from the reads as well as bases with a sequencing quality score less than 20 from the 3' end of the reads (-q 20) (Martin 2011). We used the mitochondrial genome supplied with the *A. millepora* reference genome to distinguish and exclude mitochondrial from nuclear reads using BBsplit (v. 38.22) (Bushnell 2014). We mapped reads to the *A. millepora* reference using Bowtie2 (v. 2.4.4) (Langmead and Salzberg 2012). We used samtools view (v. 1.13.0) to filter out reads that were not the primary alignment, PCR or optical duplicates, reads that failed platform/vendor quality checks, and supplementary alignments (-F 3840) (Li et al. 2009). We removed duplicate reads with Picard MarkDuplicates (v. 2.23.2) (Picard).

We called hyper accessible chromatin, or peaks, with MACS2 (v. 2.2.6) which reports the Poisson distribution p-values used to identify peaks (Zhang et al. 2008). We used the DiffBind (v3.12.0) R package to generate a consensus set of open chromatin regions across replicates (Stark and Brown 2012). Consensus peaks are regions of the genome exhibiting high accessibility to the transposase enzyme, with overlap by at least one base pair across samples, in this case the four genotypes of *A. millepora*. We specified that a peak must be present in at least two out of the four replicates to be included in the

consensus peak set. Additionally, we applied a minimum peak significance threshold of $5x10^{-5}$ to ensure the inclusion of highly significant peaks.

We used CHIPseeker (v1.38.0) to annotate the consensus peak set (Wang et al. 2022). To analyze the functional enrichment of open chromatin promoters, we analyzed Gene Ontology (GO) terms with the R package, topGO v. 2.50.0, comparing peak enrichment to all annotated genes in *A. millepora* (Alexa and Rahnenfuhrer 2022, Fuller et al. 2020).

Heat stress treatment effect on gene expression

We used the R Package DESeq2 v. 1.36.0 (Love et al. 2014; R Core Team 2023) to test the effects of thermal history, genotype, and heat stress on gene expression in our samples. To visualize these effects, we first performed principal component analysis (PCA). Next, we identified the genes with a significant change in expression due to heat stress. First, we created a 'DESeqDataSet' object and included an experimental design formula to determine the overall heat-stress effect while controlling for differences due to genotype (design = ~condition.genotype + condition.stress.treatment). We filtered for genes with a depth of at least 10 reads in all samples and normalized data with the variance stabilizing transformation. We defined "heat stress genes" with an absolute value of the $\log_2$ fold change greater than 2 and with an adjusted p-value less than 0.05. To analyze the functional enrichment of heat response genes, we analyzed Gene Ontology (GO) terms with the R package, topGO v. 2.50.0, comparing the set of heat response genes against a background of all genes that passed our quality filters. Enriched GO terms were identified with the classic Fisher's test with a p-value of less than 0.01 and at least 10 transcripts within each category (Alexa and Rahnenfuhrer 2022, Fuller et al. 2020).

Testing the relationship between open chromatin promoters and gene expression

We combined ATACSeq and transcriptome data to characterize genome-wide effects of chromatin hyper-accessibility on gene expression. We collated the genes for which we have expression and the genes proximal to the consensus peaks to assess the relationship between gene expression variation and degree

of accessibility. We categorized genes into quintiles based on their mean overall expression, where the fifth quintile represents genes with the highest expression. To calculate the accessibility of a region, we performed a $\log_{10}$ transformation of the average of the normalized read counts covering open chromatin regions. We plotted the accessibility as a function of the distance to the transcription start site (TSS) for each expression quintile using the geom_smooth function of ggplot2 v. 3.51.

In addition to mean expression, we also tested whether chromatin accessibility affected expression variation, which would be produced by a combination of plasticity, genetic effects, and noise. We used DESeq2 to extract the matrix of normalized gene counts and calculated the standard deviation of the normalized counts across samples. We removed one outlier gene with a standard deviation greater than $2x10^4$. For genes proximal to the consensus peaks with available gene expression variation data, we categorized genes into quintiles based on the standard deviation of normalized counts. The fifth quintile represented genes with "variable" expression, while the first quintile represented genes with "stable" expression. We then plotted the accessibility as a function of the distance to the transcription start site (TSS) for genes with stable and variable expression using the geom_smooth function of ggplot2 v. 3.5.1.

We combined the gene expression data and open chromatin promoter data to investigate the relationship between the open chromatin of promoters and the transcriptional response to heat stress. We used the R package CHIPseeker 1.38.0 to read and annotate raw peak file output from MACS2 (Wang et al. 2022). We filtered for peaks that are annotated as ‘promoter’ and had a peak significance threshold $\leq 5x10^{-5}$. We selected genes that had accessible promoters in at least two genotypes. Next, we used DESeq2 to contrast gene expression between samples exposed to 24.5°C and 36°C. We filtered for genes with more than ten reads across all samples. We used the ‘ashr’ method to shrink $\log_2$ fold change values and calculated the absolute values of the $\log_2$ fold changes, or the magnitude of the response. We filtered out genes with an adjusted p-value > 0.05.

Our primary hypothesis was that gene promoters are poised to facilitate an imminent transcriptional response to heat stress, presumably by histone modifications that yield open chromatin and regulatory protein binding. We used a Fisher's exact test to test the significance of the overlap between heat response genes and genes with open promoters. We defined heat response genes as genes with a response magnitude ≥ 2. Next, we tested if open promoters are associated with a larger response to heat stress. We performed an unpaired Wilcoxon test to compare the overall mean expression and the response magnitude of heat response genes with open and closed promoters. To test the response directionality between heat response genes with open or closed promoters, we performed an unpaired Wilcoxon test of the $\log_2$ fold change in gene expression.

To analyze functional enrichment of heat response genes with open promoters and closed promoters, we analyzed Gene Ontology (GO) terms with the R package, topGO v. 2.50.0, comparing the set of heat response genes with open promoters against a background of all gene transcripts that passed our quality filters. Enriched GO terms were identified with the classic Fisher's test with a p-value < 0.01 and at least 10 transcripts within each category (Alexa and Rahnenfuhrer 2022, Fuller et al. 2020).

Results

Phenotypic effects from heat stress

We found a significant decrease in algal symbiont photosystem II efficiency in heat-stressed fragments (Figure 2.2 A, Wilcoxon test, $p \leq 0.0001$). Additionally, heat-stressed fragments had a higher visual bleaching response, indicated by a higher R channel intensity (Figure 2.2 B, T-test, $p \leq 0.0001$). The R channel intensity estimates red-light absorbing chlorophyll pigment degradation. Across all heat stress assays, the heat-stressed fragments have significantly reduced GR activity compared to the control fragment counterparts (Figure 2.2 C, Wilcoxon test, $p \leq 0.01$). GR activity, an emerging biomarker for coral health, reduces reactive oxygen species (ROS) to a peroxide byproduct, thereby mitigating the downstream deleterious effects on DNA homeostasis caused by ROS (Majerová and Drury 2022). These results collectively indicate that heat stress is detrimental for both the symbionts and coral's homeostasis.

Transcriptional response to heat stress

We used RNA 3'TagSeq to evaluate the transcriptomic response to heat stress in *A. millepora*. Reads were binned based on alignment to either the *Symbiodinium goreaui* or the *A. millepora* genome. On average, 1,201,288 reads were derived from symbiont transcripts, and an average of 2,327,833 reads were from *A. millepora* transcripts. We observed an average of 61.3% uniquely mapped coral-derived reads to the *A. millepora* reference genome.

We used DESeq to assess the transcriptional response to heat stress. After filtering for genes with at least 10 reads across all samples, we evaluated the transcriptional response for 19,649 genes. We found that heat treatment is the largest source of variation, followed by genotype (Figure 2.2 D). Thermal history did not explain any variation in the gene expression response to heat. Comparing control to heat stressed fragments, 2,227 genes were differentially expressed. Among these heat response genes, 268 GO terms were significantly enriched, with cellular pathways for oxidative stress, unfolding protein binding, transcription, immunity, and apoptosis being particularly notable (Supplement Table 2.S1). These GO terms align with previous reports of *A. millepora* heat stress, where genes associated with oxidative stress, symbiont detection, symbiosis maintenance, and transcription are differentially expressed (Bellantuono et al. 2012; Granados-Cifuentes et al. 2013). These processes are also well documented to be associated with heat stress in other reef-building coral species (Louis et al. 2017).

ATAC-seq

We successfully performed ATAC-seq on *A. millepora.* After trimming raw reads, we obtained an average of 42,586,471 paired-end reads across all four replicates. On average, 4.8% of reads were derived from mitochondria, which is a low and acceptable amount of mitochondrial contamination (Montefiori et al. 2017). An average of 66.3% of reads were derived from nuclear DNA, and we achieved a primary read alignment rate of 90.1%.

Using MACS2 for peak calling, we identified an average of 32,206 peaks across the four genotypes, with 11,096 regions meeting our criteria for inclusion in the consensus set. This number of consensus peaks is lower than the open chromatin regions reported in other invertebrate ATAC-seq studies, possibly reflecting the conservative nature of our peak summary approach (Weizman and Levy 2019; Gatzmann et al. 2018). We found that 5,553 open chromatin regions were distal to genic regions (Figure 2.3). Genic open chromatin occurred more frequently in introns relative to exons (Figure 2.3), consistent with what is seen in *Strongylocentrotus purpuratus* (Bogan et al. 2023). The relatively high representation of introns among genic peaks underscores the growing recognition of their role in regulating gene expression (Rose 2018; Bogan et al. 2023).

Accessible gene promoters interact with gene regulatory proteins that control transcription initiation and regulation (Danino et al. 2015; Yang and Hansen 2024). Approximately 36% percent of the consensus peaks were annotated as promoters, which is higher than the typical 25% observed in other studies (Yan et al. 2020). This might indicate that the regulatory regions in our samples were more active. Open chromatin promoter GO terms were linked to critical biological processes that regulate a wide range of molecular functions and cellular activities (Table 2.1). Specifically, these terms are predominantly associated with immune system regulation, viral interactions and responses, gene expression and transcription regulation, cellular processes and metabolism, and regulation of development and differentiation (Table 2.1). The enrichment supports the expectation that open chromatin promoters play a key role in higher-level gene expression regulation (Klemm et al. 2019).

Testing the relationship between accessible chromatin promoters and gene expression

We investigated the genome-wide effects of chromatin hyper-accessibility on gene expression. We observed that 1,919 genes in our expression data had open chromatin promoters after collating the consensus peak set with gene expression data. Genes with the highest expression (5th quintile) have more accessible chromatin around the TSS than genes with lower expression (Figure 2.4 A). Genes with more

accessible chromatin promoters exhibited the least expression variation (Figure 2.4 B). This is consistent with observations of low-methylated genes in crayfish (Gatzmann et al. 2018).

Of the 2,227 heat response genes, 371 had accessible chromatin promoters. Surprisingly, heat response genes were significantly less likely to have accessible chromatin promoters (Fisher's exact test, p-value = 3.9×10^{-14}, odds ratio < 1). This could possibly indicate that the heat response genes with open chromatin promoters in ambient conditions may be closed, but epigenetically poised to rapidly respond to heat stress. While the overall mean expression of heat response genes with accessible promoters was similar to those with inaccessible promoters (Figure 2.5 A, Wilcoxon test, $p = 0.98$), the former exhibited higher magnitude of $\log_2$ fold changes following heat stress (Figure 2.5 B, Wilcoxon test, $p < 0.01$). Therefore, accessible chromatin promoters appear to play a small but significant role in mediating gene expression necessary for responding to heat stress.

Heat response genes with open promoters were enriched for biological processes GO terms only, whereas the heat response genes with closed promoters were enriched for all three types of GO terms (i.e. biological processes, molecular functions and cellular components) (Table 2.2). A prevalent signal in heat response genes with open promoters is for regulation of kinase and phosphorylation activity, which are critical for cellular responses to heat stress. Other regulatory biological responses enriched in this subset of genes pertain to regulation of immune responses to heat stress, and regulation of apoptosis and cell death. In contrast, the heat response genes with closed promoters exhibit diverse functional enrichment (Table 2.2). Notable stress responses in this category are transcriptional regulation, transmembrane transport and ion binding, signaling and receptor activity, extracellular matrix and cell adhesion, and immune responses. A key functional contrast between these two classes of heat response genes is observed in their regulatory behavior under heat stress. Specifically, heat response genes with open promoters are, on average, upregulated, whereas heat response genes with closed promoters are downregulated (Figure 2.6; Wilcoxon test, $p < 0.001$). Altogether, these results suggest a functional

distinction where genes with open promoters primarily enhance regulatory pathways critical for immediate cellular stress responses, while genes with closed promoters exhibit a broader array of stress-induced functions, reflecting a potentially delayed response to heat stress.

Discussion

Ecological epigenetics aims to understand how non-genetic sources of phenotypic variation influence evolutionary trajectories and improve predictions of species responses to changing climates (Lamka et al. 2022). Previous ecological epigenomic studies have primarily focused on the role of DNA methylation in regulating gene expression for ecologically relevant traits. This focus is driven by the well-established link between DNA methylation and gene expression, the environmentally induced fluctuations in DNA methylation, and the relative ease of generating such data from natural populations (Eirin-Lopez and Putnam 2019; Hofmann 2017; Suzuki and Bird 2008). However, evidence suggests that in various species, fluctuations in DNA methylation play a negligible role in causing short-term changes in gene expression (Abbott et al. 2024; Bewick et al. 2019; Dixon and Matz 2022; Guerrero and Bay 2024). Environmental stressors lead to changes in histone structure in reef building corals, and chromatin accessibility changes are linked with heat exposure in *E. pallida*, suggesting an important role for chromatin organization as a short-term regulator in corals capable of responding to environmental cues (Rodriguez-Casariego et al. 2018; Roquis et al. 2022; Weizman and Levy 2019). In this study, we investigated the relationship between gene expression and chromatin accessibility, contributing to the growing body of knowledge on how species mediate gene expression in response to environmental cues. Our ATAC-seq data revealed a predominance of open chromatin regions in distal intergenic regions, promoters, and introns, highlighting the importance of chromatin accessibility in gene regulation. We also show that genes with accessible chromatin promoters had increased expression and reduced variability. Heat response genes with open promoters on average were upregulated, suggesting that these genes are primed for an immediate heat stress response. Since genes with high expression variability and closed promoters are likely poised to respond to environmental cues, future research should focus on characterizing the mechanisms that enable this potential for gene expression plasticity.

Phenotypic and Transcriptional Responses to Heat Stress

Heat stress impacted both symbiont and coral homeostasis, yet thermal history did not significantly affect the physiological or gene expression responses to heat stress. Previous studies have found that *Acropora* corals exhibit diminished sensitivity to higher temperatures following exposure to warmer conditions, a response that is influenced by the duration of exposure and the time elapsed since that exposure (Bay and Palumbi 2015; Bellantuono et al. 2012; Middlebrook et al. 2008). For example, a previous study on *A. nana* found that an elevated temperature of just 2°C for 7 days led to increased tolerance to acute heat stress (Bay and Palumbi 2015). Under similar acclimation conditions, we saw no difference in thermal tolerance based on thermal history in *A. millepora*. One possible explanation is that the acclimation temperature was not warm enough to induce an acclimation response. Alternatively, the corals used in our experiment, which were raised in thermally stable aquaria, have lost the plastic capacity of wild-raised corals and thus do not exhibit the strong acclimation response seen in other studies. The functional enrichment of GO terms associated with heat response genes aligns with previous findings on the essential cellular processes involved in responding to heat stress (Bellantuono et al. 2012; Granados-Cifuentes et al. 2013; Louis et al. 2017).

Open chromatin regions in the *A. millepora* genome

We used ATAC-seq, a highly sensitive assay, to map open chromatin regions in the *A. millepora* genome (Buenrostro et al. 2013; Buenrostro et al. 2015). Chromatin accessibility is a critical epigenetic layer that interacts with other regulatory mechanisms, and its role in mediating gene expression in response to environmental cues is increasingly being studied in ecologically relevant species (Klemm et al. 2019; Lamka et al. 2022; Turner 2009). In our study, open distal regions constituted the majority of the identified peaks, which is consistent with the higher proportion of distal intergenic regions typically reported in ATAC-seq experiments (Yan et al. 2020). This contrasts with results in the cnidarian model *Exaiptasia pallida*, which demonstrate lower proportion of intergenic distal accessible regions, suggesting species-specific differences (Weizman and Levy 2019). Open distal chromatin regions are increasingly recognized for their role in gene expression regulation and are hypothesized to be evolutionarily

significant (Pliner et al. 2018; Roscito et al. 2018; Weizman and Levy 2019; Yan et al. 2020; Horvath et al. 2021). For example, open intergenic chromatin regions in the plant species, *Capsella grandiflora*, serve as a reservoir for mutations with regulatory functions, often having minimal fitness effects, thereby allowing them to accumulate over time (Horvath et al. 2021). Further exploration of genetic variation within open distal regions in *A. millepora* and other ecologically relevant species could shed light on the evolutionary mechanisms that shape gene regulation variation.

Functional enrichment signifies that genes with open chromatin promoters in ambient conditions are involved in regulating immune responses, viral processes, and gene silencing mechanisms, indicating their role in controlling essential cellular operations. Open promoters facilitate binding of transcriptional activators, enhancing gene expression (Cairns 2009). Enrichment of genes with open promoters, such as those involved in cellular metabolic processes and RNA nuclease activity, suggest that accessibility of these promoters is important to maintaining baseline cellular functions. On the other hand, the enrichment of terms related to the immune response regulation and responses to external stimuli suggests that promoters are poised to rapidly respond to environmental cues (Puri et al. 2015). Specifically, the presence of positive and negative regulation of immune system processes at baseline suggests a finely-tuned system that maintained immune stability while being prepared for activation. Similarities in functional enrichment of genes with open promoters between symbiotic *E. pallida* and *A. millepora* such as regulation of gene expression and responses to stress and stimuli suggest that some patterns of chromatin accessibility may be conserved across cnidarians (Weizman and Levy 2019).

Enriched regulatory processes observed in ambient conditions may reveal novel gene expression mechanisms, offering insights into important pathways that could explain adaptive processes in coral, which have yet to be fully explored (Eirin-Lopez and Putnam 2019). For instance, the enrichment for gene silencing by regulation of non-coding RNA (ncRNA) and microRNA (miRNA) supports the growing recognition that regulatory RNAs are critical for stress responses in corals (Huang et al. 2019;

Liew et al. 2014). Studies in various taxa demonstrate that ncRNAs play specific roles in responding to stressors such as temperature and may contribute to gene expression changes linked to phenotypic plasticity (Heo and Sung 2011; Kindgren et al. 2018; Eirin-Lopez and Putnam 2019; Jha et al. 2023). Further investigation into these regulatory mechanisms in coral and other ecologically relevant species will be critical for understanding how these organisms adapt to changing environments, and represents an exciting avenue for future research.

Relationship Between Open Chromatin Promoters and Gene Expression

In our study, genes with the highest expression and lowest expression variability exhibited high chromatin accessibility around the TSS. This relationship between expression, expression variation, and chromatin accessibility was also identified in marbled crayfish and is closely associated with gene-body DNA methylation (Gatzmann et al. 2018). Specifically, genes with high expression and high promoter accessibility were found to be depleted of DNA methylation across the gene body (Gatzmann et al. 2018). Additionally, Gatzmann et al. demonstrate that heavy gene-body methylation is associated with reduced chromatin accessibility at promoters of genes with stable expression, suggesting a role for DNA methylation in maintaining transcriptional consistency (Gatzmann et al. 2018). Although we did not assess DNA methylation in this study, the relationship between DNA methylation and gene expression observed in other invertebrates, including multiple *Acropora* species, could inform future hypotheses about the interaction between DNA methylation and chromatin accessibility to regulate gene expression in reef-building corals (Gatzmann et al. 2018). Specifically, housekeeping genes–those with stable expression necessary to maintain basal homeostatic processes–tend to be more densely methylated in invertebrates compared to environmentally responsive genes (Dixon and Matz 2022; Gatzmann et al. 2018). Additionally, gene expression variability–a measure that captures gene expression noise and environmental response–tends to decrease as gene-body methylation increases (Dixon and Matz 2022; Gatzmann et al. 2018; Guerrero and Bay 2024). These findings support the hypothesis that chromatin accessibility and DNA methylation synergistically mediate gene expression homeostasis (Gatzmann et al. 2018; Li et al. 2018).

It is compelling to speculate on the histone modifications that may influence the basal chromatin state of both housekeeping and environmentally responsive genes. Our finding that genes with the highest expression exhibit the highest promoter accessibility is consistent with findings in mouse embryonic stem cells (Clark et al. 2018). In mouse embryonic fibroblasts, Shoaib et al. note a positive correlation between histone H4 lysine 20 mono-methylation (H4K20me1) and chromatin accessibility to facilitate gene expression, especially in housekeeping genes (Shoaib et al. 2021). Previous studies indicate that histone H4 is highly conserved between cnidarians and mice, suggesting that these regulatory mechanisms might be evolutionarily conserved (Roquis et al. 2022). However, despite the conservation of histone amino-acid sequences, epigenetic layers, including DNA methylation patterns, generally differ between cnidarians and mammals. For instance, vertebrate genomes are densely methylated with the exception of within regulatory regions (Klughammer et al. 2023; Suzuki and Bird 2008). In contrast, invertebrate genomes exhibit sparse methylation, where higher methylation concentration occurs across gene-bodies and is positively associated with gene expression (Dixon and Matz 2022; Roberts and Gavery 2012). This divergence indicates that while certain aspects of histone modification might be conserved, their interactions with other epigenetic factors can vary across species.

Despite the divergence in genome-wide methylation patterns between mammalian somatic cells and invertebrates, mammalian oocytes, preimplantation embryos, and placenta cells exhibit a DNA methylation landscape that, along with its relationship to gene expression relationship, is similar to invertebrates (Demond and Kelsey 2020; Smallwood et al. 2011). This similarity may offer insight into conserved regulatory histone modifications. In these sparsely methylated mammalian tissues, poised chromatin marks essential for early embryonic development include histone modifications such as trimethylation of histone H3 at lysine 4 (H3K4me3), acetylation of histone H3 at lysine 27 (H3K27ac), and ubiquitination and acetylation of histone H2A variant Z (Dijkwel and Tremethick 2022; reviewed in Sotomayor-Lugo et al. 2024). For instance, when the H3K4me3 footprint around the TSS is wider than

5kb, this histone mark is associated with activated transcription and maintains stable DNA methylation percentages (Liu et al. 2016; Sotomayor-Lugo et al. 2024). Transient expression of genes is associated with the co-occurrence of H3K4me3 and H3K27ac, where H3K27ac is a embryonic stage-specific modification to influence the time-sensitive gene expression (Sotomayor-Lugo et al. 2024; Wu et al. 2023). The chromatin accessibility in regions with the H3K4me3 epigenetic mark depends on how broad the signal is around the TSS and protein complex associations, ultimately resulting in a context-dependent dynamic chromatin structure (Beacon et al. 2021). Together, these findings suggest a possible conserved role for these histone post-translational modifications in mediating gene expression, DNA methylation and chromatin accessibility. However, the interactions between these factors are complex, and future research is needed to dissect context-dependent interplay between specific histone modifications, chromatin state, and gene expression in corals and other invertebrates (Beck et al. 2012; Corvalan and Coller 2021).

Accessible chromatin promoters established under ambient conditions appear to play a small but significant role in mediating gene expression plasticity required to respond to heat stress. Promoters can be poised to repress expression under ambient conditions while simultaneously remaining primed to rapidly respond to various cellular stimuli (Puri et al. 2015). In our study, we identified a set of heat response genes with promoters poised to respond to heat stress. These genes were primarily upregulated compared to heat response genes with closed promoters in ambient conditions. A recent study by Himanen et al. (2022) demonstrated that heat shock transcription factors (HSFs) can reprogram transcription by either directly or indirectly facilitating the release of paused RNA polymerase II in open chromatin near the TSS. HSFs are also known to play a crucial role in coral thermal-tolerance (Cleves et al. 2020; Hayes and King 1995; Ishii et al. 2019; Meyer et al. 2011). In our study, functional enrichment analyses of the poised heat response genes suggest that they are involved in high-level regulatory processes, including gene expression and protein modifications. The essential cellular cascades regulated by heat response genes with poised promoters are linked to immune responses, stress responses,

apoptosis, and post-translational modifications. These findings offer insight into how transcription initiation may occur in genes with poised promoters during heat stress in ecologically relevant species.

Conclusion

Our findings highlight the significant role of chromatin accessibility in regulating gene expression in response to environmental stressors, enhancing our understanding of ecological epigenomics beyond the historical focus on DNA methylation. While the acute regulatory role of DNA methylation remains unclear, our findings underscore chromatin accessibility as a key mechanism influencing gene expression, particularly through open chromatin promoters associated with heat response genes. We demonstrate how these promoters mediate essential cellular processes. Additionally, our study shows how chromatin accessibility can inform broader hypotheses about mechanisms regulating gene expression. Future research will be needed to further explore the regulatory roles of chromatin and how their interactions with other epigenetic factors to improve predictions and strategies for mitigating the effects of climate change on vulnerable species.

References

Abbott, E., Loockerman, C., & Matz, M. V. (2024). Modifications to gene body methylation do not alter gene expression plasticity in a reef-building coral. *Evolutionary Applications*, *17*(2), e13662.

Ackermann, A. M., Wang, Z., Schug, J., Naji, A., & Kaestner, K. H. (2016). Integration of ATAC-seq and RNA-seq identifies human alpha cell and beta cell signature genes. *Molecular Metabolism*, *5*(3), 233–244.

Alexa, A., & Rahnenfuhrer, J. (2024). topGO: Enrichment Analysis for Gene Ontology. R package version 2.56.0.

Anders, S., Pyl, P. T., & Huber, W. (2015). HTSeq--a Python framework to work with high-throughput sequencing data. *Bioinformatics* , *31*(2), 166–169.

Bay, R. A., & Palumbi, S. R. (2015). Rapid Acclimation Ability Mediated by Transcriptome Changes in Reef-Building Corals. *Genome Biology and Evolution*, *7*(6), 1602–1612.

Beacon, T. H., Delcuve, G. P., López, C., Nardocci, G., Kovalchuk, I., van Wijnen, A. J., & Davie, J. R. (2021). The dynamic broad epigenetic (H3K4me3, H3K27ac) domain as a mark of essential genes. *Clinical Epigenetics*, *13*(1), 138.

Beck, D. B., Oda, H., Shen, S. S., & Reinberg, D. (2012). PR-Set7 and H4K20me1: at the crossroads of genome integrity, cell cycle, chromosome condensation, and transcription. *Genes & Development*, *26*(4), 325–337.

Bellantuono, A. J., Granados-Cifuentes, C., Miller, D. J., Hoegh-Guldberg, O., & Rodriguez-Lanetty, M. (2012). Coral thermal tolerance: tuning gene expression to resist thermal stress. *PloS One*, *7*(11), e50685.

Bewick, A. J., Zhang, Y., Wendte, J. M., Zhang, X., & Schmitz, R. J. (2019). Evolutionary and experimental loss of gene body methylation and its consequence to gene expression. *G3* , *9*(8), 2441–2445.

Bogan, S. N., Strader, M. E., & Hofmann, G. E. (2023). Associations between DNA methylation and gene regulation depend on chromatin accessibility during transgenerational plasticity. *BMC Biology*, *21*(1), 1–18.

Buenrostro, J. D., Giresi, P. G., Zaba, L. C., Chang, H. Y., & Greenleaf, W. J. (2013). Transposition of native chromatin for fast and sensitive epigenomic profiling of open chromatin, DNA-binding proteins and nucleosome position. *Nature Methods*, *10*(12), 1213–1218.

Buenrostro, J. D., Wu, B., Chang, H. Y., & Greenleaf, W. J. (2015). ATAC-seq: A Method for Assaying Chromatin Accessibility Genome-Wide. *Current Protocols in Molecular Biology / Edited by Frederick M. Ausubel ... [et Al.]*, *109*, 21.29.1-21.29.9.

Bushnell, B. (2014). *BBMap: A Fast, Accurate, Splice-Aware Aligner* (No. LBNL-7065E). Lawrence Berkeley National Lab. (LBNL), Berkeley, CA (United States). https://www.osti.gov/servlets/purl/1241166

Cairns, B. R. (2009). The logic of chromatin architecture and remodelling at promoters. *Nature*, *461*(7261), 193–198.

Clark, S. J., Argelaguet, R., Kapourani, C.-A., Stubbs, T. M., Lee, H. J., Alda-Catalinas, C., Krueger, F., Sanguinetti, G., Kelsey, G., Marioni, J. C., Stegle, O., & Reik, W. (2018). scNMT-seq enables joint profiling of chromatin accessibility DNA methylation and transcription in single cells. *Nature Communications*, *9*(1), 781.

Cleves, P. A., Tinoco, A. I., Bradford, J., Perrin, D., Bay, L. K., & Pringle, J. R. (2020). Reduced thermal tolerance in a coral carrying CRISPR-induced mutations in the gene for a heat-shock transcription factor. *Proceedings of the National Academy of Sciences of the United States of America*, *117*(46), 28899–28905.

Corvalan, A. Z., & Coller, H. A. (2021). Methylation of histone 4's lysine 20: a critical analysis of the state of the field. *Physiological Genomics*, *53*(1), 22–32.

Danino, Y. M., Even, D., Ideses, D., & Juven-Gershon, T. (2015). The core promoter: At the heart of gene expression. *Biochimica et Biophysica Acta*, *1849*(8), 1116–1131.

Demond, H., & Kelsey, G. (2020). The enigma of DNA methylation in the mammalian oocyte. *F1000Research*, *9*, 146.

Di, C., Yuan, J., Wu, Y., Li, J., Lin, H., Hu, L., Zhang, T., Qi, Y., Gerstein, M. B., Guo, Y., & Lu, Z. J. (2014). Characterization of stress-responsive lncRNAs in Arabidopsis thaliana by integrating expression, epigenetic and structural features. *The Plant Journal: For Cell and Molecular Biology*, *80*(5), 848–861.

Dijkwel, Y., & Tremethick, D. J. (2022). The role of the histone variant H2A.Z in metazoan development. *Journal of Developmental Biology*, *10*(3), 28.

Dimond, J. L., & Roberts, S. B. (2016). Germline DNA methylation in reef corals: patterns and potential roles in response to environmental change. *Molecular Ecology*, *25*(8), 1895–1904.

Dimond, J. L., & Roberts, S. B. (2020). Convergence of DNA Methylation Profiles of the Reef Coral Porites astreoides in a Novel Environment. *Frontiers in Marine Science*, *6*, 792.

Dixon, G., Liao, Y., Bay, L. K., & Matz, M. V. (2018). Role of gene body methylation in acclimatization and adaptation in a basal metazoan. *Proceedings of the National Academy of Sciences of the United States of America*, *115*(52), 13342–13346.

Dixon, G., & Matz, M. (2022). Changes in gene body methylation do not correlate with changes in gene expression in Anthozoa or Hexapoda. *BMC Genomics*, *23*(1), 234.

Dobin, A., Davis, C. A., Schlesinger, F., Drenkow, J., Zaleski, C., Jha, S., Batut, P., Chaisson, M., & Gingeras, T. R. (2013). STAR: ultrafast universal RNA-seq aligner. *Bioinformatics* , *29*(1), 15–21.

Eirin-Lopez, J. M., & Putnam, H. M. (2019). Marine Environmental Epigenetics. *Annual Review of Marine Science*, *11*, 335–368.

Feil, R., & Fraga, M. F. (2012). Epigenetics and the environment: emerging patterns and implications. *Nature Reviews. Genetics*, *13*(2), 97–109.

Fishman, B., & Tauber, E. (2024). Epigenetics and seasonal timing in animals: a concise review. *Journal of Comparative Physiology. A, Neuroethology, Sensory, Neural, and Behavioral Physiology*, *210*(4), 565–574.

Fuller, Z. L., Mocellin, V. J. L., Morris, L. A., Cantin, N., Shepherd, J., Sarre, L., Peng, J., Liao, Y., Pickrell, J., Andolfatto, P., Matz, M., Bay, L. K., & Przeworski, M. (2020). Population genetics of the coral *Acropora millepora*: Toward genomic prediction of bleaching. *Science*, *369*(6501). https://doi.org/10.1126/science.aba4674

Gatzmann, F., Falckenhayn, C., Gutekunst, J., Hanna, K., Raddatz, G., Carneiro, V. C., & Lyko, F. (2018). The methylome of the marbled crayfish links gene body methylation to stable expression of poorly accessible genes. *Epigenetics & Chromatin*, *11*(1), 57.

Gomez-Campo, K., Sanchez, R., Martinez-Rugerio, I., Yang, X., Maher, T., Osborne, C. C., Enriquez, S., Baums, I. B., Mackenzie, S. A., & Iglesias-Prieto, R. (2023). Phenotypic plasticity for improved light harvesting, in tandem with methylome repatterning in reef-building corals. *Molecular Ecology*, e17246.

Granados-Cifuentes, C., Bellantuono, A. J., Ridgway, T., Hoegh-Guldberg, O., & Rodriguez-Lanetty, M. (2013). High natural gene expression variation in the reef-building coral Acropora millepora: potential for acclimative and adaptive plasticity. *BMC Genomics*, *14*, 228.

Guerrero, L., & Bay, R. (2024). Patterns of methylation and transcriptional plasticity during thermal acclimation in a reef-building coral. *Evolutionary Applications*, *17*(7), e13757.

Hayes, R. L., & King, C. M. (1995). Induction of 70-kD heat shock protein in scleractinian corals by elevated temperature: significance for coral bleaching. *Molecular Marine Biology and Biotechnology*, *4*(1), 36–42.

Heo, J. B., & Sung, S. (2011). Vernalization-mediated epigenetic silencing by a long intronic noncoding RNA. *Science (New York, N.Y.)*, *331*(6013), 76–79.

Himanen, S. V., Puustinen, M. C., Da Silva, A. J., Vihervaara, A., & Sistonen, L. (2022). HSFs drive transcription of distinct genes and enhancers during oxidative stress and heat shock. *Nucleic Acids Research*, *50*(11), 6102–6115.

Hofmann, G. E. (2017). Ecological Epigenetics in Marine Metazoans. *Frontiers in Marine Science*, *4*, 4.

Horvath, R., Josephs, E. B., Pesquet, E., Stinchcombe, J. R., Wright, S. I., Scofield, D., & Slotte, T. (2021). Selection on accessible chromatin regions in Capsella grandiflora. *Molecular Biology and Evolution*. https://doi.org/10.1093/molbev/msab270

Huang, C., Leng, D., Sun, S., & Zhang, X. D. (2019). Re-analysis of the coral Acropora digitifera transcriptome reveals a complex lncRNAs-mRNAs interaction network implicated in Symbiodinium infection. *BMC Genomics*, *20*(1), 48.

Ishii, Y., Maruyama, S., Takahashi, H., Aihara, Y., Yamaguchi, T., Yamaguchi, K., Shigenobu, S., Kawata, M., Ueno, N., & Minagawa, J. (2019). Global shifts in gene expression profiles accompanied with environmental changes in cnidarian-dinoflagellate endosymbiosis. *G3 (Bethesda, Md.)*, *9*(7), 2337–2347.

Jha, U. C., Nayyar, H., Roychowdhury, R., Prasad, P. V. V., Parida, S. K., & Siddique, K. H. M. (2023). Non-coding RNAs (ncRNAs) in plant: Master regulators for adapting to extreme temperature conditions. *Plant Physiology and Biochemistry*, *205*(108164), 108164.

Jueterbock, A., Boström, C., Coyer, J. A., Olsen, J. L., Kopp, M., Dhanasiri, A. K. S., Smolina, I., Arnaud-Haond, S., Van de Peer, Y., & Hoarau, G. (2020). The seagrass methylome is associated with variation in photosynthetic performance among clonal shoots. *Frontiers in Plant Science*, *11*, 571646.

Kilvitis, H. J., Alvarez, M., Foust, C. M., Schrey, A. W., Robertson, M., & Richards, C. L. (2014). Ecological Epigenetics. In C. R. Landry & N. Aubin-Horth (Eds.), *Ecological Genomics: Ecology and the Evolution of Genes and Genomes* (pp. 191–210). Springer Netherlands.

Kindgren, P., Ard, R., Ivanov, M., & Marquardt, S. (2018). Transcriptional read-through of the long non-coding RNA SVALKA governs plant cold acclimation. *Nature Communications*, *9*(1), 4561.

Klemm, S. L., Shipony, Z., & Greenleaf, W. J. (2019). Chromatin accessibility and the regulatory epigenome. *Nature Reviews. Genetics*, *20*(4), 207–220.

Klughammer, J., Romanovskaia, D., Nemc, A., Posautz, A., Seid, C. A., Schuster, L. C., Keinath, M. C., Lugo Ramos, J. S., Kosack, L., Evankow, A., Printz, D., Kirchberger, S., Ergüner, B., Datlinger, P., Fortelny, N., Schmidl, C., Farlik, M., Skjærven, K., Bergthaler, A., … Bock, C. (2023). Comparative analysis of genome-scale, base-resolution DNA methylation profiles across 580 animal species. *Nature Communications*, *14*(1), 232.

Lamka, G. F., Harder, A. M., Sundaram, M., Schwartz, T. S., Christie, M. R., DeWoody, J. A., & Willoughby, J. R. (2022). Epigenetics in Ecology, Evolution, and Conservation. *Frontiers in Ecology and Evolution*, *10*. https://doi.org/10.3389/fevo.2022.871791

Lancaster, L. T., Fuller, Z. L., Berger, D., Barbour, M. A., Jentoft, S., & Wellenreuther, M. (2022). Understanding climate change response in the age of genomics. *The Journal of Animal Ecology*, *91*(6), 1056–1063.

Langmead, B., & Salzberg, S. L. (2012). Fast gapped-read alignment with Bowtie 2. *Nature Methods*, *9*(4), 357–359.

Li, H., Handsaker, B., Wysoker, A., Fennell, T., Ruan, J., Homer, N., Marth, G., Abecasis, G., Durbin, R., & 1000 Genome Project Data Processing Subgroup. (2009). The Sequence Alignment/Map format and SAMtools. *Bioinformatics* , *25*(16), 2078–2079.

Li, Y., Liew, Y. J., Cui, G., Cziesielski, M. J., Zahran, N., Michell, C. T., Voolstra, C. R., & Aranda, M. (2018). DNA methylation regulates transcriptional homeostasis of algal endosymbiosis in the coral model Aiptasia. *Science Advances*, *4*(8), eaat2142.

Liew, Y. J., Aranda, M., Carr, A., Baumgarten, S., Zoccola, D., Tambutté, S., Allemand, D., Micklem, G., & Voolstra, C. R. (2014). Identification of microRNAs in the coral Stylophora pistillata. *PloS One*, *9*(3), e91101.

Lindner, M., Laine, V. N., Verhagen, I., Viitaniemi, H. M., Visser, M. E., van Oers, K., & Husby, A. (2020). Epigenetic mediation of the onset of reproduction in a songbird. In *Cold Spring Harbor Laboratory* (p. 2020.02.01.929968). https://doi.org/10.1101/2020.02.01.929968

Louis, Y. D., Bhagooli, R., Kenkel, C. D., Baker, A. C., & Dyall, S. D. (2017). Gene expression biomarkers of heat stress in scleractinian corals: Promises and limitations. *Comparative Biochemistry and Physiology. Toxicology & Pharmacology: CBP*, *191*, 63–77.

Love, M. I., Huber, W., & Anders, S. (2014). Moderated estimation of fold change and dispersion for RNA-seq data with DESeq2. *Genome Biology*, *15*(12), 550.

Majerová, E., & Drury, C. (2022). Thermal preconditioning in a reef-building coral alleviates oxidative damage through a BI-1-mediated antioxidant response. *Frontiers in Marine Science*, *9*. https://doi.org/10.3389/fmars.2022.971332

Martin, M. (2011). Cutadapt removes adapter sequences from high-throughput sequencing reads. *EMBnet.Journal*, *17*(1), 10.

Meyer, E., Aglyamova, G. V., & Matz, M. V. (2011). Profiling gene expression responses of coral larvae (Acropora millepora) to elevated temperature and settlement inducers using a novel RNA-Seq procedure: RNA-Seq EXPRESSION PROFILING CORAL LARVAE. *Molecular Ecology*, *20*(17), 3599–3616.

Montefiori, L., Hernandez, L., Zhang, Z., Gilad, Y., Ober, C., Crawford, G., Nobrega, M., & Jo Sakabe, N. (2017). Reducing mitochondrial reads in ATAC-seq using CRISPR/Cas9. *Scientific Reports*, *7*(1), 2451.

Noguera, J. C., & Velando, A. (2019). Bird embryos perceive vibratory cues of predation risk from clutch mates. *Nature Ecology & Evolution*, *3*(8), 1225–1232.

Picard. (n.d.). Retrieved April 20, 2023, from http://broadinstitute.github.io/picard/

Pliner, H. A., Packer, J. S., McFaline-Figueroa, J. L., Cusanovich, D. A., Daza, R. M., Aghamirzaie, D., Srivatsan, S., Qiu, X., Jackson, D., Minkina, A., Adey, A. C., Steemers, F. J., Shendure, J., & Trapnell, C. (2018). Cicero predicts cis-regulatory DNA interactions from single-cell chromatin accessibility data. *Molecular Cell*, *71*(5), 858-871.e8.

Puri, D., Gala, H., Mishra, R., & Dhawan, J. (2015). High-wire act: the poised genome and cellular memory. *The FEBS Journal*, *282*(9), 1675–1691.

Putnam, H. M., Davidson, J. M., & Gates, R. D. (2016). Ocean acidification influences host DNA methylation and phenotypic plasticity in environmentally susceptible corals. *Evolutionary Applications*, *9*(9), 1165–1178.

R Core Team (2023). R: A Language and Environment for Statistical Computing. R Foundation for Statistical Computing, Vienna, Austria. https://www.R-project.org/.

Roberts, S. B., & Gavery, M. R. (2012). Is There a Relationship between DNA Methylation and Phenotypic Plasticity in Invertebrates? *Frontiers in Physiology*, *2*, 116.

Rodriguez-Casariego, J. A., Cunning, R., Baker, A. C., & Eirin-Lopez, J. M. (2022). Symbiont shuffling induces differential DNA methylation responses to thermal stress in the coral Montastraea cavernosa. *Molecular Ecology*, *31*(2), 588–602.

Rodriguez-Casariego, J. A., Ladd, M. C., Shantz, A. A., Lopes, C., Cheema, M. S., Kim, B., Roberts, S. B., Fourqurean, J. W., Ausio, J., Burkepile, D. E., & Eirin-Lopez, J. M. (2018). Coral epigenetic responses to nutrient stress: Histone H2A.X phosphorylation dynamics and DNA methylation in the staghorn coral Acropora cervicornis. *Ecology and Evolution*, *8*(23), 12193–12207.

Rodríguez-Casariego, J. A., Mercado-Molina, A. E., Garcia-Souto, D., Ortiz-Rivera, I. M., Lopes, C., Baums, I. B., Sabat, A. M., & Eirin-Lopez, J. M. (2020). Genome-wide DNA methylation analysis reveals a conserved epigenetic response to seasonal environmental variation in the staghorn coral Acropora cervicornis. *Frontiers in Marine Science*, *7*, 560424.

Roquis, D., Cosseau, C., Brener Raffalli, K., Romans, P., Masanet, P., Mitta, G., Grunau, C., & Vidal-Dupiol, J. (2022). The tropical coral Pocillopora acuta displays an unusual chromatin structure and shows histone H3 clipping plasticity upon bleaching. *Wellcome Open Research*, *6*, 195.

Roscito, J. G., Sameith, K., Parra, G., Langer, B. E., Petzold, A., Moebius, C., Bickle, M., Rodrigues, M. T., & Hiller, M. (2018). Phenotype loss is associated with widespread divergence of the gene regulatory landscape in evolution. *Nature Communications*, *9*(1), 4737.

Rose, A. B. (2018). Introns as gene regulators: A brick on the accelerator. *Frontiers in Genetics*, *9*, 672.

Shoaib, M., Chen, Q., Shi, X., Nair, N., Prasanna, C., Yang, R., Walter, D., Frederiksen, K. S., Einarsson, H., Svensson, J. P., Liu, C. F., Ekwall, K., Lerdrup, M., Nordenskiöld, L., & Sørensen, C. S. (2021). Histone H4 lysine 20 mono-methylation directly facilitates chromatin openness and promotes transcription of housekeeping genes. *Nature Communications*, *12*(1), 4800.

Smallwood, S. A., Tomizawa, S.-I., Krueger, F., Ruf, N., Carli, N., Segonds-Pichon, A., Sato, S., Hata, K., Andrews, S. R., & Kelsey, G. (2011). Dynamic CpG island methylation landscape in oocytes and preimplantation embryos. *Nature Genetics*, *43*(8), 811–814.

Sotomayor-Lugo, F., Iglesias-Barrameda, N., Castillo-Aleman, Y. M., Casado-Hernandez, I., Villegas-Valverde, C. A., Bencomo-Hernandez, A. A., Ventura-Carmenate, Y., & Rivero-Jimenez, R. A. (2024). The dynamics of histone modifications during mammalian zygotic genome activation. *International Journal of Molecular Sciences*, *25*(3). https://doi.org/10.3390/ijms25031459

Stark, R., & Brown, G. D. (2012). *DiffBind : Differential binding analysis of ChIP-Seq peak data*. https://www.semanticscholar.org/paper/DiffBind-%3A-Differential-binding-analysis-of-peak-Stark-Brown/c60a315c43b2e4acf3db8076d85ade500378dcdb

Suzuki, M. M., & Bird, A. (2008). DNA methylation landscapes: provocative insights from epigenomics. *Nature Reviews. Genetics*, *9*(6), 465–476.

Tsompana, M., & Buck, M. J. (2014). Chromatin accessibility: a window into the genome. *Epigenetics & Chromatin*, *7*(1), 33.

Turner, B. M. (2009). Epigenetic responses to environmental change and their evolutionary implications. *Philosophical Transactions of the Royal Society of London. Series B, Biological Sciences*, *364*(1534), 3403–3418.

Voolstra, C. R., Buitrago-López, C., Perna, G., Cárdenas, A., Hume, B. C. C., Rädecker, N., & Barshis, D. J. (2020). Standardized short-term acute heat stress assays resolve historical differences in coral thermotolerance across microhabitat reef sites. *Global Change Biology*. https://doi.org/10.1111/gcb.15148

Wang, Q., Li, M., Wu, T., Zhan, L., Li, L., Chen, M., Xie, W., Xie, Z., Hu, E., Xu, S., & Yu, G. (2022). Exploring Epigenomic Datasets by ChIPseeker. *Current Protocols*, *2*(10), e585.

Weizman, E., & Levy, O. (2019). The role of chromatin dynamics under global warming response in the symbiotic coral model Aiptasia. *Communications Biology*, *2*, 282.

Winters, G., Holzman, R., Blekhman, A., Beer, S., & Loya, Y. (2009). Photographic assessment of coral chlorophyll contents: Implications for ecophysiological studies and coral monitoring. *Journal of Experimental Marine Biology and Ecology*, *380*(1), 25–35.

Yan, F., Powell, D. R., Curtis, D. J., & Wong, N. C. (2020). From reads to insight: a hitchhiker's guide to ATAC-seq data analysis. *Genome Biology*, *21*(1), 22.

Yang, J. H., & Hansen, A. S. (2024). Enhancer selectivity in space and time: from enhancer-promoter interactions to promoter activation. *Nature Reviews. Molecular Cell Biology*, *25*(7), 574–591.

Ying, H., Hayward, D. C., Klimovich, A., Bosch, T. C. G., Baldassarre, L., Neeman, T., Forêt, S., Huttley, G., Reitzel, A. M., Fraune, S., Ball, E. E., & Miller, D. J. (2022). The Role of DNA Methylation in

Genome Defense in Cnidaria and Other Invertebrates. *Molecular Biology and Evolution*, *39*(2). https://doi.org/10.1093/molbev/msac018

Zhang, Y., Liu, T., Meyer, C. A., Eeckhoute, J., Johnson, D. S., Bernstein, B. E., Nusbaum, C., Myers, R. M., Brown, M., Li, W., & Liu, X. S. (2008). Model-based analysis of ChIP-Seq (MACS). *Genome Biology*, *9*(9), R137.

Figures and Tables

Figure 2.1: Experimental design. The left panel illustrates treatments designed to induce variation in thermal history. Fragments held at 24.5°C are the thermal history controls. Triangles indicate time points for heat stress assay. The right panel depicts heat stress assay temperature profile. Heat stress assays were conducted on fragments with varying thermal histories, alongside thermal history controls. We preserved tissue from this experiment for 3'TagSeq only (i.e., ATAC-seq was not performed on any of these fragments).

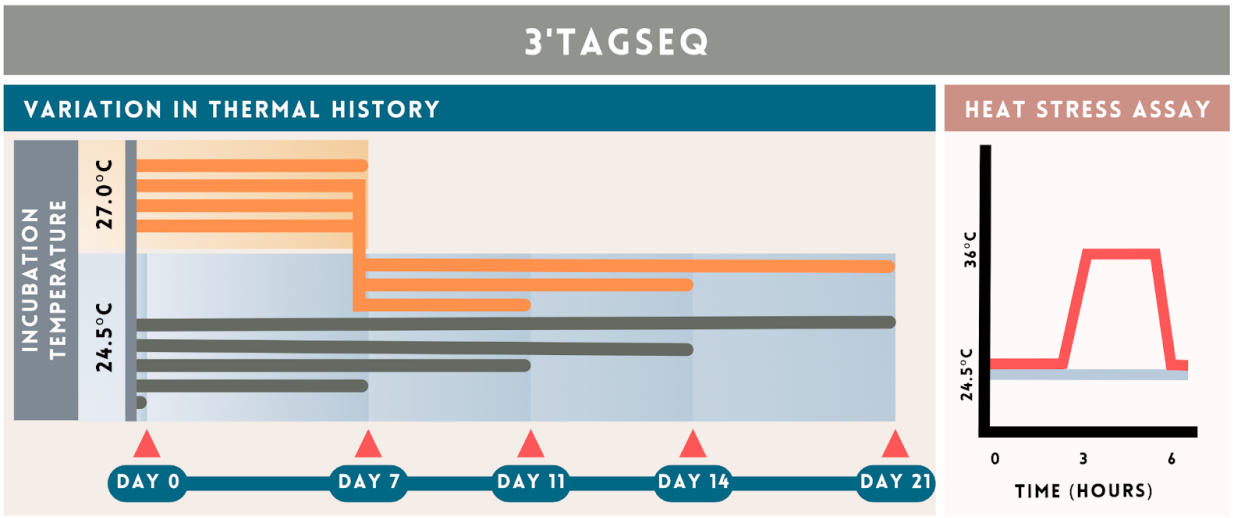

Figure 2.2: (A) Boxplot of Fv/Fm Yield showing a reduction in Fv/Fm (Photosystem II yield of algal symbiont) in heat-stressed *A. millepora* fragments compared to control fragments. (B) Boxplot of R channel intensity showing an increased R channel intensity (higher visible bleaching score) in heat-stressed *A. millepora* fragments compared to the control fragments. (C) Boxplot of glutathione reductase (GR) activity showing reduced GR activity in heat-stressed *A. millepora* fragments have reduced GR activity compared to the control fragments. (D) PCA of gene expression in heat-stressed and control fragments of *A. millepora* reveals distinct clustering along the PC1 axis, separating the heat-stressed fragments from the controls.

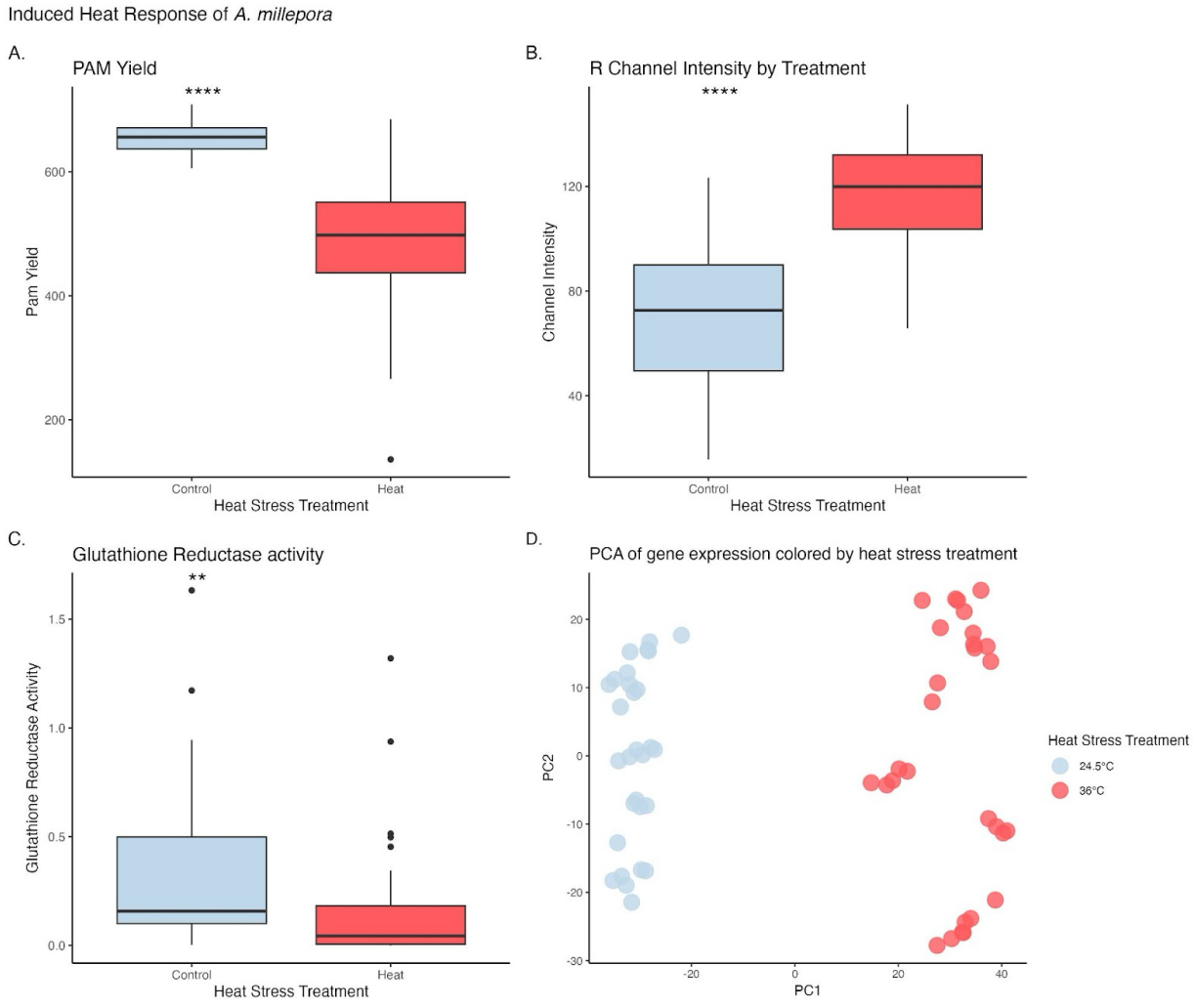

Figure 2.3: Annotated open chromatin regions in *A. millepora.* Distal intergenic regions compose 50.05% of the open regions, and promoters compose 35.80% of the open regions.

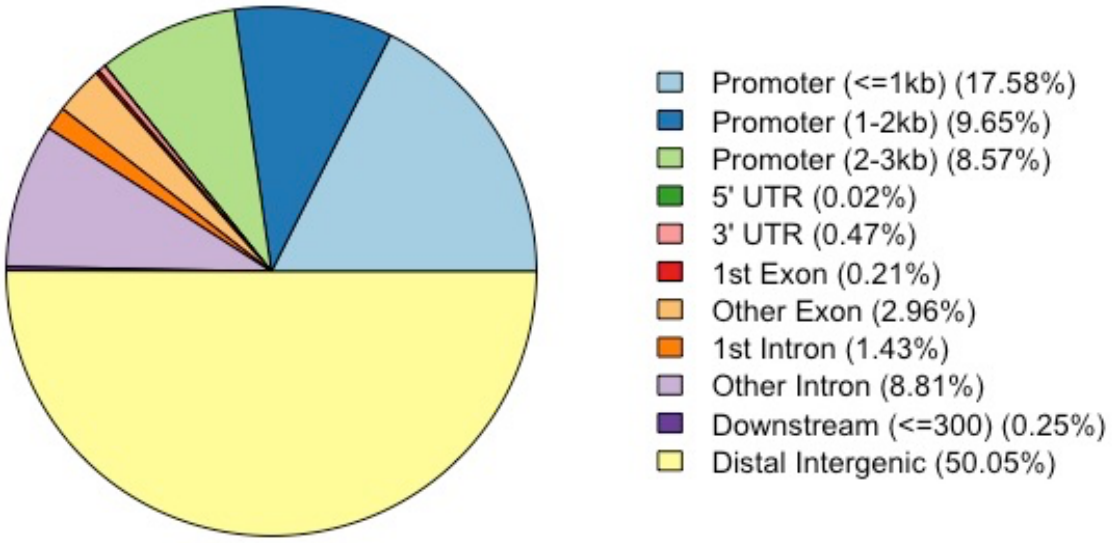

Figure 2.4: (A) Relationship between promoter accessibility and gene expression. Genes in the 5th quintile of overall mean expression exhibit the highest chromatin accessibility around the transcription start site (TSS) compared to the genes in lower expression quintiles. (B) Relationship between promoter accessibility and gene expression variation. Genes with stable expression exhibit higher chromatin accessibility around the TSS compared to genes with variable expression.

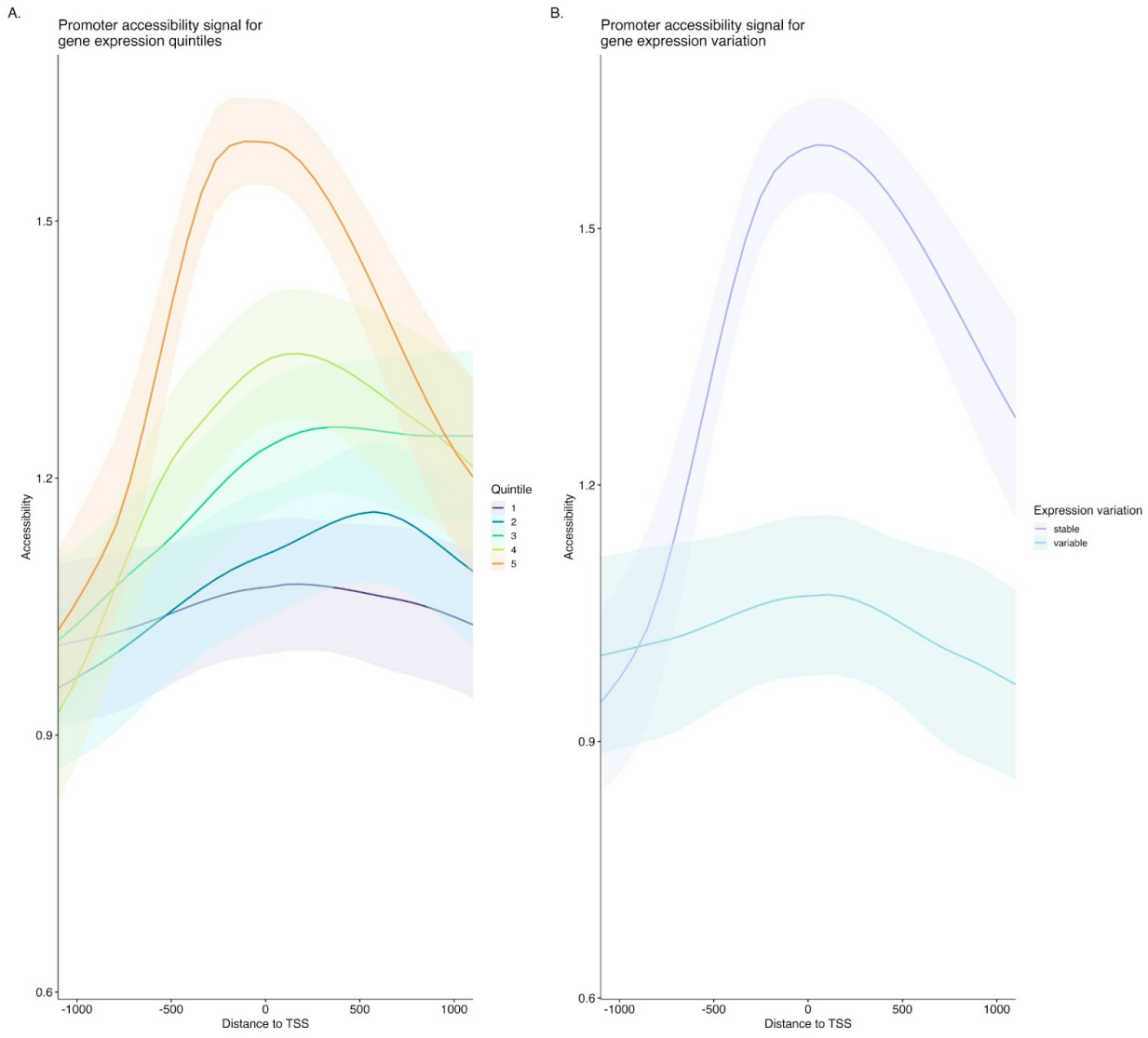

Figure 2.5: (A) Mean gene expression of heat response genes with open and closed (inaccessible) promoters. Heat response genes with open promoters exhibit no significant difference in mean expression as heat response genes with closed promoters (p-value = 0.98). (B) Log_2 fold change of heat response genes with open and closed promoters. Heat response genes with open promoters exhibit a larger magnitude of response to heat stress compared to those with closed promoters (p-value < 0.01).

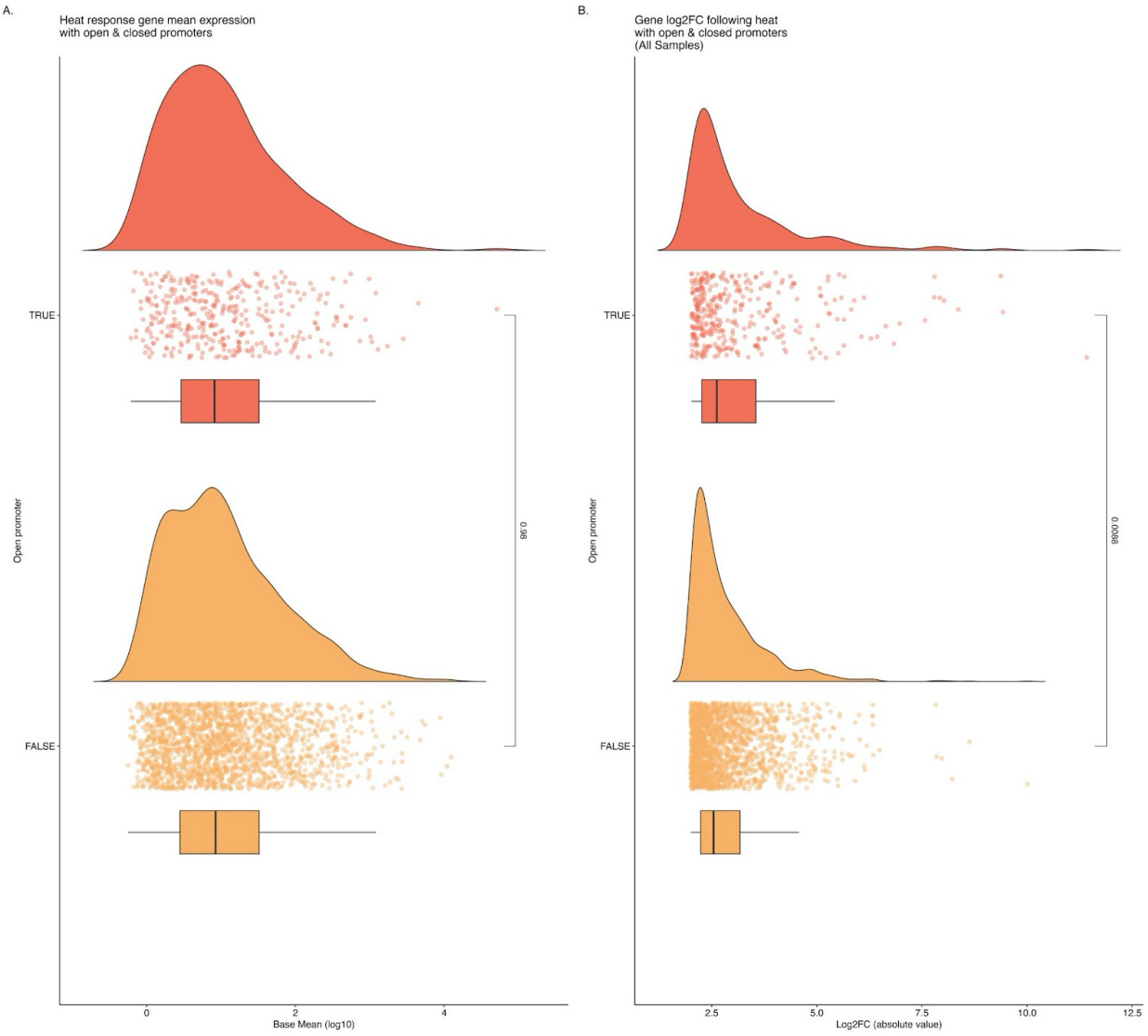

Figure 2.6: Boxplot of directional log_2 fold change of heat response genes with open and closed promoters. Heat response genes are generally upregulated following heat stress compared to those with closed promoters (p-value < 0.001).

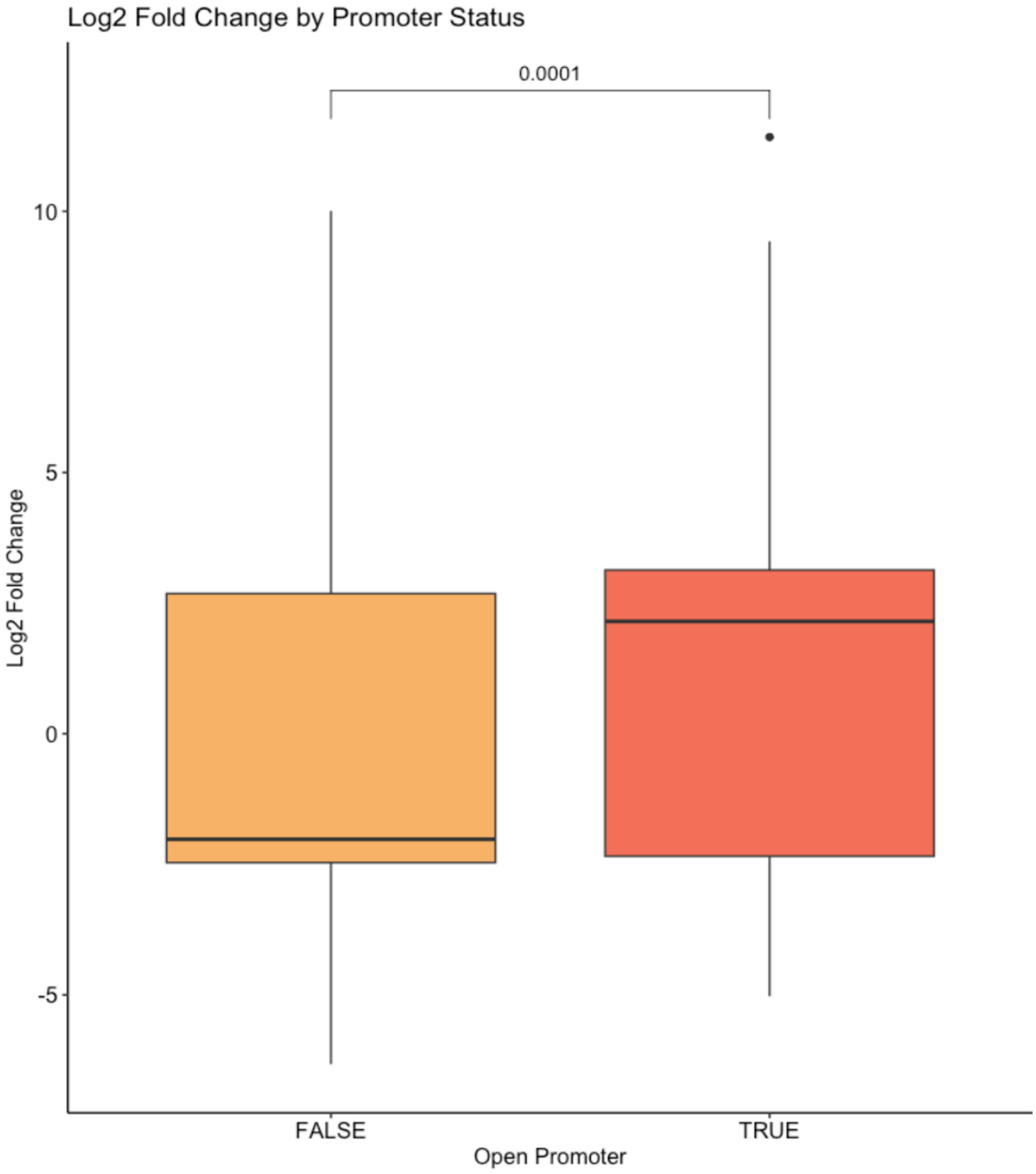

Table 2.1: Gene Ontology (GO) terms of open chromatin promoters. Table shows the results from a GO enrichment analysis of open chromatin promoters using the R package, topGO v. 2.50.0. We compared the list of open chromatin promoters in the consensus against a background of all *A. millepora* annotated transcripts. Enriched GO terms were identified with the classic Fisher's test with a p-value < 0.01 and at least 10 genes within each category. GO terms are contained within ontology types: Biological Processes (BP), Cellular Components (CC), and Molecular Functions (MF).

Type	GO ID	Term	p-value
BP	GO:0001817	regulation of cytokine production	0.00011
BP	GO:0002684	positive regulation of immune system process	0.00011
BP	GO:0031333	negative regulation of protein-containing complex assembly	0.00012
BP	GO:0075733	intracellular transport of virus	0.00013
BP	GO:0002682	regulation of immune system process	0.00015
BP	GO:0046794	transport of virus	0.00015
BP	GO:0038061	non-canonical NF-kappaB signal transduction	0.00017
BP	GO:0048147	negative regulation of fibroblast proliferation	0.00019
BP	GO:0050777	negative regulation of immune response	0.0002
BP	GO:0043207	response to external biotic stimulus	0.00021
BP	GO:0051707	response to other organism	0.00021
BP	GO:0050688	regulation of defense response to virus	0.00022
BP	GO:0009607	response to biotic stimulus	0.00023
BP	GO:0002832	negative regulation of response to biotic stimulus	0.00028
BP	GO:0075732	viral penetration into host nucleus	0.00031
BP	GO:0032479	regulation of type I interferon production	0.00032
BP	GO:0032606	type I interferon production	0.00032
BP	GO:0001816	cytokine production	0.00036
BP	GO:0043170	macromolecule metabolic process	0.00041
BP	GO:0031348	negative regulation of defense response	0.00043
BP	GO:0043433	negative regulation of DNA-binding transcription factor activity	0.00043
BP	GO:0032635	interleukin-6 production	0.00045
BP	GO:0032675	regulation of interleukin-6 production	0.00045
BP	GO:0035278	miRNA-mediated gene silencing by inhibition of translation	0.00064
BP	GO:0016032	viral process	0.00076
BP	GO:0010172	embryonic body morphogenesis	0.00076
BP	GO:0002376	immune system process	0.00112
BP	GO:0010629	negative regulation of gene expression	0.00123
BP	GO:0043254	regulation of protein-containing complex assembly	0.00132
BP	GO:0072089	stem cell proliferation	0.00151
BP	GO:0009617	response to bacterium	0.00155
BP	GO:0044237	cellular metabolic process	0.00165
BP	GO:0050678	regulation of epithelial cell proliferation	0.00183
BP	GO:0032102	negative regulation of response to external stimulus	0.00218
BP	GO:0010586	miRNA metabolic process	0.00218
BP	GO:0051090	regulation of DNA-binding transcription factor activity	0.00285
BP	GO:0006807	nitrogen compound metabolic process	0.00298
BP	GO:0035195	miRNA-mediated post-transcriptional gene silencing	0.00356

BP	GO:0044238	primary metabolic process	0.00415
BP	GO:0016567	protein ubiquitination	0.00421
BP	GO:0002683	negative regulation of immune system process	0.00451
BP	GO:0035194	regulatory ncRNA-mediated post-transcriptional gene silencing	0.00559
BP	GO:0032446	protein modification by small protein conjugation	0.00572
BP	GO:0060964	regulation of miRNA-mediated gene silencing	0.00582
BP	GO:0002224	toll-like receptor signaling pathway	0.00618
BP	GO:0048145	regulation of fibroblast proliferation	0.00658
BP	GO:0050680	negative regulation of epithelial cell proliferation	0.00668
BP	GO:0048144	fibroblast proliferation	0.00717
BP	GO:0061351	neural precursor cell proliferation	0.00779
BP	GO:0050673	epithelial cell proliferation	0.00827
BP	GO:0032197	retrotransposition	0.00828
BP	GO:0060966	regulation of gene silencing by regulatory ncRNA	0.00828
BP	GO:1900368	regulation of post-transcriptional gene silencing by regulatory ncRNA	0.00828
BP	GO:0010558	negative regulation of macromolecule biosynthetic process	0.0092
BP	GO:0045321	leukocyte activation	0.00924
BP	GO:0006313	DNA transposition	0.00961
CC	GO:0033655	host cell cytoplasm part	0.00017
CC	GO:0097228	sperm principal piece	0.0002
CC	GO:0042025	host cell nucleus	0.00026
CC	GO:0000943	retrotransposon nucleocapsid	0.00082
CC	GO:0030666	endocytic vesicle membrane	0.00093
CC	GO:0030670	phagocytic vesicle membrane	0.00439
CC	GO:0035770	ribonucleoprotein granule	0.0052
CC	GO:0036464	cytoplasmic ribonucleoprotein granule	0.0062
MF	GO:0004540	RNA nuclease activity	0.00019
MF	GO:1990381	ubiquitin-specific protease binding	0.00021
MF	GO:0003677	DNA binding	0.00024
MF	GO:0016787	hydrolase activity	0.0011
MF	GO:0035198	miRNA binding	0.00297
MF	GO:0016303	1-phosphatidylinositol-3-kinase activity	0.00377
MF	GO:0051082	unfolded protein binding	0.00385
MF	GO:0061980	regulatory RNA binding	0.00662
MF	GO:0001727	lipid kinase activity	0.00725

Table 2.2: Gene Ontology (GO) terms of heat response genes with open or closed chromatin promoters. Table shows the results from a GO enrichment analysis of heat response genes with open chromatin promoters in at least 2 replicates using the R package, topGO v. 2.50.0. We compared the list of heat response genes with open and closed chromatin promoters against a background of all transcripts that passed our quality filters. Enriched GO terms were identified with the classic Fisher's test with a p-value < 0.01 and at least 10 genes within each category. GO terms are contained within ontology types: Biological Processes (BP), Cellular Components (CC), and Molecular Functions (MF).

Promoter State	Type	GO ID	Term	p-value
Open	BP	GO:0071900	regulation of protein serine/threonine kinase activity	0.00018
Open	BP	GO:0045859	regulation of protein kinase activity	0.0007
Open	BP	GO:0001932	regulation of protein phosphorylation	0.00162
Open	BP	GO:0034097	response to cytokine	0.0018
Open	BP	GO:0043549	regulation of kinase activity	0.00233
Open	BP	GO:0042325	regulation of phosphorylation	0.00378
Open	BP	GO:0001944	vasculature development	0.0038
Open	BP	GO:0006950	response to stress	0.00404
Open	BP	GO:0042981	regulation of apoptotic process	0.00463
Open	BP	GO:0043067	regulation of programmed cell death	0.006
Open	BP	GO:0001568	blood vessel development	0.00604
Open	BP	GO:0071345	cellular response to cytokine stimulus	0.00766
Open	BP	GO:0009617	response to bacterium	0.00817
Open	BP	GO:0043066	negative regulation of apoptotic process	0.0091
Open	BP	GO:0019752	carboxylic acid metabolic process	0.00955
Open	BP	GO:0097190	apoptotic signaling pathway	0.00976
Closed	BP	GO:0045621	positive regulation of lymphocyte differentiation	0.0001
Closed	BP	GO:0046631	alpha-beta T cell activation	0.0001
Closed	BP	GO:0060021	roof of mouth development	0.0001
Closed	BP	GO:0051094	positive regulation of developmental process	0.00012
Closed	BP	GO:0035239	tube morphogenesis	0.00012
Closed	BP	GO:0050793	regulation of developmental process	0.00014
Closed	BP	GO:0051093	negative regulation of developmental process	0.00014
Closed	BP	GO:0009887	animal organ morphogenesis	0.00015
Closed	BP	GO:0015849	organic acid transport	0.00015
Closed	BP	GO:0046942	carboxylic acid transport	0.00015
Closed	BP	GO:0046323	glucose import	0.00015
Closed	BP	GO:0042446	hormone biosynthetic process	0.00016
Closed	BP	GO:0072006	nephron development	0.00016
Closed	BP	GO:0002521	leukocyte differentiation	0.00016
Closed	BP	GO:0072359	circulatory system development	0.00019
Closed	BP	GO:0050866	negative regulation of cell activation	0.00021
Closed	BP	GO:0050870	positive regulation of T cell activation	0.00022
Closed	BP	GO:1903039	positive regulation of leukocyte cell-cell adhesion	0.00022
Closed	BP	GO:0048514	blood vessel morphogenesis	0.00023
Closed	BP	GO:1902107	positive regulation of leukocyte differentiation	0.00025
Closed	BP	GO:1903708	positive regulation of hemopoiesis	0.00025
Closed	BP	GO:0030856	regulation of epithelial cell differentiation	0.00026

Closed	BP	GO:1902106	negative regulation of leukocyte differentiation	0.00029
Closed	BP	GO:0002460	adaptive immune response based on somatic recombination of immune receptors built from immunoglobulin superfamily domains	0.0003
Closed	BP	GO:0055085	transmembrane transport	0.00034
Closed	BP	GO:1903131	mononuclear cell differentiation	0.00035
Closed	BP	GO:0071363	cellular response to growth factor stimulus	0.00035
Closed	BP	GO:1903706	regulation of hemopoiesis	0.00038
Closed	BP	GO:1903707	negative regulation of hemopoiesis	0.00038
Closed	BP	GO:0007159	leukocyte cell-cell adhesion	0.00039
Closed	BP	GO:0001568	blood vessel development	0.00044
Closed	BP	GO:0015711	organic anion transport	0.00044
Closed	BP	GO:0001944	vasculature development	0.00045
Closed	BP	GO:0009888	tissue development	0.00045
Closed	BP	GO:0050863	regulation of T cell activation	0.00047
Closed	BP	GO:0061448	connective tissue development	0.00047
Closed	BP	GO:0048522	positive regulation of cellular process	0.00049
Closed	BP	GO:0070848	response to growth factor	0.00053
Closed	BP	GO:0002376	immune system process	0.00055
Closed	BP	GO:0072080	nephron tubule development	0.00063
Closed	BP	GO:1903037	regulation of leukocyte cell-cell adhesion	0.00064
Closed	BP	GO:1902074	response to salt	0.00064
Closed	BP	GO:0010604	positive regulation of macromolecule metabolic process	0.00071
Closed	BP	GO:0002366	leukocyte activation involved in immune response	0.00082
Closed	BP	GO:0007155	cell adhesion	0.00084
Closed	BP	GO:0090287	regulation of cellular response to growth factor stimulus	0.00084
Closed	BP	GO:0009893	positive regulation of metabolic process	0.00084
Closed	BP	GO:0050865	regulation of cell activation	0.00086
Closed	BP	GO:0001525	angiogenesis	0.00086
Closed	BP	GO:0002263	cell activation involved in immune response	0.00091
Closed	BP	GO:0042221	response to chemical	0.00092
Closed	BP	GO:0007167	enzyme-linked receptor protein signaling pathway	0.00094
Closed	BP	GO:0006955	immune response	0.00098
Closed	BP	GO:0001503	ossification	0.00099
Closed	BP	GO:0051249	regulation of lymphocyte activation	0.00099
Closed	BP	GO:0006694	steroid biosynthetic process	0.00101
Closed	BP	GO:0072009	nephron epithelium development	0.00101
Closed	BP	GO:0006915	apoptotic process	0.00101
Closed	BP	GO:0002819	regulation of adaptive immune response	0.00102
Closed	BP	GO:0002252	immune effector process	0.00104
Closed	BP	GO:0001658	branching involved in ureteric bud morphogenesis	0.00105
Closed	BP	GO:0060324	face development	0.00108
Closed	BP	GO:0008219	cell death	0.00112
Closed	BP	GO:0045596	negative regulation of cell differentiation	0.00113
Closed	BP	GO:0016125	sterol metabolic process	0.00116
Closed	BP	GO:1901700	response to oxygen-containing compound	0.00119
Closed	BP	GO:0034764	positive regulation of transmembrane transport	0.00129
Closed	BP	GO:0012501	programmed cell death	0.00129
Closed	BP	GO:0051247	positive regulation of protein metabolic process	0.00133
Closed	BP	GO:0007154	cell communication	0.00135
Closed	BP	GO:0007169	transmembrane receptor protein tyrosine kinase signaling pathway	0.00137
Closed	BP	GO:0048705	skeletal system morphogenesis	0.0016
Closed	BP	GO:0002443	leukocyte mediated immunity	0.00165
Closed	BP	GO:0051173	positive regulation of nitrogen compound metabolic process	0.00167
Closed	BP	GO:0043549	regulation of kinase activity	0.00181
Closed	BP	GO:0009636	response to toxic substance	0.00181
Closed	BP	GO:0035264	multicellular organism growth	0.00181

Closed	BP	GO:0044344	cellular response to fibroblast growth factor stimulus	0.00182
Closed	BP	GO:0002822	regulation of adaptive immune response based on somatic recombination of immune receptors built from immunoglobulin superfamily domains	0.00185
Closed	BP	GO:0007166	cell surface receptor signaling pathway	0.00187
Closed	BP	GO:0060675	ureteric bud morphogenesis	0.00194
Closed	BP	GO:0072171	mesonephric tubule morphogenesis	0.00194
Closed	BP	GO:0002768	immune response-regulating cell surface receptor signaling pathway	0.00209
Closed	BP	GO:0033674	positive regulation of kinase activity	0.00213
Closed	BP	GO:0051251	positive regulation of lymphocyte activation	0.00226
Closed	BP	GO:0045595	regulation of cell differentiation	0.00229
Closed	BP	GO:0006952	defense response	0.00234
Closed	BP	GO:0002695	negative regulation of leukocyte activation	0.00234
Closed	BP	GO:0010035	response to inorganic substance	0.00247
Closed	BP	GO:0065008	regulation of biological quality	0.00251
Closed	BP	GO:0000122	negative regulation of transcription by RNA polymerase II	0.00256
Closed	BP	GO:0051250	negative regulation of lymphocyte activation	0.00257
Closed	BP	GO:0022409	positive regulation of cell-cell adhesion	0.00271
Closed	BP	GO:0061326	renal tubule development	0.00271
Closed	BP	GO:0009725	response to hormone	0.00271
Closed	BP	GO:0030154	cell differentiation	0.00277
Closed	BP	GO:0008203	cholesterol metabolic process	0.00283
Closed	BP	GO:0048869	cellular developmental process	0.00283
Closed	BP	GO:0002449	lymphocyte mediated immunity	0.0029
Closed	BP	GO:0071774	response to fibroblast growth factor	0.00297
Closed	BP	GO:0002250	adaptive immune response	0.00298
Closed	BP	GO:0045860	positive regulation of protein kinase activity	0.00308
Closed	BP	GO:0002694	regulation of leukocyte activation	0.00316
Closed	BP	GO:0031328	positive regulation of cellular biosynthetic process	0.00329
Closed	BP	GO:0034762	regulation of transmembrane transport	0.00331
Closed	BP	GO:0072593	reactive oxygen species metabolic process	0.00342
Closed	BP	GO:0008217	regulation of blood pressure	0.00343
Closed	BP	GO:0031214	biomineral tissue development	0.00343
Closed	BP	GO:0031325	positive regulation of cellular metabolic process	0.00359
Closed	BP	GO:0035556	intracellular signal transduction	0.00366
Closed	BP	GO:0001656	metanephros development	0.00368
Closed	BP	GO:0006468	protein phosphorylation	0.00372
Closed	BP	GO:0002711	positive regulation of T cell mediated immunity	0.00378
Closed	BP	GO:0046777	protein autophosphorylation	0.0039
Closed	BP	GO:0002429	immune response-activating cell surface receptor signaling pathway	0.00392
Closed	BP	GO:0007165	signal transduction	0.00393
Closed	BP	GO:0010557	positive regulation of macromolecule biosynthetic process	0.00396
Closed	BP	GO:0008543	fibroblast growth factor receptor signaling pathway	0.00399
Closed	BP	GO:0009605	response to external stimulus	0.00404
Closed	BP	GO:0002682	regulation of immune system process	0.00406
Closed	BP	GO:0001932	regulation of protein phosphorylation	0.0042
Closed	BP	GO:0023052	signaling	0.00438
Closed	BP	GO:0072073	kidney epithelium development	0.0044
Closed	BP	GO:1902652	secondary alcohol metabolic process	0.00444
Closed	BP	GO:0009891	positive regulation of biosynthetic process	0.00447
Closed	BP	GO:0042325	regulation of phosphorylation	0.00449
Closed	BP	GO:0051781	positive regulation of cell division	0.00453
Closed	BP	GO:0001101	response to acid chemical	0.00458
Closed	BP	GO:0030183	B cell differentiation	0.00469
Closed	BP	GO:0010628	positive regulation of gene expression	0.0047
Closed	BP	GO:0048646	anatomical structure formation involved in morphogenesis	0.00477

Closed	BP	GO:0019220	regulation of phosphate metabolic process	0.00483
Closed	BP	GO:0045321	leukocyte activation	0.00491
Closed	BP	GO:0051174	regulation of phosphorus metabolic process	0.00503
Closed	BP	GO:0060429	epithelium development	0.00526
Closed	BP	GO:0050776	regulation of immune response	0.00549
Closed	BP	GO:0009314	response to radiation	0.0057
Closed	BP	GO:0045785	positive regulation of cell adhesion	0.00587
Closed	BP	GO:0008610	lipid biosynthetic process	0.00587
Closed	BP	GO:0051402	neuron apoptotic process	0.00589
Closed	BP	GO:0042476	odontogenesis	0.00602
Closed	BP	GO:0006865	amino acid transport	0.00626
Closed	BP	GO:0001934	positive regulation of protein phosphorylation	0.0063
Closed	BP	GO:0045859	regulation of protein kinase activity	0.00632
Closed	BP	GO:0043279	response to alkaloid	0.0064
Closed	BP	GO:0006629	lipid metabolic process	0.00662
Closed	BP	GO:0045765	regulation of angiogenesis	0.00697
Closed	BP	GO:0070661	leukocyte proliferation	0.00699
Closed	BP	GO:0010721	negative regulation of cell development	0.00707
Closed	BP	GO:0010562	positive regulation of phosphorus metabolic process	0.00708
Closed	BP	GO:0045937	positive regulation of phosphate metabolic process	0.00708
Closed	BP	GO:0002696	positive regulation of leukocyte activation	0.00711
Closed	BP	GO:0015698	inorganic anion transport	0.0072
Closed	BP	GO:0042327	positive regulation of phosphorylation	0.00729
Closed	BP	GO:0006357	regulation of transcription by RNA polymerase II	0.00742
Closed	BP	GO:0009628	response to abiotic stimulus	0.00742
Closed	BP	GO:0072078	nephron tubule morphogenesis	0.00743
Closed	BP	GO:0072088	nephron epithelium morphogenesis	0.00743
Closed	BP	GO:0051347	positive regulation of transferase activity	0.0075
Closed	BP	GO:0002709	regulation of T cell mediated immunity	0.0075
Closed	BP	GO:0051338	regulation of transferase activity	0.00753
Closed	BP	GO:0048583	regulation of response to stimulus	0.00762
Closed	BP	GO:0016310	phosphorylation	0.00813
Closed	BP	GO:0060284	regulation of cell development	0.0082
Closed	BP	GO:0030097	hemopoiesis	0.0083
Closed	BP	GO:0001657	ureteric bud development	0.00849
Closed	BP	GO:0002824	positive regulation of adaptive immune response based on somatic recombination of immune receptors built from immunoglobulin superfamily domains	0.00858
Closed	BP	GO:0016477	cell migration	0.0087
Closed	BP	GO:0050867	positive regulation of cell activation	0.00871
Closed	BP	GO:0030282	bone mineralization	0.00877
Closed	BP	GO:1901342	regulation of vasculature development	0.00903
Closed	BP	GO:0060993	kidney morphogenesis	0.00922
Closed	BP	GO:0051703	biological process involved in intraspecies interaction between organisms	0.00939
Closed	BP	GO:0061333	renal tubule morphogenesis	0.00939
Closed	BP	GO:0072028	nephron morphogenesis	0.00987
Closed	BP	GO:0001775	cell activation	0.00993
Closed	BP	GO:0050851	antigen receptor-mediated signaling pathway	0.00995
Closed	CC	GO:0005615	extracellular space	0.00028
Closed	CC	GO:0071944	cell periphery	0.00052
Closed	CC	GO:0045177	apical part of cell	0.00073
Closed	CC	GO:0016324	apical plasma membrane	0.00197
Closed	CC	GO:0016020	membrane	0.00206
Closed	CC	GO:0005886	plasma membrane	0.00258
Closed	CC	GO:0005581	collagen trimer	0.00269

Closed	MF	GO:0030546	signaling receptor activator activity	0.0001
Closed	MF	GO:0005342	organic acid transmembrane transporter activity	0.00044
Closed	MF	GO:0046943	carboxylic acid transmembrane transporter activity	0.00044
Closed	MF	GO:0008235	metalloexopeptidase activity	0.00054
Closed	MF	GO:0046872	metal ion binding	0.00059
Closed	MF	GO:0016836	hydro-lyase activity	0.00082
Closed	MF	GO:0038024	cargo receptor activity	0.00087
Closed	MF	GO:0005506	iron ion binding	0.00089
Closed	MF	GO:0016705	oxidoreductase activity, acting on paired donors, with incorporation or reduction of molecular oxygen	0.00091
Closed	MF	GO:0043169	cation binding	0.00092
Closed	MF	GO:0000977	RNA polymerase II transcription regulatory region sequence-specific DNA binding	0.00098
Closed	MF	GO:0015370	solute:sodium symporter activity	0.00103
Closed	MF	GO:0008514	organic anion transmembrane transporter activity	0.00111
Closed	MF	GO:0008083	growth factor activity	0.00121
Closed	MF	GO:0015294	solute:monoatomic cation symporter activity	0.00122
Closed	MF	GO:0000976	transcription cis-regulatory region binding	0.0014
Closed	MF	GO:0001067	transcription regulatory region nucleic acid binding	0.0014
Closed	MF	GO:0008238	exopeptidase activity	0.00197
Closed	MF	GO:0005201	extracellular matrix structural constituent	0.00233
Closed	MF	GO:0015171	amino acid transmembrane transporter activity	0.00251
Closed	MF	GO:0004222	metalloendopeptidase activity	0.00296
Closed	MF	GO:0061135	endopeptidase regulator activity	0.00374
Closed	MF	GO:0015293	symporter activity	0.00397
Closed	MF	GO:0016829	lyase activity	0.00399
Closed	MF	GO:0008233	peptidase activity	0.00431
Closed	MF	GO:1990837	sequence-specific double-stranded DNA binding	0.00515
Closed	MF	GO:0140677	molecular function activator activity	0.00532
Closed	MF	GO:0016835	carbon-oxygen lyase activity	0.0069
Closed	MF	GO:0000987	cis-regulatory region sequence-specific DNA binding	0.00864
Closed	MF	GO:0000978	RNA polymerase II cis-regulatory region sequence-specific DNA binding	0.00866
Closed	MF	GO:0015179	L-amino acid transmembrane transporter activity	0.00907

Supplemental Tables

Supplement Table 2.S1: Gene Ontology (GO) terms of heat response genes. Table shows the results from a GO enrichment analysis of heat response genes using the R package, topGO v. 2.50.0. We compared the list of heat response genes against a background of all transcripts that passed our quality filters. Enriched GO terms were identified with the classic Fisher's test with a p-value < 0.01 and at least 10 transcripts within each category. GO terms are contained within ontology types: Biological Processes (BP), Cellular Components (CC), and Molecular Functions (MF).

Type	GO ID	Term	p-value
BP	GO:0012501	programmed cell death	0.0001
BP	GO:0007166	cell surface receptor signaling pathway	0.0001
BP	GO:0008202	steroid metabolic process	0.00011
BP	GO:0046638	positive regulation of alpha-beta T cell differentiation	0.00011
BP	GO:0001525	angiogenesis	0.00011
BP	GO:0002521	leukocyte differentiation	0.00011
BP	GO:0002819	regulation of adaptive immune response	0.00011
BP	GO:0002376	immune system process	0.00012
BP	GO:0009893	positive regulation of metabolic process	0.00012
BP	GO:0051094	positive regulation of developmental process	0.00012
BP	GO:0045860	positive regulation of protein kinase activity	0.00013
BP	GO:0042325	regulation of phosphorylation	0.00014
BP	GO:0046637	regulation of alpha-beta T cell differentiation	0.00014
BP	GO:0010604	positive regulation of macromolecule metabolic process	0.00014
BP	GO:0015849	organic acid transport	0.00015
BP	GO:0046942	carboxylic acid transport	0.00015
BP	GO:0046634	regulation of alpha-beta T cell activation	0.00015
BP	GO:0033674	positive regulation of kinase activity	0.00016
BP	GO:0045621	positive regulation of lymphocyte differentiation	0.00016
BP	GO:0006749	glutathione metabolic process	0.00016
BP	GO:0002292	T cell differentiation involved in immune response	0.00017
BP	GO:0002822	regulation of adaptive immune response based on somatic recombination of immune receptors built from immunoglobulin superfamily domains	0.00019
BP	GO:0046631	alpha-beta T cell activation	0.0002
BP	GO:0045596	negative regulation of cell differentiation	0.0002
BP	GO:0002252	immune effector process	0.0002
BP	GO:0002449	lymphocyte mediated immunity	0.00021
BP	GO:1903131	mononuclear cell differentiation	0.00022
BP	GO:0048522	positive regulation of cellular process	0.00026
BP	GO:0007159	leukocyte cell-cell adhesion	0.00028
BP	GO:0050863	regulation of T cell activation	0.00029
BP	GO:1903037	regulation of leukocyte cell-cell adhesion	0.0003
BP	GO:1903706	regulation of hemopoiesis	0.00031
BP	GO:0019220	regulation of phosphate metabolic process	0.00033
BP	GO:0071900	regulation of protein serine/threonine kinase activity	0.00033
BP	GO:0051174	regulation of phosphorus metabolic process	0.00035
BP	GO:0002711	positive regulation of T cell mediated immunity	0.00037

BP	GO:0045595	regulation of cell differentiation	0.00037
BP	GO:1901700	response to oxygen-containing compound	0.00038
BP	GO:0042221	response to chemical	0.00038
BP	GO:0002443	leukocyte mediated immunity	0.00038
BP	GO:0050866	negative regulation of cell activation	0.0004
BP	GO:0007154	cell communication	0.0004
BP	GO:0006468	protein phosphorylation	0.0004
BP	GO:0060429	epithelium development	0.00041
BP	GO:0032502	developmental process	0.00041
BP	GO:0007167	enzyme-linked receptor protein signaling pathway	0.00042
BP	GO:0050865	regulation of cell activation	0.00043
BP	GO:0071363	cellular response to growth factor stimulus	0.00043
BP	GO:0030856	regulation of epithelial cell differentiation	0.00044
BP	GO:0048856	anatomical structure development	0.00044
BP	GO:0001934	positive regulation of protein phosphorylation	0.00048
BP	GO:0002286	T cell activation involved in immune response	0.00049
BP	GO:0051338	regulation of transferase activity	0.00051
BP	GO:0048646	anatomical structure formation involved in morphogenesis	0.00052
BP	GO:0051249	regulation of lymphocyte activation	0.00053
BP	GO:0009628	response to abiotic stimulus	0.00056
BP	GO:0031325	positive regulation of cellular metabolic process	0.00056
BP	GO:0007169	transmembrane receptor protein tyrosine kinase signaling pathway	0.00057
BP	GO:0043405	regulation of MAP kinase activity	0.00057
BP	GO:0015711	organic anion transport	0.00061
BP	GO:0006955	immune response	0.00064
BP	GO:0002250	adaptive immune response	0.00065
BP	GO:0046323	glucose import	0.00067
BP	GO:0002768	immune response-regulating cell surface receptor signaling pathway	0.00068
BP	GO:0060021	roof of mouth development	0.00069
BP	GO:0009636	response to toxic substance	0.00069
BP	GO:0042981	regulation of apoptotic process	0.00073
BP	GO:0042327	positive regulation of phosphorylation	0.00077
BP	GO:0070848	response to growth factor	0.0008
BP	GO:0001503	ossification	0.00083
BP	GO:0042446	hormone biosynthetic process	0.00084
BP	GO:0007165	signal transduction	0.00086
BP	GO:0072006	nephron development	0.00096
BP	GO:0002709	regulation of T cell mediated immunity	0.00097
BP	GO:0016310	phosphorylation	0.00102
BP	GO:0010562	positive regulation of phosphorus metabolic process	0.00106
BP	GO:0045937	positive regulation of phosphate metabolic process	0.00106
BP	GO:0043067	regulation of programmed cell death	0.00107
BP	GO:0061448	connective tissue development	0.00108
BP	GO:0051251	positive regulation of lymphocyte activation	0.00109
BP	GO:0002366	leukocyte activation involved in immune response	0.0011
BP	GO:0022409	positive regulation of cell-cell adhesion	0.00112
BP	GO:0032743	positive regulation of interleukin-2 production	0.00116
BP	GO:0055085	transmembrane transport	0.0012
BP	GO:0042743	hydrogen peroxide metabolic process	0.00121
BP	GO:0071466	cellular response to xenobiotic stimulus	0.00121
BP	GO:1902106	negative regulation of leukocyte differentiation	0.00121
BP	GO:0002263	cell activation involved in immune response	0.00123
BP	GO:0002429	immune response-activating cell surface receptor signaling pathway	0.00124
BP	GO:0033993	response to lipid	0.00126
BP	GO:0090287	regulation of cellular response to growth factor stimulus	0.00127
BP	GO:0002694	regulation of leukocyte activation	0.00131

BP	GO:0032147	activation of protein kinase activity	0.00131
BP	GO:0007155	cell adhesion	0.00134
BP	GO:0051347	positive regulation of transferase activity	0.00136
BP	GO:0031328	positive regulation of cellular biosynthetic process	0.00147
BP	GO:1902074	response to salt	0.00148
BP	GO:0023052	signaling	0.00149
BP	GO:0002456	T cell mediated immunity	0.00149
BP	GO:0002824	positive regulation of adaptive immune response based on somatic recombination of immune receptors built from immunoglobulin superfamily domains	0.00158
BP	GO:1903707	negative regulation of hemopoiesis	0.0016
BP	GO:0015698	inorganic anion transport	0.00162
BP	GO:0045785	positive regulation of cell adhesion	0.00163
BP	GO:0032663	regulation of interleukin-2 production	0.00169
BP	GO:0000122	negative regulation of transcription by RNA polymerase II	0.00174
BP	GO:0045444	fat cell differentiation	0.00176
BP	GO:0071902	positive regulation of protein serine/threonine kinase activity	0.00204
BP	GO:0044344	cellular response to fibroblast growth factor stimulus	0.00204
BP	GO:0072593	reactive oxygen species metabolic process	0.00208
BP	GO:0032623	interleukin-2 production	0.0021
BP	GO:0009891	positive regulation of biosynthetic process	0.00212
BP	GO:0002708	positive regulation of lymphocyte mediated immunity	0.00229
BP	GO:0002821	positive regulation of adaptive immune response	0.00229
BP	GO:0031214	biomineral tissue development	0.0023
BP	GO:0002699	positive regulation of immune effector process	0.00234
BP	GO:0035556	intracellular signal transduction	0.00238
BP	GO:0002040	sprouting angiogenesis	0.00257
BP	GO:0003073	regulation of systemic arterial blood pressure	0.00265
BP	GO:0009605	response to external stimulus	0.00271
BP	GO:0002705	positive regulation of leukocyte mediated immunity	0.00274
BP	GO:0030183	B cell differentiation	0.00274
BP	GO:0030154	cell differentiation	0.00286
BP	GO:0010557	positive regulation of macromolecule biosynthetic process	0.00292
BP	GO:0048869	cellular developmental process	0.00293
BP	GO:0070887	cellular response to chemical stimulus	0.00294
BP	GO:0002220	innate immune response activating cell surface receptor signaling pathway	0.00296
BP	GO:0051250	negative regulation of lymphocyte activation	0.00296
BP	GO:0006950	response to stress	0.003
BP	GO:0032496	response to lipopolysaccharide	0.00303
BP	GO:0031401	positive regulation of protein modification process	0.00303
BP	GO:0006865	amino acid transport	0.00308
BP	GO:0030097	hemopoiesis	0.00309
BP	GO:0002695	negative regulation of leukocyte activation	0.00316
BP	GO:0001101	response to acid chemical	0.0032
BP	GO:0016125	sterol metabolic process	0.00327
BP	GO:0045597	positive regulation of cell differentiation	0.00332
BP	GO:0010035	response to inorganic substance	0.0034
BP	GO:0043066	negative regulation of apoptotic process	0.00341
BP	GO:0045765	regulation of angiogenesis	0.00344
BP	GO:0002682	regulation of immune system process	0.00348
BP	GO:0070661	leukocyte proliferation	0.00351
BP	GO:0045944	positive regulation of transcription by RNA polymerase II	0.00356
BP	GO:0006357	regulation of transcription by RNA polymerase II	0.00374
BP	GO:0001657	ureteric bud development	0.00375
BP	GO:0009064	glutamine family amino acid metabolic process	0.00375
BP	GO:0008543	fibroblast growth factor receptor signaling pathway	0.00377

BP	GO:0030282	bone mineralization	0.00382
BP	GO:0019221	cytokine-mediated signaling pathway	0.00382
BP	GO:0071774	response to fibroblast growth factor	0.00388
BP	GO:0002237	response to molecule of bacterial origin	0.00388
BP	GO:0016477	cell migration	0.00393
BP	GO:0048583	regulation of response to stimulus	0.00396
BP	GO:0034764	positive regulation of transmembrane transport	0.004
BP	GO:0051716	cellular response to stimulus	0.00405
BP	GO:0097190	apoptotic signaling pathway	0.00406
BP	GO:0072080	nephron tubule development	0.00419
BP	GO:0009410	response to xenobiotic stimulus	0.00419
BP	GO:0060324	face development	0.00419
BP	GO:0072073	kidney epithelium development	0.00419
BP	GO:0002696	positive regulation of leukocyte activation	0.0042
BP	GO:0042476	odontogenesis	0.00437
BP	GO:0001658	branching involved in ureteric bud morphogenesis	0.00448
BP	GO:0006952	defense response	0.0045
BP	GO:0051402	neuron apoptotic process	0.0045
BP	GO:0035264	multicellular organism growth	0.00456
BP	GO:0015807	L-amino acid transport	0.0046
BP	GO:0048880	sensory system development	0.00464
BP	GO:0031399	regulation of protein modification process	0.00469
BP	GO:1901342	regulation of vasculature development	0.0047
BP	GO:0043069	negative regulation of programmed cell death	0.00475
BP	GO:0051246	regulation of protein metabolic process	0.00484
BP	GO:1902652	secondary alcohol metabolic process	0.00487
BP	GO:0001935	endothelial cell proliferation	0.00522
BP	GO:0043406	positive regulation of MAP kinase activity	0.00529
BP	GO:0050867	positive regulation of cell activation	0.00533
BP	GO:0051781	positive regulation of cell division	0.00543
BP	GO:0001823	mesonephros development	0.00553
BP	GO:0072163	mesonephric epithelium development	0.00553
BP	GO:0072164	mesonephric tubule development	0.00553
BP	GO:0009725	response to hormone	0.00555
BP	GO:0048585	negative regulation of response to stimulus	0.00601
BP	GO:0008217	regulation of blood pressure	0.00616
BP	GO:0008203	cholesterol metabolic process	0.00636
BP	GO:0009314	response to radiation	0.00637
BP	GO:0046903	secretion	0.00641
BP	GO:0009617	response to bacterium	0.00658
BP	GO:0006694	steroid biosynthetic process	0.00676
BP	GO:0072009	nephron epithelium development	0.00676
BP	GO:0042127	regulation of cell population proliferation	0.00679
BP	GO:0002697	regulation of immune effector process	0.00696
BP	GO:0048705	skeletal system morphogenesis	0.00696
BP	GO:0005996	monosaccharide metabolic process	0.00696
BP	GO:0040011	locomotion	0.00704
BP	GO:1901701	cellular response to oxygen-containing compound	0.00705
BP	GO:0045862	positive regulation of proteolysis	0.00725
BP	GO:0010033	response to organic substance	0.00726
BP	GO:0006665	sphingolipid metabolic process	0.00726
BP	GO:0034097	response to cytokine	0.00728
BP	GO:0001654	eye development	0.00741
BP	GO:0150063	visual system development	0.00741
BP	GO:0045321	leukocyte activation	0.00764
BP	GO:0050851	antigen receptor-mediated signaling pathway	0.00777

BP	GO:0048468	cell development	0.00781
BP	GO:0060675	ureteric bud morphogenesis	0.00783
BP	GO:0072171	mesonephric tubule morphogenesis	0.00783
BP	GO:0050776	regulation of immune response	0.00799
BP	GO:0045893	positive regulation of DNA-templated transcription	0.00815
BP	GO:0051254	positive regulation of RNA metabolic process	0.00823
BP	GO:0002706	regulation of lymphocyte mediated immunity	0.00825
BP	GO:0001656	metanephros development	0.00826
BP	GO:0022407	regulation of cell-cell adhesion	0.00835
BP	GO:0050790	regulation of catalytic activity	0.00836
BP	GO:0006629	lipid metabolic process	0.00846
BP	GO:1902680	positive regulation of RNA biosynthetic process	0.00849
BP	GO:0048562	embryonic organ morphogenesis	0.00867
BP	GO:0002684	positive regulation of immune system process	0.0088
BP	GO:0009790	embryo development	0.00886
BP	GO:0071356	cellular response to tumor necrosis factor	0.00906
BP	GO:0048598	embryonic morphogenesis	0.00933
BP	GO:0044281	small molecule metabolic process	0.00938
BP	GO:0046777	protein autophosphorylation	0.00984
BP	GO:0009968	negative regulation of signal transduction	0.00989
BP	GO:0001817	regulation of cytokine production	0.00997
CC	GO:0045177	apical part of cell	0.00011
CC	GO:0005615	extracellular space	0.00023
CC	GO:0016324	apical plasma membrane	0.0004
CC	GO:0071944	cell periphery	0.00098
CC	GO:0005886	plasma membrane	0.00246
CC	GO:0016020	membrane	0.004
CC	GO:0005581	collagen trimer	0.00401
CC	GO:0005764	lysosome	0.00538
CC	GO:0005796	Golgi lumen	0.00846
MF	GO:0016616	oxidoreductase activity, acting on the CH-OH group of donors, NAD or NADP as acceptor	0.00011
MF	GO:0005342	organic acid transmembrane transporter activity	0.00011
MF	GO:0046943	carboxylic acid transmembrane transporter activity	0.00011
MF	GO:0030545	signaling receptor regulator activity	0.00017
MF	GO:0005343	organic acid:sodium symporter activity	0.00018
MF	GO:0016846	carbon-sulfur lyase activity	0.00018
MF	GO:0048018	receptor ligand activity	0.00032
MF	GO:0015294	solute:monoatomic cation symporter activity	0.00037
MF	GO:0030546	signaling receptor activator activity	0.00045
MF	GO:0000977	RNA polymerase II transcription regulatory region sequence-specific DNA binding	0.00047
MF	GO:0015370	solute:sodium symporter activity	0.00048
MF	GO:0008514	organic anion transmembrane transporter activity	0.00072
MF	GO:0015171	amino acid transmembrane transporter activity	0.00076
MF	GO:0015293	symporter activity	0.00084
MF	GO:0046872	metal ion binding	0.0011
MF	GO:0000976	transcription cis-regulatory region binding	0.00114
MF	GO:0001067	transcription regulatory region nucleic acid binding	0.00114
MF	GO:0008233	peptidase activity	0.0012
MF	GO:0015179	L-amino acid transmembrane transporter activity	0.00131
MF	GO:0005201	extracellular matrix structural constituent	0.00136
MF	GO:0008238	exopeptidase activity	0.00138
MF	GO:0016836	hydro-lyase activity	0.0015
MF	GO:0051082	unfolded protein binding	0.00159
MF	GO:0016209	antioxidant activity	0.00188

MF	GO:0043169	cation binding	0.00204
MF	GO:0008083	growth factor activity	0.00224
MF	GO:0008235	metalloexopeptidase activity	0.00304
MF	GO:0005506	iron ion binding	0.00331
MF	GO:0016705	oxidoreductase activity, acting on paired donors, with incorporation or reduction of molecular oxygen	0.00436
MF	GO:1990837	sequence-specific double-stranded DNA binding	0.00491
MF	GO:0043565	sequence-specific DNA binding	0.00531
MF	GO:0015291	secondary active transmembrane transporter activity	0.00533
MF	GO:0038024	cargo receptor activity	0.00548
MF	GO:0000978	RNA polymerase II cis-regulatory region sequence-specific DNA binding	0.00623
MF	GO:0000987	cis-regulatory region sequence-specific DNA binding	0.00701
MF	GO:0004180	carboxypeptidase activity	0.00945

Evolution of thermal tolerance in Acroporid corals

Authors: Leslie Guerrero, Brooke Benson, Camille Rumberger, Sunaina Dhillon, and Rachael Bay

Abstract

Adaptive phenotypic plasticity can allow individual organisms to alter their phenotype to optimize fitness response to environmental cues. However, this flexibility can come with costs, leading to trade-offs between performance and plasticity. Through canalization, traits initially produced via plasticity can become hard-wired over generations, and this mechanism has been proposed to contribute to adaptive diversification. In this study, we investigated molecular mechanisms of thermal tolerance evolution in *Acropora* corals. *Acropora* thermal tolerance is a complex polygenic trait, where phenotypic variation is produced by a combination of environmental and genetic effects. We found that although transcriptome-wide expression largely mirrored the phylogeny, thermal tolerance did not. Additionally, we found that species with the highest thermal tolerance had a reduced gene expression response to heat stress, a phenomenon known as transcriptional dampening. This result at a macro-evolutionary level parallels transcriptional dampening observed at the individual and population levels, suggesting a general mechanism of thermal tolerance in corals and canalization of a plastic response over evolutionary time. These findings offer insights into mechanisms defining coral 'winners and losers' in warming oceans and expand our understanding of complex trait evolution more broadly.

Introduction

Phenotypic plasticity is the phenomenon when one genotype can produce multiple phenotypes based on environmental cues (Fusco and Minelli 2010). Through evolutionary changes, organisms can become better suited to variable environments by developing and maintaining plastic traits. However, plasticity can be limited, as the machinery required to achieve plasticity across a spectrum of environments is theorized to be costly, presenting a trade-off between performance and plasticity (Scheiner and Holt 2012). For example, mechanisms enabling plasticity are lost in zebrafish adapted to stable laboratory environments (Morgan et al. 2022). While laboratory zebrafish exhibit a narrower thermal performance

range at warmer temperatures, they have a reduced capacity for thermal tolerance plasticity compared to their counterparts from natural environments (Morgan et al. 2022).

Canalization, the reduction of phenotypic variation in a trait across generations, reduces the costs associated with maintaining high levels of plasticity (Wagner et al. 1997; Dewitt et al. 1998). Canalization, and subsequent refinement, of phenotypes introduced through plasticity can result in fixed adaptive phenotypes. For instance, Levis et al. (2018) demonstrate that a fixed carnivorous morphology in a species of spadefoot toad tadpoles originated from feeding morphology plasticity in ancestral lineages. Canalization of phenotypic novelty introduced by plasticity occurs following population divergence, kickstarting rapid divergence when plastic ancestral lineages repeatedly colonize novel environments (Wund et al. 2008; Pfennig et al. 2010). This pattern is thought to lead to rapid speciation in threespine sticklebacks, cichlids, nematodes, and spiders (Schneider and Meyer 2017). A critical biological question remains: what is the mechanistic link between plasticity-induced phenotypes and fixed adaptations?

Across physiological timescales, subsets of stress response genes exhibit reduced gene expression plasticity to stressors, or 'transcriptional dampening', which can be induced in estuarine amphipods by acclimatory conditions (Collins et al. 2021). Mirroring these results, recent studies indicate that locally adapted populations exhibit a reduced gene expression response when environmental conditions change (Shaw et al. 2014; von Heckel et al. 2016; Ghalambor et al. 2015; Brennan et al. 2022; Barshis et al. 2013). Collectively, these studies show that a reduced gene expression plasticity coincides with enhanced stress tolerance at distinct timescales: 1) individuals acquiring enhanced stress tolerance after a few days of conditioning, and 2) enhanced stress tolerance between populations due to local adaptation across generations. Plasticity in gene expression responses acquired in acclimatory conditions is distinct from heritable gene expression canalization resulting from population divergence. However, the transcriptional dampening observed across different biological time-scales suggests that regulatory mechanisms finely tune gene expression to cope with environmental stressors and can be genetically fixed across adaptive timescales (Schneider and Meyer 2017).

This pattern of transcriptional dampening associated with environmental tolerance is observed at both individual and population levels in reef-building corals (Bellantuono et al. 2012; Barshis et al. 2013; Bay and Palumbi 2015). Coral reefs are particularly vulnerable to warmer temperatures, since heat stress leads to the breakdown of the relationship between the coral host and nutrient-providing intracellular symbionts, a process known as bleaching. However, thermal acclimation and local adaptation to warmer environments lead to enhanced thermal tolerance and transcriptional dampening. Acclimatory processes lead to transcriptional dampening without changing baseline expression (Bellantuono et al. 2012; Bay and Palumbi 2015). In contrast, local adaptation leads to transcriptional dampening when baseline transcription is elevated (i.e. "frontloading"), leading to a reduced gene expression response to maintain homeostasis in warmer environments (Barshis et al. 2013). At the same time, coral species exhibit differences in thermal tolerance thresholds, bleaching and recovery potential. Variation in bleaching susceptibility, both within and between genera, has been historically observed during surveys following mass bleaching events across the globe (Jaap 1979; Fitt and Warner 1995; Pratchett et al. 2013; Swain et al. 2016). Linking the community response within such surveys to molecular insight gained at the individual and species level would represent a substantial advance in our understanding of how thermal tolerance may evolve and our ability to predict coral reef futures (van Woesik et al. 2022).

To date, most coral comparative studies have investigated thermal tolerance in a few populations of a single species or a few divergent lineages (Barshis et al. 2013; Kenkel and Matz 2016; Klepac and Barshis 2020; Avila-Magaña et al. 2021; Evensen et al. 2022). Comparing adaptive trait variation between populations can inform the relative contributions of genetic diversity and plasticity, as well as associated trade-offs (Thomas et al. 2018). For example, Barshis et al. (2013) found that a population of thermally tolerant *A. hyacinthus* had constitutively higher expression—or frontloading—of 60 heat response genes in the tolerant population (Barshis et al. 2013). In contrast, comparing divergent lineages reveals deeply conserved mechanisms and lineage-specific innovations. Avila-Magaña et al. (2021) compared the thermal tolerances of Caribbean species *Pseudodiploria clivosa*, *Orbicella faveolata*, and

Siderastrea radians. They found that–while gene expression diverged among coral species and their symbionts–thermal tolerance differences between species are associated with distinct microbiome metabolic capabilities and the redundancy of metabolic pathways across coral, symbiont, and microbiome members under heat stress (Avila-Magaña et al. 2021). However, comparisons among distantly related species can be limited by reduced homology of expressed genes.

Investigating adaptive traits across a clade enhances our understanding of the evolutionary forces driving trait variation and the specific genetic and molecular mechanisms behind phenotypic variation and convergence (Whitehead and Crawford 2006; Romero et al. 2012). To investigate the molecular mechanisms underlying thermal tolerance variation among closely related species, we leveraged adaptive radiation in *Acropora*, the most speciose coral genus having undergone rapid species diversification around 25-50 million years ago (Wallace and Willis 1994; Shinzato et al. 2020),. Specifically, we use eight species collected from the same location to investigate: i) how thermal tolerance varies among species, ii) whether transcriptome-wide gene expression reflects phylogenetic or functional (i.e. thermal tolerance) patterns, and iii) whether transcriptional dampening, as seen at the individual and population levels, is also canalized across species. Together, the results provide an understanding of how thermal tolerance and potentially other complex traits evolve in closely related species and connect mechanisms across individual, population, and community levels.

Methods

Experimental design

In July 2021, we identified 38 individual coral colonies from multiple *Acropora* species in the lagoons from the north shore of Moorea, French Polynesia, for short-term acute heat stress trials (Figure 1A, CITES permit number FR2198700133-E). The species used in this study were *A. abrotanoides* (n = 6; Lamarck, 1816)*, A. hyacinthus* (n=5; Dana, 1846)*, A. lutkeni* (n=3; Crossland, 1948)*, A. nasuta* (n=3;

Dana, 1846), *A. pulchra* (n=5; Brook, 1891), *A. retusa* (n= 4; Dana, 1846), *A. robusta* (n= 4; Dana, 1846), and *A. tutuilensis* (n= 8; Hoffmeister, 1925). These numbers reflect the final sample sizes, excluding 12 colonies discarded due to species ambiguity and molecular extraction failure. We sampled four to five colonies daily to ensure consistent collection times and avoid overcrowding during each short-term acute heat stress trial. We marked GPS coordinates and collected sixteen small branches from each colony. Most trials include multiple species, except for two (Supplementary Table 1). Four branches from each colony were placed in each treatment aquarium with a holding temperature of 29°C, an approximate ambient water temperature at this site.

We used the Coral Bleaching Automated Stress System (CBASS) and the protocol described by Evensen et. al. for heat stress trials (Evensen et al. 2023). The treatment temperatures we used were 29°C (control), 34°C, 36°C, and 38°C (Figure 1B). Based on preliminary trials, these temperatures were chosen to span the full range of bleaching responses. At noon (GMT-10), CBASS ramped the tank temperature to the respective treatment temperatures for three hours, held the treatment temperature for three hours, and then lowered the temperature back to 29°C over the course of an hour. The temperature in each tank was maintained at 29°C overnight. We anchored a HOBO Pendant MX Water Temperature Data Logger in each treatment to log the temperature (Onset, USA, Mfr. Catalog ID MX2201).

Estimating thermal tolerance

To collect Fv/Fm measurements, we dark-acclimated coral branches during the ramp down to 29°C. At 7:00 PM, when the temperature in all tanks reached 29°C, we performed PAM fluorometry to measure Fv/Fm yield. We used the Mini-PAM-II with a miniature fiber optic cable (WALZ Effeltrich, Germany). We recorded Fv/Fm measurements at three random points across each sample and averaged Fv/Fm values for each fragment.

We used an ED50 dose-response logistic regression to estimate a thermal tolerance value for each coral colony (Evensen et al. 2021). To fit the dose-response curve of the Fv/Fm yield, we used the 'drm' function in the R package drc v3.0.1 (Ritz et al. 2015). This function fits a three-parameter log-logistic function with a lower limit is 0 (Ritz et al. 2015). In this model, photosystem II efficiency (Fv/Fm) for each individual was the dependent variable, and treatment temperature was the independent variable. This allowed us to determine the temperature that induces a 50% reduction in Fv/Fm yield (ED50) (Evensen et al. 2021). We validated our thermal tolerance estimations for each species by assessing coral chlorophyll content using photographic color analysis.

To perform the photographic color analysis, we used the photographic analysis described by Winters et al., 2009 to estimate the species-level visual bleaching scores of every branch the morning following each heat stress assay (Winters et al. 2009). In brief, four branches in each treatment were placed on a standard background bordered with the Kodak Color Separation Guide and Gray Scale Q-13 (Kodak, USA, Mfr. Catalog ID 1527662). We took photos with the Olympus TG-5 Waterproof Camera. Camera settings for all the photographs taken included the following: no flash, ISO = 100, F = 3.6, aperture speed of 1/60 s, and full frame metering was on. For the analysis, we normalized the image color with a macro in MATLAB called "CalibrateImageA," which adjusts RGB components in images to an *a priori* known RGB profile of Kodak grayscale. Following normalization, we randomly placed quadrats of 15 x 15 pixels (each equal to 6.5 mm^2) at different parts of the normalized coral photo. We measured color intensity for RGB in another macro called "AnalyzeIntensity" at eight points per branch. We calculated the rate of change of the red channel intensity across the thermal treatments for each species to compare the visual bleaching score.

We calculated Spearman's correlation coefficient between the species ED50 and the visual bleaching score to validate the species' thermal tolerance estimations. We removed the outlier species, *A. robusta.* ED50 is correlated with the visual beaching score, so we used ED50 as the primary metric of thermal tolerance for downstream analyses.

RNA 3’ Tag Seq

We preserved the branches from the 29°C control and 36°C treatments in RNA stabilizing solution (70g Ammonium Sulfate /100ml solution, 10 mM EDTA, 25 mM Sodium Citrate, 5.4 pH) for molecular extractions at 8:00 AM following each heat stress trial. Tissue samples were preserved in RNA stabilizing solution and stored at -80°C until RNA was extracted. We used a TRIzol protocol to isolate RNA (Invitrogen, Mfr. Catalog ID 15596026). Purified RNA was stored at -80°C until sent to the DNA Technologies and Expression Analysis Core at the UC Davis Genome Center for library preparation and sequencing. Barcoded 3'Tag-Seq libraries were prepared with 180 ng of RNA using the QuantSeq FWD kit (Lexogen, Austria) for multiplexed sequencing according to the manufacturer's recommendations. Libraries were amplified with 17 cycles of PCR. The fragment size distribution of the libraries was verified via micro-capillary gel electrophoresis on a Bioanalyzer 2100 (Agilent, USA). The libraries were quantified by fluorometry on a Qubit instrument (LifeTechnologies, Carlsbad, CA) and pooled in equimolar ratios. The libraries were sequenced on an Aviti sequencer (Element Biosciences, USA) with single-end 100 bp reads. The sequencing generated more than 4 million reads per library.

We used FastQC 0.11.9 to check the quality of raw fastq files and identify adapter sequences (https://www.bioinformatics.babraham.ac.uk/projects/fastqc). We used Cutadapt 4.1 to filter and trim reads of the universal Illumina adapter, based on the 3’ end, which has a quality score of less than 10 (Martin 2011).

At the time of this study, there were two chromosome-scale reference genomes with annotated gene models for acroporid species: *A. millepora and A. hyacinthus* (López-Nandam et al. 2023; Fuller et al. 2020). To determine whether the *A. millepora* or *A. hyacinthus* reference genome would produce the highest percentage of mapped reads and to filter reads derived from symbionts, we used BBsplit 38.22 (Bushnell 2014). BBsplit bins reads where, with default settings, the aim was to assign each read to one reference based on the reference to which the read aligns best. We used either the *A. hyacinthus* or the *A.*

millepora whole genome, along with concatenated transcriptomes of *Symbiodinium microadriaticum*, *Breviolum minutum*, *Cladocopium goreaui*, and *Durusdinium trenchii* as references for BBsplit to bin reads derived between symbiont or coral (Aranda et al. 2016; Chen et al. 2022; Cooke et al. 2020; Parkinson et al. 2016). The reference genome that returned the highest number of coral reads across all species was *A. hyacinthus*, which we used as the reference for the remainder of this study's bioinformatic steps. Using default settings, we used STAR 2.7.10b to align coral reads from all species to the *A. hyacinthus* reference genome (Dobin et al. 2013). We used SAMtools 1.13.0 to sort BAM files, then used HTSeq 2.0.3 to create read count files from the alignments (Anders et al. 2015; Li et al. 2009).

Effect of symbiont on thermal tolerance

We extracted DNA, as explained above. We amplified the ITS2 region using PCR with primer pairs SYM_VAR_5.8S2 (5'-GAATTGCAGAACTCCGTGAACC-3') and SYM_VAR_REV (5'-CGGGTTCWCTTGTYTGACTTCATGC-3') and the protocol described in Hume et al., 2018. We sequenced the PCR product with Sanger sequencing, then queried the ITS2 sequence against the Sym ITS2 sequence database using default parameters (Shi et al. 2021). We used ANOVA to test the effects of species and symbiont genus on thermal tolerance (ED50).

Acropora phylogeny

We used genetic variation extracted from Tag-Seq data to estimate evolutionary relationships among the species we sampled. For an outgroup, we additionally downloaded Tag-Seq data from a single sample of *Montipora capitata* (NCBI SRA: SRR19620976) and mapped it to the same reference. From reads mapped to the *A. hyacinthus* reference genome, we used GATK to identify single nucleotide polymorphisms (SNPs) and genotype each individual (McKenna et al. 2010). RAxML was used to estimate the phylogeny using parameters suggested for variant sites only (-m ASC_GTRCAT --asc-corr=lewis) (Stamatakis 2014). An initial tree with no outgroup was generated to verify species

groupings. Once species designations were verified, we selected the single individual from each species with highest coverage and added the *M. capitata* outgroup to estimate a species tree. To test the phylogenetic signal of thermal tolerance, we used R package phytools v. 2.3.0 to calculate the Blomberg's K and the phylogenetic signal lambda (Revell 2024).

Measuring and comparing differences in gene expression response magnitudes across species

One of our primary hypotheses was that the magnitude of the gene expression response of heat response genes is higher in more thermally sensitive species. To test for species-specific response to heat stress, we quantified heat stress using 1) PCA distance between paired control and heated samples and 2) A network approach to identify heat stress modules. Within each approach, we also examined differences in heat stress response among species

We used DESeq2 1.42.1 to investigate the difference in total transcriptional response to heat using PCA (Love et al. 2014, R Core Team 2023). We used the HTSeq count files to create a DESeqDataSet. We filtered the DESeqDataSet object for genes with a minimum count across all samples of 10 and normalized the data with the variance stabilizing transformation. We performed a principal component analysis of the samples. We calculated the Euclidean distance between each control and heat-stressed sample for each colony. We performed a Spearman correlation to test the relationship between the Euclidean distance (a proxy for the overall transcriptional response) and individual ED50 values.

For the network-based approach, we identified modules with a species-specific response to heat using a combination of weighted gene co-expression network analysis (WGCNA) and variance partitioning analysis (Langfelder and Horvath 2008; Hoffman and Schadt 2016). First, we used the R package WGCNA 1.72.5 to construct an unsigned gene co-expression network using the 'blockwiseModules' function with a soft-thresholding power of 5 and identified modules with a minimum size of 30 genes. We then performed hierarchical clustering on the topological overlap matrix (TOM) and identified modules using dynamic tree cutting with a minimum module size of 100 genes. We generated a matrix by

calculating the difference between control and heat-stressed sample eigenvalues. We performed linear regressions to identify the modules with a statistically significant relationship between the difference in the eigengene values and individual sample ED50 values, which we defined as 'heat response modules.' Next, we used the variancePartition 1.32.5 R package to quantify the variation in eigengene values explained by treatment, batch, collection site, species, species-by-treatment interaction, and residual sources of variation across identified modules (Hoffman and Schadt 2016). We calculated the average percent variation in eigengene values from the species-by-treatment interaction. Then, we used this as the threshold to filter for modules with above-average variation due to the species-by-treatment interaction. We performed linear regressions to test the relationships between eigengene values and colony thermal tolerance to identify modules of interest. We performed Gene Ontology (GO) enrichment analysis for genes in the modules meeting this criteria using the topGO package v. 2.54.0 (Rahnenfuhrer J., 2023), following differential expression analysis with DESeq2. GO terms were analyzed for biological process (BP), molecular function (MF), and cellular component (CC) ontologies using Fisher's exact test with a p-value threshold of 0.01 to identify significantly enriched GO terms.

We used DESeq to quantify the gene-level response to heat stress (formula: ~ heat treatment) and the average expression for each species. We subsetted these measures for the respective genes in the yellow and salmon modules. To assess if there is a significant difference among species for the gene expression response to heat stress, we performed ANOVA, followed by a Tukey Honest Significant Difference (HSD) test. To test the relationship between the species-level response to heat and the individual thermal tolerance, we performed a Pearson's correlation to test the correlation between the species average, the absolute value of the log2 fold-change (log2FC), and the species' average thermal tolerance (ED50). Finally, we compared the average expression among species and used ANOVA followed by Tukey HSD to identify species with significantly different average expressions.

Results

Thermal tolerance variation across Acroporid species

We found that the species exhibit diverse thermal tolerances (ANOVA, p-value = 0.00048). Among the species we captured in our sampling, *A. tutuilensis* had the lowest average estimated thermal tolerance at 34.8°C, with a range of 34.4-35.2°C (Figure 2A). The species with the highest average estimated thermal tolerance was *A. abrotanoides*, at 36.2°C, with a range of 35.4-37.6°C (Figure 2A). The estimated average thermal tolerances for the other species were as follows: 35.3°C for *A. lutkeni*, 35.5°C for *A. pulchra*, 35.7°C for *A. retusa*, 35.9°C for *A. nasuta*, 35.9°C for *A. robusta*, and 36.1°C for *A. hyacinthus* (Figure 2A).

The red channel intensity varied by species and treatment (ANOVA, p-value = 0.000115). Across all species, there was an increase in the red channel intensity under hotter treatments (Figure 2B). After removing outlier colony 211, the species with the highest visual bleaching score is *A. pulchra* (Figure 2B). In contrast, *A. abrotanoides* showed the lowest visual bleaching score among the species we studied (Figure 2B). There was a significant correlation between the bleaching score and the species' thermal tolerance estimate (Spearman's correlation, p-value < 0.01, Figure 2C). Given this significant relationship, we determined that the thermal tolerance estimate calculated from the dose-response curve would be sufficient for the remainder of our analyses.

RNA 3' Tag Seq

We used RNA 3' TagSeq to examine species-level differences in gene expression response to heat stress. Due to extraction failure, we excluded two samples from the 38 colonies: one *A. tutuilensis* (colony 35) sample and one *A. abrotanoides* (colony 45) sample. After trimming reads and filtering for quality, each remaining sample had an average of 4,842,525 reads.

After trying both reference genomes, we decided to use the *A. hyacinthus* reference genome for the

remainder of the analyses because aligning to this genome reduced the number of reads mapped to multiple loci across all samples (Figure S2). BBsplit returned an average of 2,732,608 (56% of trimmed reads) coral reads, and 285,647 (6% of trimmed reads) symbiont reads per sample. Across the species, an average of 2,282,000 reads were uniquely mapped to the *A. hyacinthus* reference genome.

Effect of symbiont on thermal tolerance

Associations with different symbiont clades can influence holobiont thermal tolerance (Palacio-Castro et al. 2023). We identified the primary symbiont associated with the colonies but could not determine the primary symbiont clade in three colonies due to low-quality sanger sequences (Table S1). Twenty-three colonies were associated with Clade A symbionts, nine with Clade C symbionts, and three with Clade D symbionts (Table S1). All *A. lutkeni, A. nasuta,* and *A. pulchra* colonies were associated with Clade A symbionts, while *A. tutuilensis* colonies were associated with Clades A, C, and D. *A. hyacinthus, A. retusa,* and *A. robusta* colonies were associated with Clades A and C, and *A. abrotanoides* colonies with Clades C and D (Figure S3). The symbiont clades identified in our sampled colonies are consistent with previous reports of symbiont associations found in Moorea (Magalon et al. 2007). Coral species significantly explained the variation in thermal tolerance (ANOVA, p-value = 0.00503). In contrast, symbiont clade alone (ANOVA, p-value = 0.13345) and the interaction between coral species and symbiont clade (ANOVA, p-value = 0.81475) did not significantly contribute to the variation in thermal tolerance. However, as symbiont clade covaries with species, the species and symbiont effects are not possible to completely disentangle. Nonetheless, considering these associations is crucial for understanding the factors influencing coral thermal tolerance (Palacio-Castro et al. 2023).

Evolution of thermal tolerance in Acropora

The phylogeny for our samples, estimated from 4,051 SNPs, is shown in Figure 3. The species in this study form two clades: One with *A. hyacinthus, A. tutuilensis,* and *A. robusta*, while the other clade comprised *A. nasuta, A. pulchra, A. restusa,* and *A. lutkeni,* and *A. abrotanoides* (Figure 3). The

placement of species agrees with previous phylogenetic studies in *Acropora* (Faith and Richards 2012). Within its clade, *A. abrotanoides* was quite divergent from other species, with a substantially longer branch than any other tip (Figure 3). The relative thermal tolerances vary between species, but do not correspond with their evolutionary relationships (Blomberg's K = 0.304, Pagel's lambda = 7.33 e-05). However, the gene expression PCA shows the variation in PC2 was explained by the phylogenetic relationship (Figure S4). This suggests that while the profile of baseline transcription among species is influenced by evolutionary history, it does not determine the species-level thermal tolerance. The observed differences in thermal tolerance are likely due to other factors not captured by the overall relative differences in gene expression alone.

Measuring and comparing gene expression response magnitudes across species

Comparing the gene expression response to heat stress among species is crucial to understanding how variation in thermal tolerance is achieved. We used two approaches to quantify the response differences among species and test the relationship with the estimated species' thermal tolerance. Using a PCA-based approach, we found that species with higher thermal tolerance had a lower magnitude response to heat stress (Spearman's correlation, p-value < 0.05; Figure 4B). This potentially indicates that these species have higher thresholds to initiate gene expression responses to heat.

In a module-based approach, we identified 54 modules of genes with correlated expression. Merging modules with topological overlap resulted in 28 well-supported co-expression modules. Then, we quantified the variation in eigengene values due to species, treatment, collection site, and the interaction between species and treatment (Figure 5A). We found that of the 13 modules with above-average variation explained by a species-specific response, the yellow and salmon modules had eigenvalues with a statistically significant relationship with the colony-level thermal tolerance (Figure 5B, linear regression, p-value = 0.0258. Figure 5C, linear regression, p-value = 0.0044). The yellow module was comprised of 2,333 genes, and the salmon module was comprised of 386 genes. The yellow module genes were

enriched for recombination processes, hormonal responses, protein localization, and processes that respond to tumor necrosis factor stimulus (Supplementary Table 2). The salmon module genes were enriched for genes associated with DNA repair, DNA metabolism, chromosome organization and segregation, and cell-cycle processes (Supplementary Table 3).

Finally, we wanted to investigate the magnitude of the gene expression response of genes within our modules of interest in the context of species thermal tolerance differences. There was variation among species in the magnitude of the gene expression response to heat stress for both yellow module (ANOVA, p-value < 2e-16, Figures 6A, S5) and salmon module genes (ANOVA, p-value < 2e-16; Figure 6B, S5). Notably, *A. abrotanoides* and *A. lutkeni* had a large response to heat stress, while *A. pulchra*, *A. nasuta*, and *A. robusta* had a relatively small response to heat stress (Figures 6A and 6B). The species' average response to heat stress was negatively correlated with the individual thermal tolerance (Figures 6C and 6D).

Our results support our primary hypothesis that gene expression plasticity is associated with differences in thermal tolerance between species. Higher thermal tolerance was associated with a smaller gene expression response to heat stress. Genes exhibiting a smaller response in more thermally tolerant species were associated with apoptosis, DNA processes and maintenance, cellular integrity, and cell cycle regulation. This might indicate that *Acropora* corals evolved mechanisms to diminish the need for drastic changes in gene expression to maintain homeostasis in thermally challenging environments as exaggerated gene expression responses can be costly (von Heckel et al. 2016).

Discussion

Thermal tolerance is a complex trait with increasing ecological relevance in the warming ocean. Understanding how variation in thermal tolerance is achieved among closely related species can aid in predicting future marine communities, yet mechanisms of such variation remain elusive in many systems.

We demonstrate that attenuated gene expression response to heat stress is associated with increased thermal tolerance among colonies from eight acroporid species. This decreased magnitude response to heat stress is similar to patterns seen both on individual (acclimation) and population (local adaptation) levels, suggesting a generalized mechanism of thermal tolerance in corals (Bellantuono et al. 2012; Bay and Palumbi 2015; Barshis et al. 2013). Understanding molecular mechanisms of ecologically relevant phenotypes is essential for predicting how species will evolve as climate change persists.

Variation and evolution of thermal tolerance across coral taxa

We present the first empirical investigation into coral thermal tolerance evolution across many closely related species in a single clade. Investigations at this intermediate level of divergence allow for explicit comparison of trait evolution and underlying mechanisms while limiting additional neutral divergence of long evolutionary timescales. We found that the relative thermal tolerance varies significantly among the eight *Acropora* species we investigated, but thermal tolerance does not align with the evolutionary relationships. This finding is consistent with a previous study that found that bleaching susceptibility evolved independently of the phylogeny of 88 scleractinian coral species (Swain et al. 2018). The discrepancy between thermal tolerance and phylogeny presents an opportunity to investigate mechanisms by which thermal tolerance evolves independently of shared ancestry.

Evolution of gene expression

Despite a lack of phylogenetic signal for thermal tolerance, the transcriptome-wide gene expression across taxa generally reflects phylogenetic relationships. The PCA of gene expression shows distinct separation of species and clustering into groups that reflect groupings within the phylogeny. Because gene expression is influenced by genetic variation, it is subject to the same evolutionary forces as sequence variation. Drift can lead to neutral variation in overall gene expression between taxa, but these variations are constrained by stabilizing selection to maintain homeostatic levels (Khaitovich et al. 2005; Whitehead

and Crawford 2006). While directional selection may alter baseline expression in particular genes associated with fitness, most genes likely evolve under a neutral model of evolutionary change, reflecting evolutionary relationships across species (López-Maury et al. 2008; Rohlfs and Nielsen 2015). Although gene expression is regulated by various molecular mechanisms, variation in gene expression across species may reflect how these underlying regulatory systems are influenced by both neutral and selective evolutionary processes (Romero et al. 2012; Franzen et al. 2021; Quiver and Lachance 2022). However, gene expression and its regulatory mechanisms interact dynamically, complicating the direct influence of drift on regulation.

Plasticity and adaptation

Our study provides evidence for canalization of gene expression response over evolutionary time. Theory suggests that plasticity leads to adaptive divergence when novel plastic phenotypes are closer to the fitness optimum in different environmental conditions (Pfennig et al. 2010). Over time, these novel phenotypes produced via plasticity become hard-wired (canalized) through evolutionary processes (Pfennig et al. 2010). For example, plasticity in jaw morphology followed by canalized jaw shape and diet led to the rapid diversification of cichlid fish species (Parsons et al. 2016). Similarly, in our study, we see that the most thermally tolerant species show a dampened gene expression response to heat stress. This result parallels the reduced gene expression response reported at both physiological and local adaptation timescales (Bellantuono et al. 2012; Bay and Palumbi 2015; Barshis et al. 2013). However, on macro-evolutionary timescales, increases in thermal tolerance are not associated with constitutive expression differences of genes in modules associated with species-specific response to heat stress. Combining these results, one possible explanation is that plastic phenotypic variance present in the ancestral lineage became canalized in different *Acropora* lineages inhabiting different environments. To fully understand the extent of divergence in thermal tolerance and associated gene expression responses, a more detailed reconstruction across the broader *Acropora* phylogeny is required.

Cellular mechanisms of thermal tolerance

Enrichment for genes downregulated during heat response of the most thermally tolerant species provides significant insights into the mechanisms underlying thermal tolerance variation. Thermally tolerant species seem to have enhanced transport of protein and other molecules within and between cells, which may assist in managing stress responses and maintaining homeostasis. Notably, thermally tolerant species responding to heat also exhibit reduced expression of genes that respond to tumor necrosis factor (TNF). Previous reports indicate that TNF is important for coral thermal tolerance (Barshis et al. 2013; Palumbi et al. 2014). In cnidarians, TNF has been shown to be involved in the heat stress response, wound healing, apoptosis, and immunity (Quistad and Traylor-Knowles 2016). Thermally tolerant species also exhibit a reduction of genes coding for intracellular non-membrane bounded organelles and nuclear chromosome cellular components in response to heat. This might indicate that the most thermally tolerant species evolved optimal protein synthesis and chromatin organization to maintain cellular homeostasis.

The most prominent signal of enhanced thermal tolerance is associated with genome stability during acute heat events. Genome instability following heat stress is largely attributed to an abundance of reactive oxygen species (ROS) that damages DNA via oxidation (Oakley and Davy 2018). The observed downregulation of DNA metabolism and repair genes in thermally tolerant species responding to heat may suggest several possible explanations: during heat stress, (a) thermally tolerant species may experience lower levels of intracellular ROS compared to thermally sensitive species, (b) they might possess enhanced ROS detection and antioxidant mechanisms to counteract ROS effects, or (c) they could be more efficient in repairing DNA damage. A caveat to these hypotheses is that they may not be mutually exclusive.

The GO terms associated with the gene expression modules that remain stable under heat stress in thermally tolerant species suggest that these species might inherently experience lower levels of intracellular ROS and possess enhanced ROS detection and antioxidant activity. In thermally sensitive

species, inhibited protein transport following heat stress may represent a strategy to conserve energy or to prevent further protein damage (Njenga et al. 2023). This contrasts with the more stable protein transport observed in thermally tolerant species, implying that the cellular environment in thermally sensitive species following a heat stress becomes more unstable, presumably due to accumulated ROS. The stable expression of genes related to lipid binding, monocarboxylic metabolic processes, and ion channel regulator activity further indicates thermally tolerant species maintain cellular membrane integrity and balance cellular energy and ions, thus preserving cellular homeostasis despite acute thermal exposure. This stability in cellular processes and lower ROS levels might explain why thermally tolerant species exhibit a reduced gene expression response related to DNA repair.

Interactions between the coral host's gene expression response and the responses of the microbiome and symbiodinium can contribute to individual variations in thermal tolerance (Avila-Magaña et al. 2021; DeSalvo et al. 2010; Howells et al. 2012; Palacio-Castro et al. 2023). Although we were unable to disentangle the effects of different symbiodinium types from the coral host's overall thermal tolerance, we observed that closely related coral species with distinct symbiont associations exhibited variation in thermal tolerance linked to a reduced gene expression response. For example, the thermal tolerance between sister species *A. hyacinthus* and *A. tutuilensis* is different, with *A. tutuilensis* exhibiting a larger gene expression response and lower thermal tolerance relative to *A. hyacinthus*. Yet, the symbiont composition in the colonies between these two species is similar. This suggests that the evolution of a coral-intrinsic tolerance mechanism, independent of symbiont types, may play a key role. Future research will be needed to investigate the complex interplay between coral hosts, symbionts and microbiomes to further understand the mechanisms driving thermal tolerance, but our results support that a coral-intrinsic reduced gene expression response associated with thermal tolerance may have evolved through the canalization of gene expression plasticity.

Conclusion

Our study highlights the complex interplay between gene expression plasticity and evolution of thermal tolerance in corals. We found that thermally tolerant species exhibit attenuated gene expression response to heat stress, a pattern consistent across individual, population and macro-evolutionary timescales. Attenuation in gene expression response, coupled with a lack of constitutive expression differences in response to heat stress, suggests that plasticity in thermal responses can become canalized over evolutionary time. Our findings align with theories of plastic phenotypes evolving into fixed traits, possibly contributing to rapid divergence. Understanding these mechanisms is crucial for predicting how vulnerable species, like corals, will cope with ongoing climate change.

References

Anders, S., Pyl, P. T., & Huber, W. (2015). HTSeq--a Python framework to work with high-throughput sequencing data. *Bioinformatics* , *31*(2), 166–169.

Aranda, M., Li, Y., Liew, Y. J., Baumgarten, S., Simakov, O., Wilson, M. C., Piel, J., Ashoor, H., Bougouffa, S., Bajic, V. B., Ryu, T., Ravasi, T., Bayer, T., Micklem, G., Kim, H., Bhak, J., LaJeunesse, T. C., & Voolstra, C. R. (2016). Genomes of coral dinoflagellate symbionts highlight evolutionary adaptations conducive to a symbiotic lifestyle. *Scientific Reports*, *6*, 39734.

Avila-Magaña, V., Kamel, B., DeSalvo, M., Gómez-Campo, K., Enríquez, S., Kitano, H., Rohlfs, R. V., Iglesias-Prieto, R., & Medina, M. (2021). Elucidating gene expression adaptation of phylogenetically divergent coral holobionts under heat stress. *Nature Communications*, *12*(1), 5731.

Barshis, D. J., Ladner, J. T., Oliver, T. A., Seneca, F. O., Traylor-Knowles, N., & Palumbi, S. R. (2013). Genomic basis for coral resilience to climate change. *Proceedings of the National Academy of Sciences of the United States of America*, *110*(4), 1387–1392.

Bay, R. A., & Palumbi, S. R. (2015). Rapid Acclimation Ability Mediated by Transcriptome Changes in Reef-Building Corals. *Genome Biology and Evolution*, *7*(6), 1602–1612.

Bellantuono, A. J., Granados-Cifuentes, C., Miller, D. J., Hoegh-Guldberg, O., & Rodriguez-Lanetty, M. (2012). Coral thermal tolerance: tuning gene expression to resist thermal stress. *PloS One*, *7*(11), e50685.

Brennan, R. S., deMayo, J. A., Dam, H. G., Finiguerra, M. B., Baumann, H., & Pespeni, M. H. (2022). Loss of transcriptional plasticity but sustained adaptive capacity after adaptation to global change conditions in a marine copepod. *Nature Communications*, *13*(1), 1147.

Brook, G. (1891). Descriptions of new species of Madrepora in the collections of the British Museum. *Annals and Magazine of Natural History*, *8*(6), 458–471.

Bushnell, B. (2014). *BBMap: A Fast, Accurate, Splice-Aware Aligner* (No. LBNL-7065E). Lawrence Berkeley National Lab. (LBNL), Berkeley, CA (United States). https://www.osti.gov/servlets/purl/1241166

Chen, Y., Shah, S., Dougan, K. E., van Oppen, M. J. H., Bhattacharya, D., & Chan, C. X. (2022). Improved Cladocopium goreaui Genome Assembly Reveals Features of a Facultative Coral Symbiont and the Complex Evolutionary History of Dinoflagellate Genes. *Microorganisms*, *10*(8). https://doi.org/10.3390/microorganisms10081662

Collins, M., Clark, M. S., Spicer, J. I., & Truebano, M. (2021). Transcriptional frontloading contributes to cross-tolerance between stressors. Evolutionary Applications, 14(2), 577–587.

Cooke, I., Ying, H., Forêt, S., Bongaerts, P., Strugnell, J. M., Simakov, O., Zhang, J., Field, M. A., Rodriguez-Lanetty, M., Bell, S. C., Bourne, D. G., van Oppen, M. J., Ragan, M. A., & Miller, D. J. (2020). Genomic signatures in the coral holobiont reveal host adaptations driven by Holocene climate change and reef specific symbionts. *Science Advances*, *6*(48). https://doi.org/10.1126/sciadv.abc6318

Crossland, C. (1948). Reef corals of the South African coast. Adlard & Son, Limited.

Dana, J. D. (1846). *United States Exploring Expedition During the Years 1838, 1839, 1840, 1841, 1842: Zoophytes*. Sherman.

Dewitt, T. J., Sih, A., & Wilson, D. S. (1998). Costs and limits of phenotypic plasticity. *Trends in Ecology & Evolution*, *13*(2), 77–81.

Dobin, A., Davis, C. A., Schlesinger, F., Drenkow, J., Zaleski, C., Jha, S., Batut, P., Chaisson, M., & Gingeras, T. R. (2013). STAR: ultrafast universal RNA-seq aligner. *Bioinformatics* , *29*(1), 15–21.

Evensen, N. R., Fine, M., Perna, G., Voolstra, C. R., & Barshis, D. J. (2021). Remarkably high and consistent tolerance of a Red Sea coral to acute and chronic thermal stress exposures. *Limnology and Oceanography*, *l11715*. https://doi.org/10.1002/lno.11715

Evensen, N. R., Parker, K. E., Oliver, T. A., Palumbi, S. R., Logan, C. A., Ryan, J. S., Klepac, C. N., Perna, G., Warner, M. E., Voolstra, C. R., & Barshis, D. J. (2023). The Coral Bleaching Automated Stress System (CBASS): A low-cost, portable system for standardized empirical assessments of coral thermal limits. *Limnology and Oceanography: Methods*, *21*(7), 421–434.

Evensen, N. R., Voolstra, C. R., Fine, M., Perna, G., Buitrago-López, C., Cárdenas, A., Banc-Prandi, G., Rowe, K., & Barshis, D. J. (2022). Empirically derived thermal thresholds of four coral species along the Red Sea using a portable and standardized experimental approach. *Coral Reefs*, *41*(2), 239–252.

Faith, D. P., & Richards, Z. T. (2012). Climate change impacts on the tree of life: changes in phylogenetic diversity illustrated for acropora corals. *Biology*, *1*(3), 906–932.

Fitt, W. K., & Warner, M. E. (1995). Bleaching patterns of four species of Caribbean reef corals. *The Biological Bulletin*, *189*(3), 298–307.

Franzen, J., Georgomanolis, T., Selich, A., Kuo, C.-C., Stöger, R., Brant, L., Mulabdić, M. S., Fernandez-Rebollo, E., Grezella, C., Ostrowska, A., Begemann, M., Nikolić, M., Rath, B., Ho, A. D., Rothe, M., Schambach, A., Papantonis, A., & Wagner, W. (2021). DNA methylation changes during long-term in vitro cell culture are caused by epigenetic drift. *Communications Biology*, *4*(1), 598.

Fuller, Z. L., Mocellin, V. J. L., Morris, L. A., Cantin, N., Shepherd, J., Sarre, L., Peng, J., Liao, Y., Pickrell, J., Andolfatto, P., Matz, M., Bay, L. K., & Przeworski, M. (2020). Population genetics of the coral *Acropora millepora*: Toward genomic prediction of bleaching. *Science*, *369*(6501). https://doi.org/10.1126/science.aba4674

Fusco, G., & Minelli, A. (2010). Phenotypic plasticity in development and evolution: facts and concepts. Introduction. *Philosophical Transactions of the Royal Society of London. Series B, Biological Sciences*, *365*(1540), 547–556.

Ghalambor, C. K., Hoke, K. L., Ruell, E. W., Fischer, E. K., Reznick, D. N., & Hughes, K. A. (2015). Non-adaptive plasticity potentiates rapid adaptive evolution of gene expression in nature. *Nature*, *525*(7569), 372–375.

Hoffman, G. E., & Schadt, E. E. (2016). variancePartition: interpreting drivers of variation in complex gene expression studies. *BMC Bioinformatics*, *17*(1), 483.

Hoffmeister, J. E. (1925). *Some Corals from American Samoa and the Fiji Islands*. Carnegie Institution of Washington.

Jaap, W. C. (1979). Observations on zooxanthellae expulsion at Middle Sambo reef, Florida keys. *Bulletin of Marine Science*, *29*(3), 414–422.

Kenkel, C. D., & Matz, M. V. (2016). Gene expression plasticity as a mechanism of coral adaptation to a variable environment. *Nature Ecology & Evolution*, *1*(1), 14.

Khaitovich, P., Pääbo, S., & Weiss, G. (2005). Toward a neutral evolutionary model of gene expression. *Genetics*, *170*(2), 929–939.

Klepac, C. N., & Barshis, D. J. (2020). Reduced thermal tolerance of massive coral species in a highly variable environment. *Proceedings. Biological Sciences*, *287*(1933), 20201379.

Lamarck, J. (1816). *Histoire naturelle des animaux sans vertèbres. Tome second. Paris: Verdière, 568 pp.*

Langfelder, P., & Horvath, S. (2008). WGCNA: an R package for weighted correlation network analysis. *BMC Bioinformatics*, *9*(1), 559.

Levis, N. A., Isdaner, A. J., & Pfennig, D. W. (2018). Morphological novelty emerges from pre-existing phenotypic plasticity. *Nature Ecology & Evolution*, *2*(8), 1289–1297.

Li, H., Handsaker, B., Wysoker, A., Fennell, T., Ruan, J., Homer, N., Marth, G., Abecasis, G., Durbin, R., & 1000 Genome Project Data Processing Subgroup. (2009). The Sequence Alignment/Map format and SAMtools. *Bioinformatics* , *25*(16), 2078–2079.

López-Maury, L., Marguerat, S., & Bähler, J. (2008). Tuning gene expression to changing environments: from rapid responses to evolutionary adaptation. *Nature Reviews. Genetics*, *9*(8), 583–593.

López-Nandam, E. H., Albright, R., Hanson, E. A., Sheets, E. A., & Palumbi, S. R. (2023). Mutations in coral soma and sperm imply lifelong stem cell renewal and cell lineage selection. *Proceedings. Biological Sciences*, *290*(1991), 20221766.

Love, M. I., Huber, W., & Anders, S. (2014). Moderated estimation of fold change and dispersion for RNA-seq data with DESeq2. *Genome Biology*, *15*(12), 550.

Magalon, H., Flot, J.-F., & Baudry, E. (2007). Molecular identification of symbiotic dinoflagellates in Pacific corals in the genus Pocillopora. *Coral Reefs*, *26*(3), 551–558.

Martin, M. (2011). Cutadapt removes adapter sequences from high-throughput sequencing reads. *EMBnet.Journal*, *17*(1), 10.

McKenna, A., Hanna, M., Banks, E., Sivachenko, A., Cibulskis, K., Kernytsky, A., Garimella, K., Altshuler, D., Gabriel, S., Daly, M., & DePristo, M. A. (2010). The Genome Analysis Toolkit: a MapReduce framework for analyzing next-generation DNA sequencing data. *Genome Research*, *20*(9), 1297–1303.

Morgan, R., Andreassen, A. H., Åsheim, E. R., Finnøen, M. H., Dresler, G., Brembu, T., Loh, A., Miest, J. J., & Jutfelt, F. (2022). Reduced physiological plasticity in a fish adapted to stable temperatures. *Proceedings of the National Academy of Sciences of the United States of America*, *119*(22), e2201919119.

Njenga, R., Boele, J., Öztürk, Y., & Koch, H.-G. (2023). Coping with stress: How bacteria fine-tune protein synthesis and protein transport. *The Journal of Biological Chemistry*, *299*(9), 105163.

Oakley, C. A., & Davy, S. K. (2018). Cell biology of coral bleaching. In *Ecological Studies* (pp. 189–211). Springer International Publishing.

Palacio-Castro, A. M., Smith, T. B., Brandtneris, V., Snyder, G. A., van Hooidonk, R., Maté, J. L., Manzello, D., Glynn, P. W., Fong, P., & Baker, A. C. (2023). Increased dominance of heat-tolerant symbionts creates resilient coral reefs in near-term ocean warming. *Proceedings of the National Academy of Sciences of the United States of America*, *120*(8), e2202388120.

Palumbi, S. R., Barshis, D. J., Traylor-Knowles, N., & Bay, R. A. (2014). Mechanisms of reef coral resistance to future climate change. *Science (New York, N.Y.)*, *344*(6186), 895–898.

Parkinson, J. E., Baumgarten, S., Michell, C. T., Baums, I. B., LaJeunesse, T. C., & Voolstra, C. R. (2016). Gene Expression Variation Resolves Species and Individual Strains among Coral-Associated Dinoflagellates within the Genus Symbiodinium. *Genome Biology and Evolution*, *8*(3), 665–680.

Parsons, K. J., Concannon, M., Navon, D., Wang, J., Ea, I., Groveas, K., Campbell, C., & Albertson, R. C. (2016). Foraging environment determines the genetic architecture and evolutionary potential of trophic morphology in cichlid fishes. *Molecular Ecology*, *25*(24), 6012–6023.

Pfennig, D. W., Wund, M. A., Snell-Rood, E. C., Cruickshank, T., Schlichting, C. D., & Moczek, A. P. (2010). Phenotypic plasticity's impacts on diversification and speciation. *Trends in Ecology & Evolution*, *25*(8), 459–467.

Pratchett, M. S., McCowan, D., Maynard, J. A., & Heron, S. F. (2013). Changes in bleaching susceptibility among corals subject to ocean warming and recurrent bleaching in Moorea, French Polynesia. *PloS One*, *8*(7), e70443.

Quistad, S. D., & Traylor-Knowles, N. (2016). Precambrian origins of the TNFR superfamily. *Cell Death Discovery*, *2*(1), 16058.

Quiver, M. H., & Lachance, J. (2022). Adaptive eQTLs reveal the evolutionary impacts of pleiotropy and tissue-specificity while contributing to health and disease. *HGG Advances*, *3*(1), 100083.

R Core Team (2023). _R: A Language and Environment for Statistical Computing_. R Foundation for Statistical Computing, Vienna, Austria. <https://www.R-project.org/>.

Revell, L. J. (2024). phytools 2.0: an updated R ecosystem for phylogenetic comparative methods (and other things). *PeerJ*, *12*, e16505.

Ritz, C., Baty, F., Streibig, J. C., & Gerhard, D. (2015). Dose-response analysis using R. *PloS One*, *10*(12), e0146021.

Rivera, H. E., Aichelman, H. E., Fifer, J. E., Kriefall, N. G., Wuitchik, D. M., Wuitchik, S. J. S., & Davies, S. W. (2021). A framework for understanding gene expression plasticity and its influence on stress tolerance. *Molecular Ecology*, *30*(6), 1381–1397.

Rohlfs, R. V., & Nielsen, R. (2015). Phylogenetic ANOVA: The Expression Variance and Evolution Model for Quantitative Trait Evolution. *Systematic Biology*, *64*(5), 695–708.

Romero, I. G., Ruvinsky, I., & Gilad, Y. (2012). Comparative studies of gene expression and the evolution of gene regulation. *Nature Reviews. Genetics*, *13*(7), 505–516.

Schneider, R. F., & Meyer, A. (2017). How plasticity, genetic assimilation and cryptic genetic variation may contribute to adaptive radiations. *Molecular Ecology*, *26*(1), 330–350.

Scheiner, S. M., & Holt, R. D. (2012). The genetics of phenotypic plasticity. X. Variation versus uncertainty. *Ecology and Evolution*, *2*(4), 751–767.

Shaw, J. R., Hampton, T. H., King, B. L., Whitehead, A., Galvez, F., Gross, R. H., Keith, N., Notch, E., Jung, D., Glaholt, S. P., Chen, C. Y., Colbourne, J. K., & Stanton, B. A. (2014). Natural selection canalizes expression variation of environmentally induced plasticity-enabling genes. *Molecular Biology and Evolution*, *31*(11), 3002–3015.

Shi, T., Niu, G., Kvitt, H., Zheng, X., Qin, Q., Sun, D., Ji, Z., & Tchernov, D. (2021). Untangling ITS2 genotypes of algal symbionts in zooxanthellate corals. *Molecular Ecology Resources*, *21*(1), 137–152.

Shinzato, C., Khalturin, K., Inoue, J., Zayasu, Y., Kanda, M., Kawamitsu, M., Yoshioka, Y., Yamashita, H., Suzuki, G., & Satoh, N. (2020). Eighteen coral genomes reveal the evolutionary origin of Acropora strategies to accommodate environmental changes. *Molecular Biology and Evolution*. https://doi.org/10.1093/molbev/msaa216

Stamatakis, A. (2014). RAxML version 8: a tool for phylogenetic analysis and post-analysis of large phylogenies. *Bioinformatics (Oxford, England)*, *30*(9), 1312–1313.

Swain, T. D., Bold, E. C., Osborn, P. C., Baird, A. H., Westneat, M. W., Backman, V., & Marcelino, L. A. (2018). Physiological integration of coral colonies is correlated with bleaching resistance. *Marine Ecology Progress Series*, *586*, 1–10.

Swain, T. D., Vega-Perkins, J. B., Oestreich, W. K., Triebold, C., DuBois, E., Henss, J., Baird, A., Siple, M., Backman, V., & Marcelino, L. (2016). Coral bleaching response index: a new tool to standardize and compare susceptibility to thermal bleaching. *Global Change Biology*, *22*(7), 2475–2488.

Thomas, L., Rose, N. H., Bay, R. A., López, E. H., Morikawa, M. K., Ruiz-Jones, L., & Palumbi, S. R. (2018). Mechanisms of Thermal Tolerance in Reef-Building Corals across a Fine-Grained Environmental Mosaic: Lessons from Ofu, American Samoa. *Frontiers in Marine Science*, *4*, 338.

van Woesik, R., Shlesinger, T., Grottoli, A. G., Toonen, R. J., Vega Thurber, R., Warner, M. E., Marie Hulver, A., Chapron, L., McLachlan, R. H., Albright, R., Crandall, E., DeCarlo, T. M., Donovan, M. K., Eirin-Lopez, J., Harrison, H. B., Heron, S. F., Huang, D., Humanes, A., Krueger, T., … Zaneveld, J. (2022). Coral-bleaching responses to climate change across biological scales. *Global Change Biology*, *28*(14), 4229–4250.

von Heckel, K., Stephan, W., & Hutter, S. (2016). Canalization of gene expression is a major signature of regulatory cold adaptation in temperate Drosophila melanogaster. *BMC Genomics*, *17*, 574.

Wagner, G. P., Booth, G., & Bagheri-Chaichian, H. (1997). A population genetic theory of canalization. *Evolution; International Journal of Organic Evolution*, *51*(2), 329–347.

Wallace, C., & Willis, B. (1994). SYSTEMATICS OF THE CORAL GENUS ACROPORA: Implications of new biological findings for species concepts. *Annual Review of Ecology, Evolution, and Systematics*, *25*, 237–262.

Whitehead, A., & Crawford, D. L. (2006). Variation within and among species in gene expression: raw material for evolution: REVIEW OF GENE EXPRESSION VARIATION. *Molecular Ecology*, *15*(5), 1197–1211.

Winters, G., Holzman, R., Blekhman, A., Beer, S., & Loya, Y. (2009). Photographic assessment of coral chlorophyll contents: Implications for ecophysiological studies and coral monitoring. *Journal of Experimental Marine Biology and Ecology*, *380*(1), 25–35.

Wund, M. A., Baker, J. A., Clancy, B., Golub, J. L., & Foster, S. A. (2008). A test of the "flexible stem" model of evolution: ancestral plasticity, genetic accommodation, and morphological divergence in the threespine stickleback radiation. *The American Naturalist*, *172*(4), 449–462.

Figures and Tables

Figure 3.1: (A) Map of Moorea, French Polynesia, with sampling sites labeled. (B) Example of temperature profile used in this experiment where the x-axis is time spanning 18 hours and y-axis is the treatment temperature. X-axis is marked with the time that Fv/Fm yield was measured with PAM fluorometry and tissue was preserved.

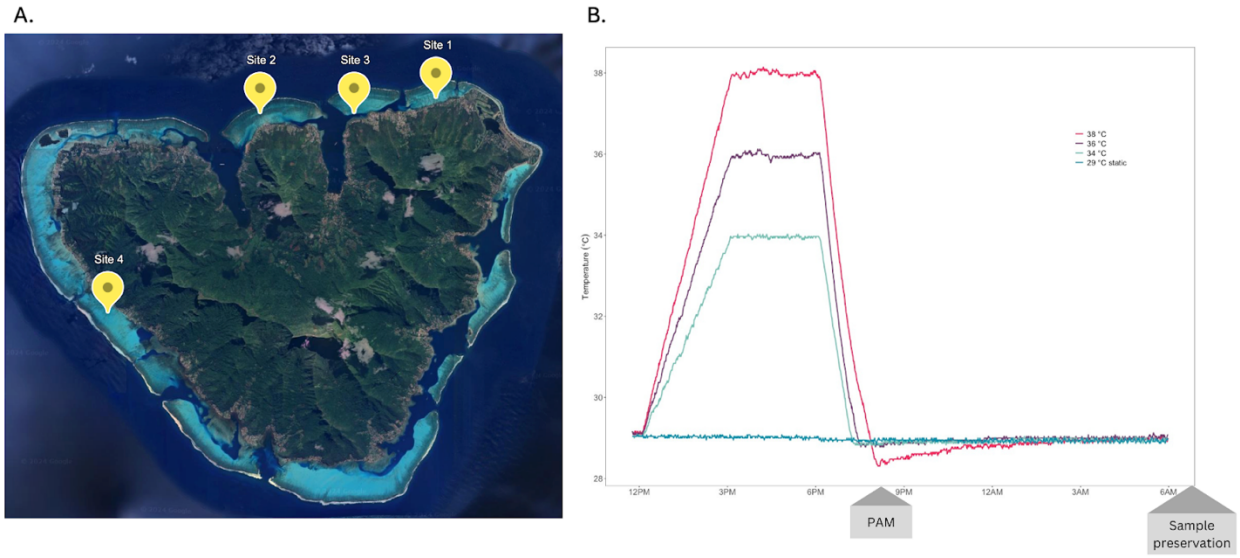

Figure 3.2: (A) Distribution of the ED50 for each species. Vertical lines correspond to the species' mean ED50. The y-axis indicates the number of samples for each species. (B) Red channel intensity changes across treatments separated by species. The depicted slope represents the rate of change in chlorophyll concentration due to treatment for each species, referred to as the species' visual bleaching score. Outlier samples of *A. robusta* with markedly higher red channel intensity in the control treatment are included. (C) Correlation between the species' visual bleaching score and the species-level thermal tolerance estimation. Outlier *A. robusta* colony 211 was removed to calculate the visual bleaching score (Red Channel Slope) for this species.

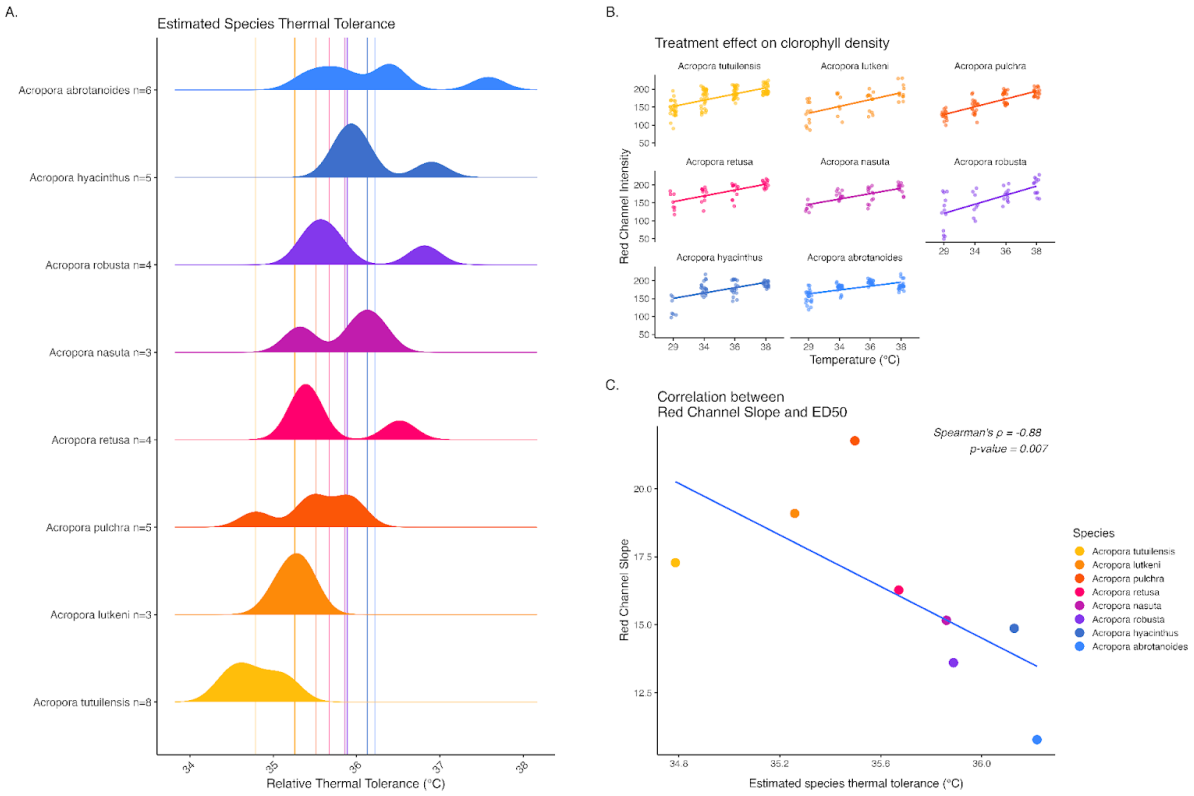

Figure 3.3: Phylogeny of coral species we sampled using 4,051 SNPs from 3' TagSeq data. The outgroup for the phylogeny was a species of *Montipora.* Illustrative photos of species diversity are included where the species from from the top to the bottom are: *A. pulchra, A. nasuta, A. lutkeni, A. retusa, A. abrotanoides, A. hyacinthus, A. tutiliensis,* and *A. robusta.*

Figure 3.4: (A) PCA of gene expression response to heat colored by species. (B) Spearman correlation between the euclidean distance calculated from the PCA and the colony-level thermal tolerance.

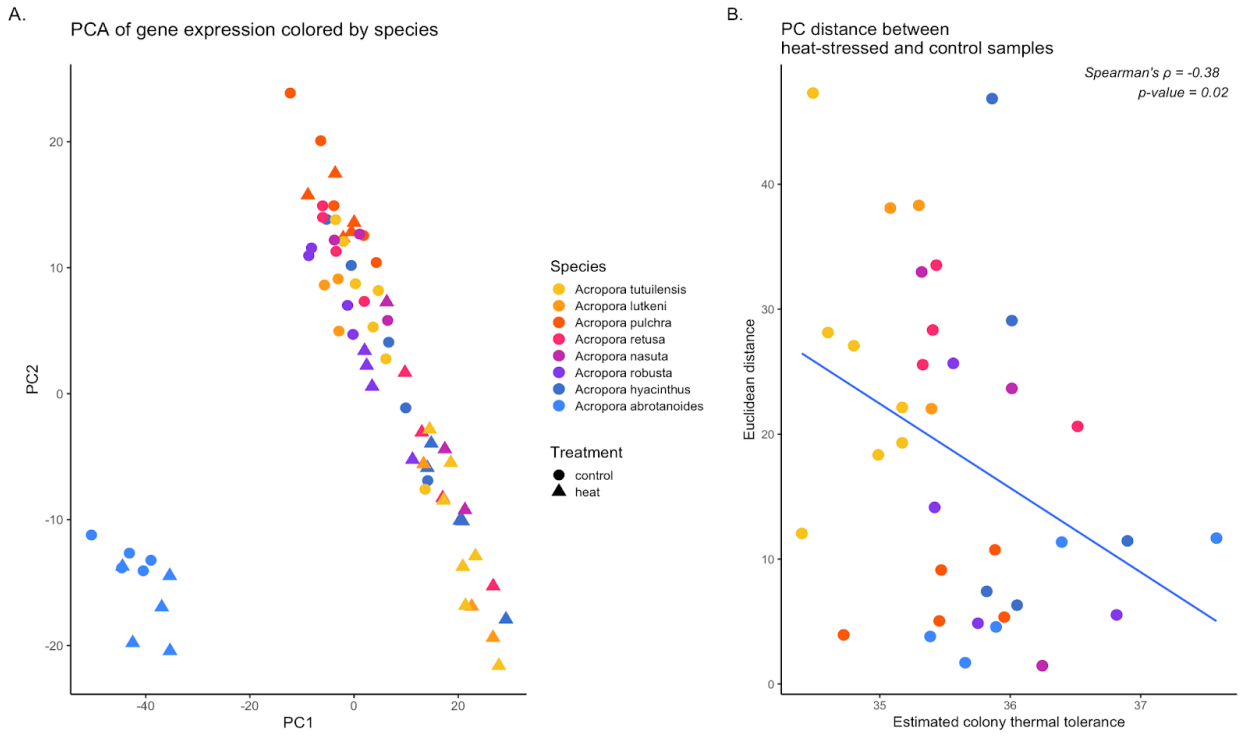

Figure 3.5: (A) Bar plot of percentage of variation in 28 well-supported gene expression modules contributed from treatment, species, collection site, and residuals. Vertical dashed line is the average variation due to the interaction between species and treatment. Modules with higher than average percent-variation due to the interaction between species and treatment were tested for a significant relationship between colony thermal tolerance and eigengene expression value. (B) Significant positive relationship of colony thermal tolerance and 'yellow' eigengene values (linear regression, p-value = 0.0258). (C) Significant positive relationship of colony thermal tolerance and 'salmon' eigengene values (linear regression, p-value = 0.0044).

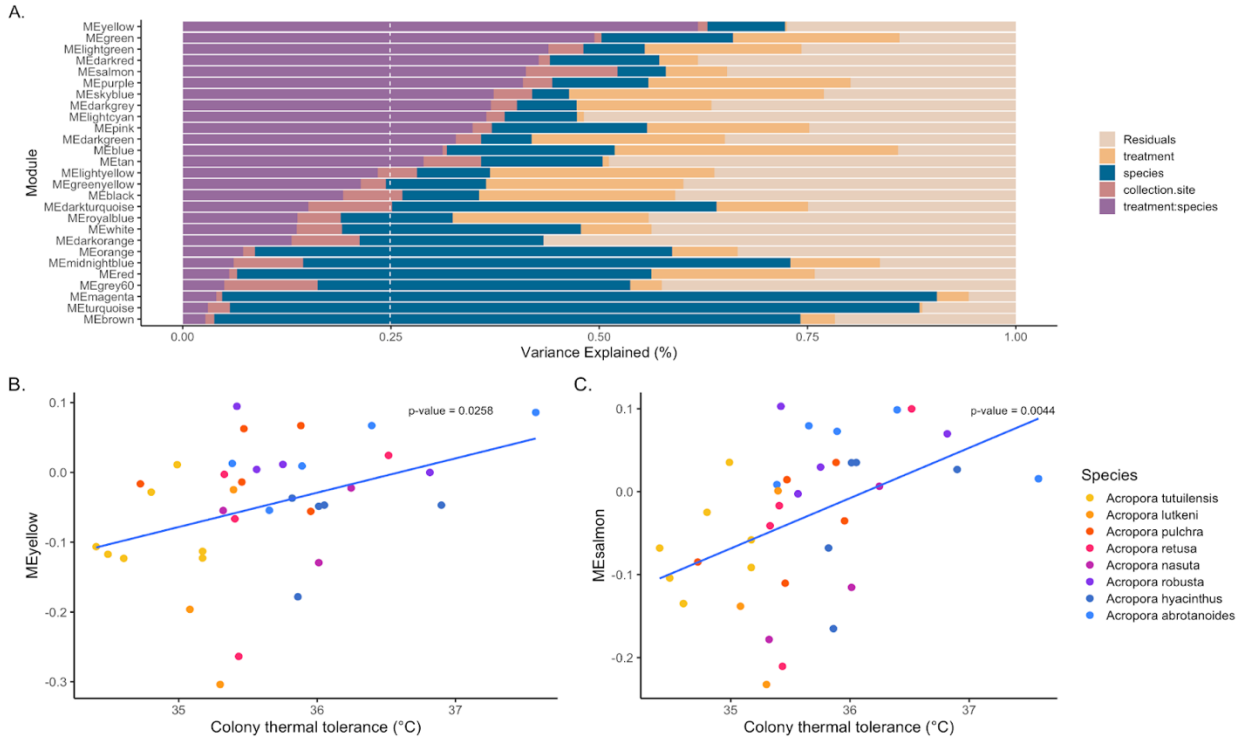

Figure 3.6: Comparison across species of expression of genes in the ‘yellow’ and ‘salmon’ modules. (A) log2-fold change across species of genes in the ‘yellow’ module. (B) log2-fold change across species of genes in the ‘salmon’ module. (C) Negative correlation between the average absolute value of the log2 fold change expression of genes in the ‘yellow’ module and colony thermal tolerance (Pearson’s correlation coefficient = -0.44, p-value = 0.006). (D) Negative correlation between the average absolute value of the log2 fold change expression of genes in the ‘salmon’ module and colony thermal tolerance (Pearson’s correlation coefficient = -0.349, p-value = 0.032). (E) Overall expression means of genes in ‘yellow’ modules of control and heat-stressed samples across species. (F) Overall expression means of genes in ‘salmon’ modules of control and heat-stressed samples across species.

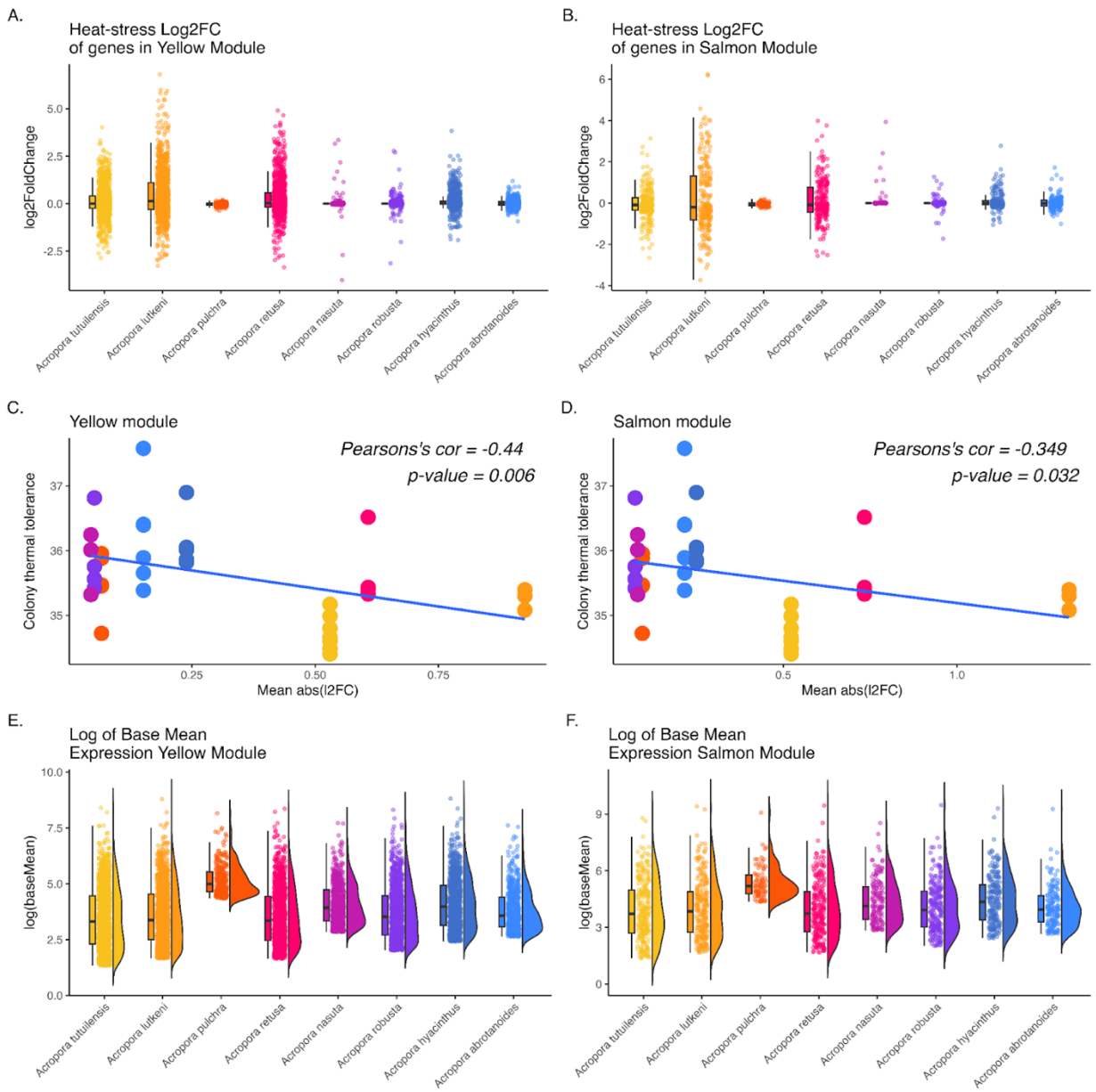
A.
Heat-stress Log2FC
of genes in Yellow Module
log2FoldChange
Acropora tutuilensis
Acropora lutkeni
Acropora pulchra
Acropora retusa
Acropora nasuta
Acropora robusta
Acropora hyacinthus
Acropora abrotanoides
B.
Heat-stress Log2FC
of genes in Salmon Module
log2FoldChange
C.
Yellow module
Pearsons's cor = -0.44
p-value = 0.006
Colony thermal tolerance
Mean abs(l2FC)
D.
Salmon module
Pearsons's cor = -0.349
p-value = 0.032
Colony thermal tolerance
Mean abs(l2FC)
E.
Log of Base Mean
Expression Yellow Module
log(baseMean)
F.
Log of Base Mean
Expression Salmon Module
log(baseMean)

Supplemental Figures and Tables

Table 3.S1: Colony sampling metadata shows species in each trial, sampling coordinates and site, and symbiont clade association. Rows are colored by species. We are missing some coordinates due to equipment failure.

Species	Colony ID	Sampling Date	Trial	Lat	Long	Site	Symbiont Clade
Acropora abrotanoides	c033	7/9/21	7	*na*	*na*	1	C
Acropora abrotanoides	c045	7/12/21	9	*na*	*na*	2	*na*
Acropora abrotanoides	c075	7/17/21	14	-17.54572	-149.89703	4	D
Acropora abrotanoides	c076	7/17/21	14	-17.54592	-149.89703	4	C
Acropora abrotanoides	c077	7/17/21	14	-17.54586	-149.89745	4	C
Acropora abrotanoides	c078	7/17/21	14	-17.54531	-149.8979	4	D
Acropora hyacinthus	c011	7/5/21	3	-17.47709	-149.78798	1	C
Acropora hyacinthus	c017	7/6/21	4	-17.47732	-149.78828	1	A
Acropora hyacinthus	c018	7/6/21	4	-17.4772	-149.78822	1	*na*
Acropora hyacinthus	c038	7/11/21	8	-17.47729	-149.78699	1	A
Acropora hyacinthus	c051	7/13/21	10	-17.47572	-149.78645	1	C
Acropora lutkeni	c047	7/12/21	9	*na*	*na*	2	A
Acropora lutkeni	c196	7/28/21	23	-17.47654	-149.79088	1	A
Acropora lutkeni	c210	7/29/21	24	-17.48227	-149.48659	2	A
Acropora nasuta	c012	7/5/21	3	-17.47728	-149.78796	1	A
Acropora nasuta	c037	7/11/21	8	-17.37729	-149.787	1	A
Acropora nasuta	c120	7/22/21	18	-17.47675	-149.78975	1	A
Acropora pulchra	c004	7/4/21	2	-17.47773	-149.78734	1	A
Acropora pulchra	c007	7/4/21	2	-17.47732	-149.78735	1	A
Acropora pulchra	c009	7/5/21	3	-17.49171	-149.82848	1	A
Acropora pulchra	c013	7/5/21	3	-17.47736	-149.78789	1	A
Acropora pulchra	c016	7/6/21	4	-17.47759	-149.78784	1	A
Acropora retusa	c030	7/8/21	6	-17.47629	-149.78709	1	C
Acropora retusa	c032	7/9/21	7	-17.47558	-149.78786	1	C
Acropora retusa	c040	7/11/21	8	-17.4764	-149.78714	1	A
Acropora retusa	c094	7/20/21	16	-17.47742	-149.78963	1	A
Acropora robusta	c090	7/20/21	16	-17.47762	-149.78873	1	A
Acropora robusta	c123	7/22/21	18	-17.47568	-149.79036	1	C
Acropora robusta	c167	7/26/21	21	-17.47863	-149.79138	1	A
Acropora robusta	c211	7/29/21	24	-17.4823	-149.84653	2	A
Acropora tutuilensis	c014	7/6/21	4	-17.4778	-149.78749	1	A
Acropora tutuilensis	c024	7/8/21	6	-17.47606	-149.78691	1	A
Acropora tutuilensis	c035	7/9/21	7	-17.47536	-149.78795	1	*na*
Acropora tutuilensis	c066	7/15/21	12	*na*	*na*	3	A
Acropora tutuilensis	c071	7/16/21	13	*na*	*na*	3	A
Acropora tutuilensis	c122	7/22/21	18	-17.47578	-149.79024	1	C
Acropora tutuilensis	c137	7/24/21	20	-17.48254	-149.84612	2	D
Acropora tutuilensis	c164	7/26/21	21	-17.47779	-149.79135	1	A

Table 3.S2: Table shows the results from a GO enrichment analysis of the 'yellow' module genes using the R package, topGO v. 2.50.0. We compared the list of 'yellow' module genes against a background of all transcripts that passed our quality filters. Enriched GO terms were identified with the classic Fisher's test with a p-value < 0.01 and at least 10 transcripts within each category. GO terms are contained within ontology types: Biological Processes (BP), Molecular Functions (MF), and Cellular Components (CC).

Type	**GO ID**	**Term**	**p-value**
BP	GO:1904950	negative regulation of establishment of protein localization	0.0038
BP	GO:0032355	response to estradiol	0.0048
BP	GO:0007131	reciprocal meiotic recombination	0.0053
BP	GO:0140527	reciprocal homologous recombination	0.0053
BP	GO:0035825	homologous recombination	0.0063
BP	GO:0120254	olefinic compound metabolic process	0.0068
BP	GO:0032787	monocarboxylic acid metabolic process	0.0074
BP	GO:0034612	response to tumor necrosis factor	0.0079
BP	GO:0051224	negative regulation of protein transport	0.0079
BP	GO:0051051	negative regulation of transport	0.0086
BP	GO:0010817	regulation of hormone levels	0.0099
MF	GO:0099106	ion channel regulator activity	0.0032
MF	GO:0008289	lipid binding	0.0038
MF	GO:0016247	channel regulator activity	0.0039
CC	GO:0043292	contractile fiber	0.0079

Table 3.S3: Table shows the results from a GO enrichment analysis of the 'salmon' module genes using the R package, topGO v. 2.50.0. We compared the list of 'salmon' module genes against a background of all transcripts that passed our quality filters. Enriched GO terms were identified with the classic Fisher's test with a p-value < 0.01 and at least 10 transcripts within each category. GO terms are contained within ontology types: Biological Processes (BP) and Cellular Components (CC). No Molecular Functions ontology types were found in this gene module.

Type	**GO ID**	**Term**	**p-value**
BP	GO:0000819	sister chromatid segregation	0.00021
BP	GO:0140014	mitotic nuclear division	0.00028
BP	GO:1903047	mitotic cell cycle process	0.00066
BP	GO:0006259	DNA metabolic process	0.00095
BP	GO:0006281	DNA repair	0.00153
BP	GO:0051052	regulation of DNA metabolic process	0.00248
BP	GO:0006974	DNA damage response	0.00272
BP	GO:0000278	mitotic cell cycle	0.00317
BP	GO:0098813	nuclear chromosome segregation	0.00437
BP	GO:0060249	anatomical structure homeostasis	0.00452
BP	GO:0022402	cell cycle process	0.00488
BP	GO:0051276	chromosome organization	0.00912
BP	GO:0007059	chromosome segregation	0.00934
CC	GO:0000228	nuclear chromosome	0.0052
CC	GO:0043228	non-membrane-bounded organelle	0.0069
CC	GO:0043232	intracellular non-membrane-bounded organelle	0.0069

Figure 3.S1: Boxplot of red-channel intensity. Colony outliers of *A. robusta* are circled.

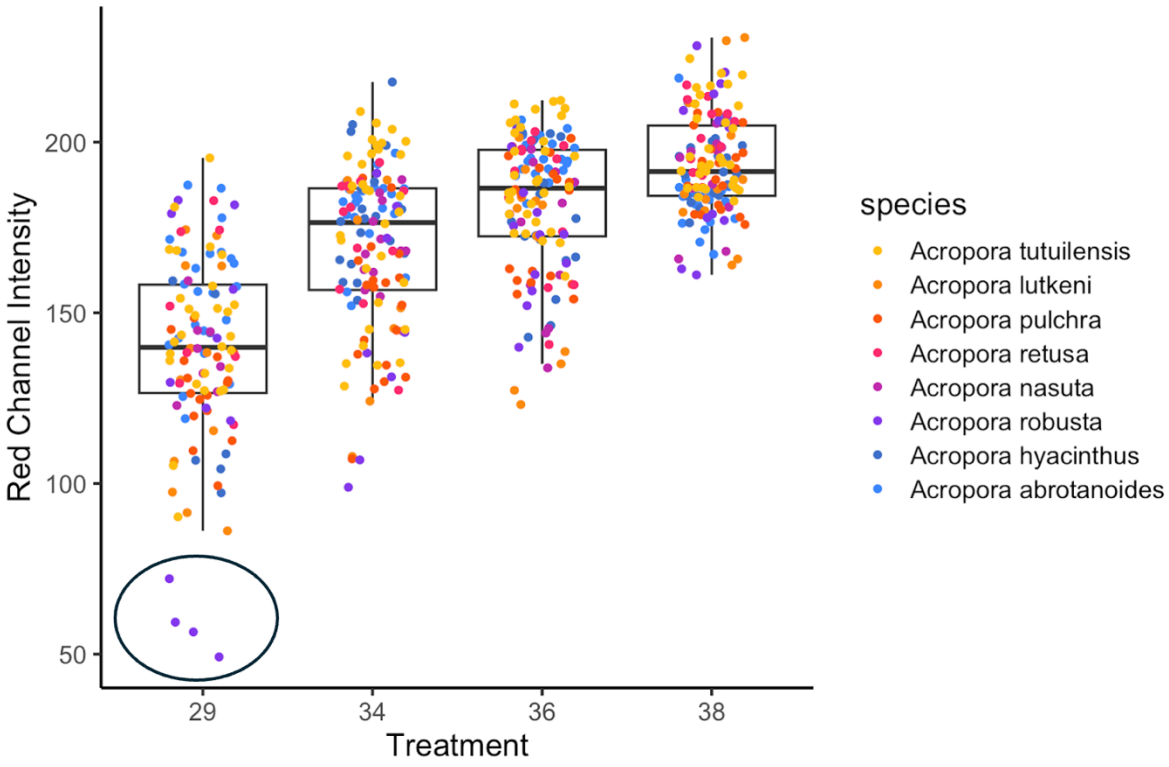

Figure 3.S2: 3'Tag Seq mapping efficiency of reads for all samples to each respective reference genome.

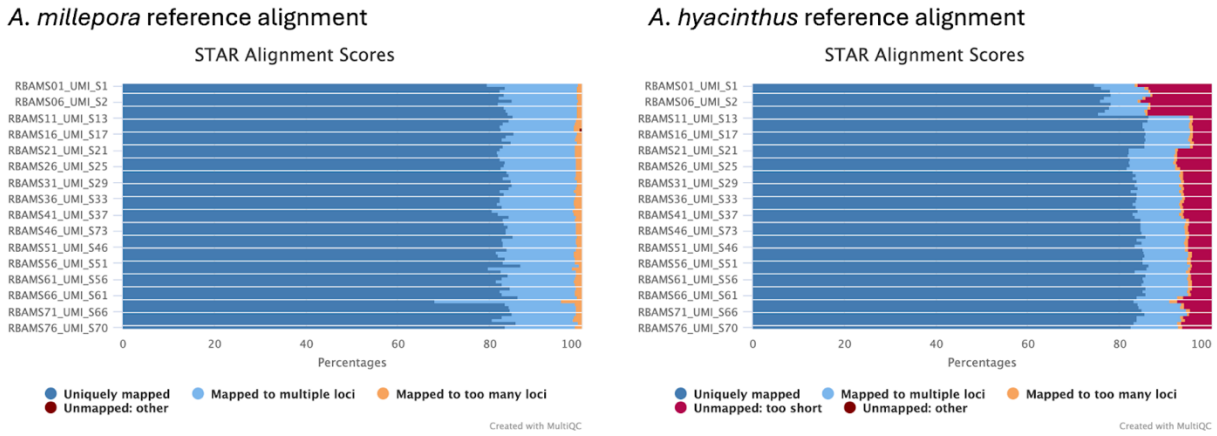

Figure 3.S3: Symbiodinium clade distribution across species.

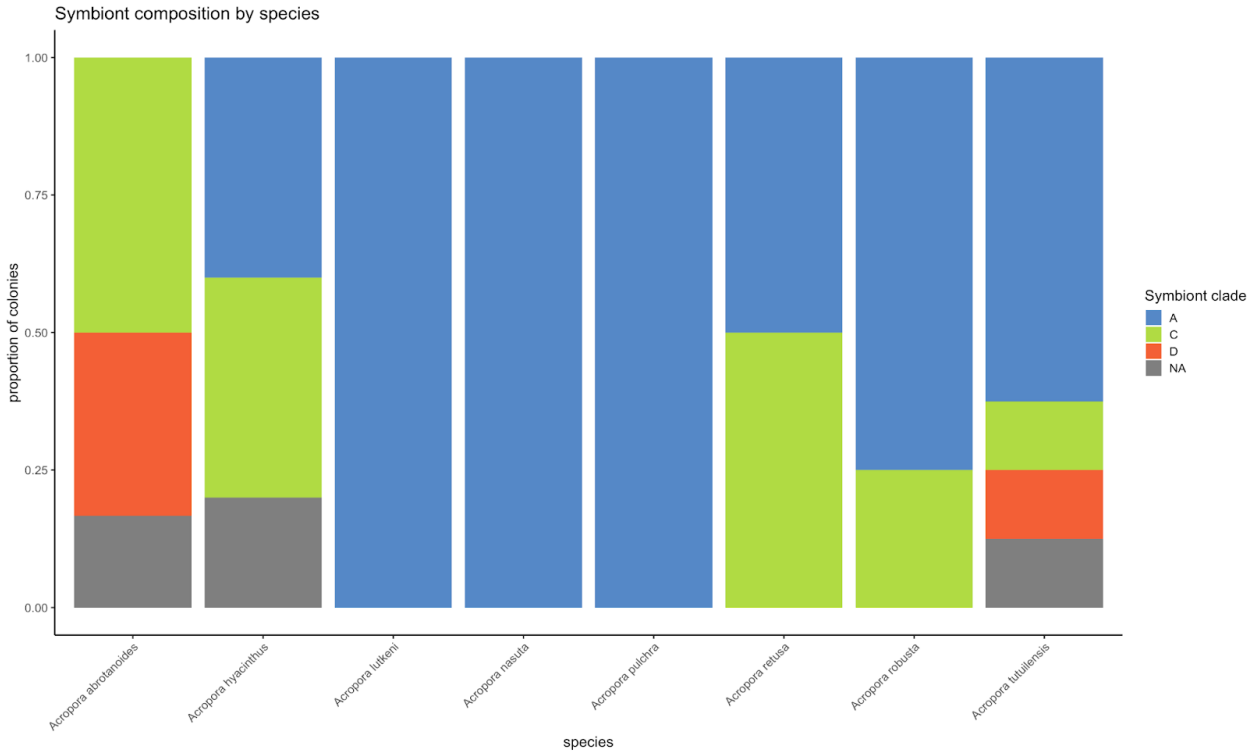

Figure 3.S4: PCA with divergent *A. abrotanoides* removed to visualize gene expression. Variation in PC1 is influenced by treatment and variation in PC2 mirrors phylogeny.

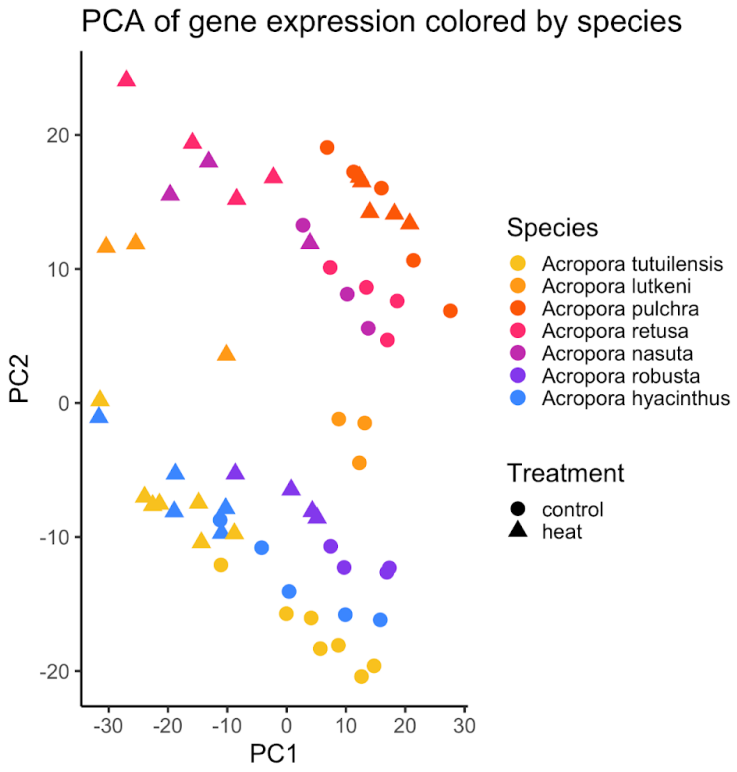

Figure 3.S5: Tukey HSD post-hoc comparisons of the mean difference in response magnitude of genes in the ‘yellow’ module (top) and the ‘salmon’ module (bottom). Error bars represent the 95% confidence interval.